INJECTABLE BIOPOLYMER GEL COMPOSITIONS FOR NEURAL TISSUE REPAIR

By

SAMESHA ROSÁNNE BARNES

A DISSERTATION PRESENTED TO THE GRADUATE SCHOOL
OF THE UNIVERSITY OF FLORIDA IN PARTIAL FULFILLMENT
OF THE REQUIREMENTS FOR THE DEGREE OF
DOCTOR OF PHILOSOPHY

UNIVERSITY OF FLORIDA

2009

This work is dedicated to my mother, Mrs. Rosemary Dorsey Barnes, who gave me wings and allowed me to fly.

ACKNOWLEDGMENTS

First and foremost I would like to acknowledge my lord and savior, Jesus Christ, who has brought me to this expected end. Apart from him I can do nothing. I especially thank my mother, Mrs. Rosemary D. Barnes, father, Mr. Samuel A. Barnes, brothers Reginald and Vincent Barnes, sister Tiara Barnes, and godsister Sarah Stubblefield for all of their love and support throughout my academic career. I would like to thank my advisor and chair, Dr. Eugene Goldberg, for his continued support and patience during this process. I appreciate him for believing in me to the end and pushing me across the finish line. I also thank the members of my supervisory committee, Dr. Chris Batich, Dr. Anthony Brennan, Dr. Henry Hess, and Dr. Paul Reier for helping me to reach this goal. It was truly an honor to be connected to such giants in the field. I would also like to acknowledge the late Dr. Abbas Zaman, Dr. Brij Moudgil and Dr. Charles Beatty for their contributions to my academic development at the University of Florida.

I acknowledge Gil Sanchez and Dr. Scott Brown from the Particle Engineering Research Center for assistance with rheological characterization. From the McKnight Brain Institute, I acknowledge Dr. Michael Lane, Barbara O'Steen, and Alex Jones from the Reier Research group and Drs. Irina Madorsky and Lucia Notterpek for their expertise and generosity in conducting the animal and Schwann cell studies. I also acknowledge Dr. Taili Thula, Paul Martin, Scott Cooper and Chelsea Magin from the Department of Materials Science and Engineering for their research assistance. I especially thank my former undergraduate mentees, David Cepeda, Julianne Huegel, David Walker and Bequita Gaines, for all of their contributions which were vital to the completion of this work. I also thank all the members of the Goldberg, Brennan and Batich research groups, past and present, that have been an essential part of my graduate experience.

I would like to give special acknowledgement to Ayana Johnson, Tara Washington, Dr. Shema Freeman, Jennifer Wrighton, Dr. Anne Donnelly, Dr. Todd White, Dr. Danyell Wilson,

Dr. Charlee Bennett, Dr. Erika Knight Styles, Dr. Anika Odukale Edwards, Dr. John Azeke, and Dr. Jompo Moloye-Olabisi, Dr. Margaret Kayo, and Dr. Daniel Urbaniak for being my cheerleaders and support system throughout my graduate career. Special appreciation is also given to my extended family, friends and colleagues for their support and encouragement along the way: Bill and Cynthia Jones, Shirley Benning, Carolyn Hayes, Delores Merriweather, the late Robert Howard, Geneva Stallings, Lily Hamilton, Linda McClellan, Penny McCloud, Monique McCane, Kecia and Cedric Rouse, Tambra Rainey, Pastor Eric Thomas, Kimberly Hayes, Kimberly Coward, Katara Starkey, Danisha Duncan-Phillips, Gwendolyn Saffo, Wendy Fletcher-Shannon, Dr. Sally Williams, Dr. Barbara Henry, Betty Floyd, Christina Scott, Kyana Stewart, Ashon and Takisha Nesbitt, Antoinette Black, Kevin Holloway, Leah Woodward, Kennesha Adolphin, Ian Fletcher, Anntwanique Edwards, Dr. Carla Phillips, Dr. Iris Enriquez-Schumaker, Dr. Amanda Ely, Dr. Leslie Wilson, Dr. Lizandra Williams, Dr. Jeremiah Abiade, Dr. Robert Crosby and the members of BGSO.

I would also like to thank the Department of Materials Science and Engineering Academic Service Coordinators, Martha McDonald, Doris Harlow and Jennifer Horton, the Southeast Alliance for Graduate Education and the Professoriate (SEAGEP), and the Office of Graduate Minority Programs (OGMP) for their support and commitment to my success.

TABLE OF CONTENTS

LIST OF TABLES

LIST OF FIGURES

LIST OF ABBREVIATIONS

ALG	alginate
ANOVA	analysis of variance
BDNF	brain derived neurotrophic factor
BSA	bovine serum albumin
CMC	carboxymethylcellulose
CNS	central nervous system
CSPG	chondroitin sulfate proteoglycan
DRG	dorsal root ganglion
ECM	extracellular matrix
ESC	embryonic stem cell
G	guluronic acid residue in alginate
GDL	glucono-delta-lactone
HA	hyaluronic acid
IKVAV	Ile-Lys-Val-Ala-Val peptide sequence
M	mannuronic acid residue in alginate
MP	methylprednisolone
NGF	nerve growth factor
NSC	neural stem cell
NT-3	neurotrophin-3
OEC	olfactory ensheathing cell
PEG	polyethylene glycol
PHEMA	poly(2-hydroxyethylmethacrylate)
PHPMA	poly(N-[2-hydroxypropyl] methacrylamide)
PGA	poly(glycolic acid)

PLA	poly(lactic acid)
PLGA	poly(lactic acid-co-glycolic acid)
PNS	peripheral nervous system
RGD	Arg-Gly-Asp peptide sequence
SCI	spinal cord injury
SEM	scanning electron microscopy

Abstract of Dissertation Presented to the Graduate School
of the University of Florida in Partial Fulfillment of the
Requirements for the Degree of Doctor of Philosophy

INJECTABLE BIOPOLYMER GEL COMPOSITIONS FOR NEURAL TISSUE REPAIR

By

Samesha Rosánne Barnes

December 2009

Chair: Eugene Goldberg
Major: Materials Science and Engineering

Injuries to the brain, spinal cord or other central nervous system (CNS) tissues trigger a cascade of biochemical events that result in an environment that is unfavorable for axonal regeneration and re-establishment of functional connections. Advances in understanding of the cellular and molecular mechanisms underlying spinal cord injury (SCI) over the past twenty years have resulted in the development of a number of therapeutic approaches to treating this critical problem. Biomaterial constructs represent an important and perhaps essential component of spinal cord repair strategies; however the functional and restorative potential of these approaches has not yet been realized.

This research focused on the development, synthesis and properties of biopolymer gel compositions for neural tissue repair. The primary goal was to prepare injectable gels which could function to bridge the lesion, prevent development or progression of a cystic cavity and provide a favorable terrain for axonal regeneration by delivering cells or other growth-promoting factors to the injured spinal cord. Homogeneous alginate (ALG), alginate-carboxymethylcellulose (ALG-CMC) and alginate-hyaluronic acid (ALG-HA) gels suitable for soft tissue engineering applications were synthesized via ionic crosslinking. Gradual gelation was achieved by slow liberation of calcium ions from calcium carbonate by reaction with D-

glucono-delta-lactone (GDL). In situ-forming ALG, ALG-CMC and ALG-HA gels have not previously been studied as biopolymer matrices for SCI repair.

All compositions were injectable through a 22-gauge needle prior to crosslinking. Gelation timing was evaluated as a function of biopolymer composition, calcium content, and temperature, and ranged from one to three hours for the conditions studied. Swelling and stability of gels were evaluated *in vitro*, and oscillatory tests were used to examine rheological properties. The potential for ALG, ALG-CMC and ALG-HA gels as transplantation matrices was investigated by incorporating Schwann cells in gel compositions *in vitro*.

A pilot animal study was conducted to demonstrate proof of concept *in vivo* using a clinically relevant SCI model in adult rats. Study animals received midline cervical contusion injuries at C3/C4 using an Infinite Horizon impactor and were treated with an ALG-CMC gel one week later. Histology revealed that the compositions integrated well with host spinal cord tissue and did not initiate a significant inflammatory response. Treated animals also showed minimal evidence of cystic cavitation. Results suggest that injectable alginate-based compositions have significant potential for minimally-invasive treatment of SCI and should undergo further investigation and optimization for neural tissue repair.

CHAPTER 1
INTRODUCTION

Significance of Spinal Cord Injury in the United States

Damage to the spinal cord is a life-altering experience for those who suffer from these injuries. An insult to the spinal cord disrupts communication with the brain below the level of injury and frequently leaves SCI victims with limited use of limbs, chronic pain, and other complications; the higher the injury along the spinal cord, the more catastrophic the consequences. Over 250,000 people in the United States live with SCI, and more than half of these patients were young adults between the ages of 16 and 30 at the time of injury (NSCISC, 2007). Most SCIs are caused by automobile accidents, falls, and gun shots, and approximately 12,000 new injuries occur each year resulting in lifelong medical expenses that often exceed $1 million per patient.

It was once believed that the CNS had no inherent ability to repair itself. However, decades of research has proven otherwise. It has been discovered that both regenerative and degenerative processes are triggered following CNS trauma, but the end result is an environment that is usually inhibitory to neural tissue repair. The permanent nature of SCI is largely due to the inability of axons to regenerate in the presence of physical and chemical barriers that develop around the wounded area; and the progressive nature of these injuries results in damage that is exacerbated over time. There has been no cure or effective treatment for SCI, but a number of factors have been identified to encourage axonal growth and re-establish functional connections. Hence, a growing body of research aimed at CNS tissue repair and regeneration. Accordingly, research proposed here was dedicated to achieving CNS repair by development of biopolymer-cell compositions with neuroregenerative properties.

Clinical Treatment of Acute SCI

The current clinical standard for acute SCI is high-dose treatment with methylprednisolone (MP) (Figure 1-1), a synthetic glucocorticosteroid. MP is administered within 8 hours of injury as a bolus of 30 mg/kg followed by 23-hour infusion of 5.4 mg/kg/hour based on recommendations from the National Acute Spinal Cord Injury Studies (NASCIS I, II, III) (Bracken et al., 1984; 1990; 1997; Bracken, 2002). The primary neuroprotective benefit of MP is believed to be reduction of inflammation and inhibition of oxygen free radical-induced lipid peroxidation (Hall, 1992; Kwon et al., 2004). MP was found to improve motor function recovery when delivered within 8 hours of injury and further improvement was reported when therapy is extended for 48 hours, especially when the initial bolus cannot be delivered within the first 3 to 8 hours after injury (Bracken, 2002). Others argue that MP offers only modest improvements in neurological function and when the risks of side-effects associated with high-dose steroid therapy are considered, the use of MP therapy as the standard of care for acute SCI cannot be justified (Gerndt et al., 1997; Short et al., 2000; Rabchevsky et al., 2002; Hugenholtz, 2003; Qian et al., 2005; Miller, 2008). Sustained delivery of MP from poly(lactic-co-glycolic acid) (PLGA) nanoparticles has recently been investigated and found to result in decreased lesion volume and enhanced behavioral recovery compared to standard MP treatment (Kim et al., 2009).

Specific Aims

The objective of this research was to develop biopolymer gel compositions for neural tissue repair using SCI as a model. Our primary goal was to synthesize injectable gels which would provide a favorable terrain for axonal regeneration by bridging the lesion site, preventing development (acute SCI) or progression (chronic SCI) of a cystic cavity, and functioning as a carrier matrix for transplanted cells or growth-promoting substances. This project was divided into two specific aims:

Aim 1: Synthesis and Characterization of Injectable Biopolymer Gel Compositions via Gradual Ionic Crosslinking of Alginate

Injectable alginate-carboxymethylcellulose (ALG-CMC) and alginate-hyaluronic acid (ALG-HA) gels were prepared via ionic crosslinking. Homogeneous gels of varying compositions were prepared and gradually crosslinked by the slow release of Ca^{2+} ions from $CaCO_3$ by reaction with D-glucono-δ-lactone (GDL). Gelation time was assessed at room and physiological temperatures using the inverted tube method. Modulus of gels was determined using a Paar-Physica UDS 200 rheometer with a cone-and-plate measuring cell, and morphology was examined by scanning electron microscopy (SEM). *In vitro* swelling and dissolution were evaluated for select compositions in artificial cerebrospinal fluid (aCSF) at 37 °C.

Aim 2: *In Vitro* and *In Vivo* Evaluations of Injectable Biopolymer Gel Compositions as a Matrix for Neural Tissue Repair

Suitability of gel compositions for cellular transplantation was evaluated by incorporating Schwann cells *in vitro*. Cell viability was examined using an alamarBlue assay. Cervical contusion lesions were introduced in the spinal cord of adult rats at C3/C4 using an Infinite Horizon spinal cord impactor, and biopolymer gel was injected one week post-injury and allowed to gel *in situ*. Rats were allowed to recover for one week before histological evaluation was conducted.

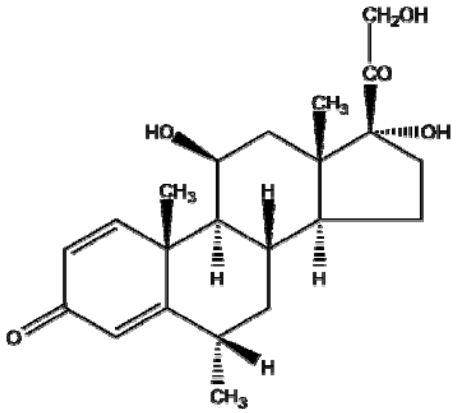

Figure 1-1. Structure of methylprednisolone.

CHAPTER 2
BACKGROUND

Physical trauma to the spinal cord causes immediate mechanical damage, vascular disruption and cell death, typically as a result of compression or tearing of tissue by the vertebral column. An intricate sequence of cellular and molecular events is subsequently triggered that includes both regenerative and degenerative processes. As early as 15 minutes after injury axons begin to swell causing surrounding myelin to peel away and rupture (Profyris et al., 2004). As a result, axonal contents are released into the extracellular space along with myelin fragments. Crushing or severing of axons physically divides the axon into two parts leading to the eventual degeneration of the distal segment in a process called Wallerian degeneration (Reier and Lane, 2008).

Within hours, activated macrophages and microglia invade the area and clear out myelin and axonal debris (Fawcett and Asher, 1999; Darian-Smith, 2009) but also secrete pro-inflammatory cytokines such as tumor necrosis factor (TNF-α), interleukin-1 (IL-1) and interleukin-2 (IL-6) that can compound tissue damage (Kwon et al., 2004). Breakdown of myelin debris by phagocytic cells elevates levels of myelin-derived proteins Nogo, myelin-associated glycoprotein (MAG) and oligodendrocyte myelin glycoprotein (OMgp) which have been shown to suppress plasticity and inhibit axonal growth and regeneration in the CNS (Grandpre and Strittmatter, 2001). Immediately after injury astrocytes undergo reactive gliosis and migrate to the damaged area. Within 3 to 5 days of injury, these reactive astrocytes begin to wall-off the injury and upregulate chondroitin sulfate proteoglycans (CSPGs) which are potent inhibitors of axonal regeneration (McGraw et al., 2001). The resulting glial scar is prominent in areas where the blood-brain barrier (BBB) has been most significantly breached accompanied by

a larger population of activated macrophages (Busch and Silver, 2007). The result is an inhibitory environment that is not conducive for repair.

Approaches to SCI Repair

The peripheral and central nervous systems differ in their response to injury which impacts the extent of axonal regeneration and functional recovery following trauma (Figure 2-1). Damage to the adult mammalian CNS was considered to be permanent until the early 1980s when its regenerative potential was demonstrated by elongation of transected CNS axons into peripheral nerve grafts (Richardson et al., 1980; David and Aguayo, 1981; Benfey and Aguayo, 1982). These landmark studies unambiguously showed that some CNS axons could undergo significant regrowth following injury if presented with a favorable environment. Since that time, advancement in the understanding of SCI mechanisms has led to considerable progress in developing treatments to promote axonal regeneration and functional recovery. The progressive nature of CNS injury makes it imperative that an effective strategy be developed that will minimize or halt further development of secondary damage and provide a favorable environment for regrowth of spared axons through the lesion.

A number of strategies been investigated that have been be categorized to offer neuroprotection, promote axonal growth, bridge the lesion, restore axonal conduction or to promote plasticity (Ramer et al., 2005), and many recent studies have focused on combining more than one approach (Ikegami et al., 2005; Ji et al., 2005; López-Vales et al., 2006; Bunge, 2008). Neuroprotective pharmaceutical agents such as methylprednisolone, GM-1 ganglioside, and minocycline have been studied to prevent loss of undamaged neural cells to secondary injury processes but the efficacy of some of these agents has been debated (Hall and Springer, 2004; Baptiste and Fehlings, 2006). Axonal regeneration has been encouraged through the neutralization of growth inhibitors, including antibody blocking of Nogo-66 receptor function

(Grandpre and Strittmatter, 2001; Li et al., 2005; Tian et al., 2005; Yu et al., 2008) and enzymatic degradation of CSPGs in the glial scar by chondroitinase ABC (Yick et al., 2003; Chau et al., 2004; García-Alías et al., 2008; Tester and Howland, 2008) . Also nerve growth factor (NGF), neurotrophin-3 (NT-3), brain-derived neurotrophic factor (BDNF) and other neurotrophic substances have been extensively used in partnership with other treatments to support axonal elongation. Due to the complexity of SCI, an effective treatment will ultimately consist of complementary approaches and will likely incorporate transplanted cells (Reier, 2004; Willerth and Sakiyama-Elbert, 2008). Major cell-based therapies are reviewed in the following section.

Cellular Transplantation Strategies

Schwann Cells

Unlike the CNS, axons in the peripheral nervous system (PNS) undergo significant elongation and regeneration following injury. The robust regenerative capacity of the PNS has largely been linked to Schwann cells, myelin-producing glia surrounding peripheral nerves, making them a prime candidate for transplantation in the injured spinal cord. When peripheral nerves are severed, macrophages invade the area and remove myelin and axonal debris resulting from Wallerian degeneration. Schwann cells in the distal segment proliferate and line up in tubes (bands of Bunger) along the basal lamina, up-regulating neurotrophins and ECM molecules that promote axonal regeneration. Growth cones in the proximal segment are directed through the Schwann cell tubes towards the distal segment: ultimately the ends are reconnected and remeyelinated and function is restored (Hall, 2001; Dezawa, 2002). In severe injuries where there is no residual distal segment, Schwann cells can be generated by precursors in proximal nerves, and these can stimulate a limited degree of regeneration and functional recovery (Purves et al., 2008).

Schwann cell transplantation in the spinal cord has been extensively investigated over the past twenty years and has been shown to promote repair and functional recovery (Martin et al., 1996; Guest et al., 1997; Xu et al., 1997; Oudega et al., 2001; Dezawa, 2002; Oudega et al., 2005; Rasouli et al., 2006; Agudo et al., 2008; Lavdas et al., 2008). Recently, intraspinal injection was found to be a more effective route for delivering autologous activated Schwann cells to the contused rat spinal cord, resulting in enhanced axonal regeneration, myelination and hindlimb locomotor recovery compared to intravenous or intrathecal delivery (Ban et al., 2009). In recent clinical trials, four adult patients with chronic mid-thoracic SCI received rehabilitation and treatment with autologous Schwann cells from the sural nerve (Saberi et al., 2008). Study patients experienced transient paresthesia and muscle spasms in lower limbs, but did not show signs of infection or neurological decline up to one year following cell transplantation. These results suggest that autologous Schwann cell transplantation is safe; however no sensory or motor function improvement was demonstrated.

Olfactory Ensheathing Cells

The mammalian olfactory neuroepithelium is unique in its ability to continuously renew itself for a lifetime, with neurogenesis occurring into adulthood (Ramón-Cueto and Avila, 1998), so when the olfactory system is injured, neurogenesis is enhanced and new axonal connections are established (Franssen et al., 2007). Olfactory ensheathing cells are glial cells that enwrap axons of olfactory neurons and guide them from the neuroepithelium in the nasal cavity to the olfactory bulb in the brain. The ability of OECs to permit axonal growth across the PNS to CNS interface into adulthood is a key factor in the regenerative capacity of the olfactory system (Franssen et al., 2007), and these cells may work in concert with other olfactory cells such as meningeal cells, olfactory nerve fibroblasts and olfactory mucosa cells (Barnett and Chang, 2004). OECs are similar to Schwann cells in many respects in that they exhibit: secretion of

neurotrophic factors, expression of ECM and cell adhesion molecules, stimulation of axonal regeneration and remyelination (Kocsis et al., 2009), and both are available for autologous transplantation. However, OECs have been shown to intermingle better with astrocytes and induce lower expression of inhibitory CSPGs than Schwann cells *in vitro* and *in vivo* (Lakatos et al., 2000; Lakatos et al., 2003). There has been considerable research involving acute and chronic transplantation of OECs in a variety of spinal cord injury models during the past 15 years (Ramón-Cueto and Nieto-Sampedro, 1994; Li et al., 1997, 1998; Bartolomei and Greer, 2000; Ramón-Cueto et al., 2000; García-Alías et al., 2004; Ramer et al., 2004; López-Vales et al., 2006; Franssen et al., 2007; Guest et al., 2008) as well as in the optic nerve (Li et al., 2003; Li et al., 2008). Clinical trials involving transplantation of OECs or olfactory tissue have also been conducted in Australia (Feron et al., 2005; Mackay-Sim et al., 2008), China (Zheng et al., 2007) and Portugal (Lima et al., 2006).

Macrophages/Microglia

Microglia are brain macrophage found throughout the adult CNS that play a key role in its immune function. There has been ongoing debate over whether these cells behave in a neuroprotective or neurotoxic manner in the injured CNS. Following CNS trauma, microglia become activated and secrete cytotoxic pro-inflammatory cytokines and free radicals (Stopek, 2003; Kitamura et al., 2009); however a pro-regenerative role is supported by activated microglial expression of neurotrophins, growth factors and ECM molecules as well as phagocytosis of cellular debris (Dougherty et al., 2000; Stopek et al., 2002; Kitamura et al., 2009). It has been proposed that microglia may exist in more than one type of activated state depending on the trigger which determines the effect these cells will have in response to trauma (Streit, 2002). The neuroprotective train of thought has lead to consideration of microglia for SCI repair in a few studies.

Prewitt et. al. co-transplanted microglia-coated nitrocellulose membranes along with fetal spinal cord tissue into adult rat lesions and found that increasing the concentration of activated macrophage/microglia at the injury site enhanced growth of sensory axons (1997). These results were presumed to be due to expression of cytokines and interaction with surrounding cells. Rabchevsky and Streit observed enhanced regeneration and substantial axonal extension into microglia-gelfoam grafts implanted into the injured adult rat spinal cord (1997; Streit, 2001). The authors concluded that cultured microglia in the grafts created a favorable environment for regeneration determined from neurite growth, vascularization, laminin expression and infiltration of growth-promoting host cells, e.g. Schwann cells. Microglial grafts were later revisited in studies by Stopek who implanted microglia-seeded alginate scaffolds into partial transection lesions in rats (2003). Seeded scaffolds were found to increase neurological function during spontaneous vertical exploration compared to untreated controls and to integrate well with host tissue. Transplantation of microglia for SCI repair has not been reported in recent years.

Stem and Progenitor Cells

Because of their ability to differentiate into specialized cells, stem and progenitor cells are of great interest for replacement of lost, injured or diseased cells and tissues. Embryonic stem cells (ESCs) are pluripotent and self-renewing and can be directed to differentiate into neurons and glia. This makes ESCs particularly attractive for SCI repair. Transplanted ESC-derived neurons have been shown survive and differentiate in the spinal cord and to promote functional recovery following injury (McDonald et al., 1999; Deshpande et al., 2006). Potential development of teratomas and risk of immunorejection in addition ethical issues have somewhat hampered ESC research for use in the spinal cord (Tewarie et al., 2009). However the first human clinical trials involving ESCs were recently approved by the United States FDA (Alper, 2009).

Neural stem cells (NSCs) are multipotent, self-renewing cells that generate neurons, astrocytes and glia that have been isolated from the developing and adult brain, spinal cord and optic nerve (Coutts and Keirstead, 2008). Adult NSCs have gained popularity as an alternative to embryonic cells as they have potential for autologous or donor-matched treatment and circumvent ethical concerns (Louro and Pearse, 2008). Also, a number of studies have investigated transplantation of neural progenitor cells as well as adult stems cells derived from bone marrow (e.g. hematopoietic stem cells and bone marrow stromal cells) and dermis as reviewed by Bareyre (Bareyre, 2008). Clinical trials involving stem and progenitor cells have also been conducted.

Tissue Engineering in the Injured CNS

The limited availability of autologous neural tissue and immunological risks related to allografts have led to investigation of tissue engineering approaches to CNS repair employing natural or synthetic polymeric scaffolds (Novikova et al., 2003). Development of biopolymer matrices is especially important as interest in cellular replacement therapies for SCI discussed above continues to grow (Reier, 2004; Ronsyn et al., 2008; Willerth and Sakiyama-Elbert, 2008). Therefore methods will be required for more effective delivery of donor tissue or bioactive substances into human spinal cord lesions which are typically larger and more complex than those created in the laboratory setting (Friedman et al., 2002; Kakulas, 2004; Guo et al., 2007).

The overall goal of neural tissue engineering is to provide an environment where scaffolds, cells, and bioactive molecules interact synergistically to promote tissue repair (Samadikuchaksaraei, 2007). This is approached by bridging the lesion with biomaterial constructs that will create a more permissive terrain for axonal regeneration either alone or in combination with growth-promoting cell types, neurotrophic molecules, or substances that neutralize inhibitory factors. There has been extensive exploration of biomaterial constructs for

CNS repair over the past decade as reviewed in the literature (Harvey, 2000; Geller and Fawcett, 2002; Nomura et al., 2006; Samadikuchaksaraei, 2007; Nisbet et al., 2008; Zhong and Bellamkonda, 2008). A variety of natural and synthetic polymers in the form of sponges or gels have been utilized, and effects of scaffold properties, e.g. scaffold architecture (Wong et al., 2008), have been explored. Linearly-oriented axonal growth and encapsulation of stem cells into biocompatible polymers have been issues of great interest (Teng et al., 2002; Silva et al., 2004; Stokols and Tuszynski, 2004; Nisbet et al., 2009). However, failure to achieve significant axonal growth beyond inhibitory host-implant glial interfaces is a challenge that has not been fully resolved (Geller and Fawcett, 2002). The following sections review some of the key polymers that have been investigated for CNS repair.

Natural Biopolymers

Agarose

Agarose (Figure 2-2) is a linear polysaccharide derived from red algae that forms thermoreversible gels in the temperature range of 17- 40 °C. Agarose gels have been shown to support outgrowth of dorsal root ganglion (DRG) neurites in vitro, and neurite extension was found to be inversely related to gel concentration and stiffness (Bellamkonda et al., 1995; Dillon et al., 1998; Balgude et al., 2001). Laminin-modified agarose hydrogel scaffolds enhanced DRG and PC12 neurite outgrowth *in vitro* (Yu et al., 1999). Additionally, loading the modified agarose scaffolds with NGF-loaded lipid microtubules stimulated directional DRG neurite extension. Freeze-dried agarose scaffolds with linearly oriented channels filled with collagen gel supported axonal ingrowth when implanted in the injured spinal cord (Stokols and Tuszynski, 2006). Regeneration was enhanced for scaffolds containing BDNF. In situ-forming agarose gels loaded with BDNF-loaded microtubules allowed axonal ingrowth and reduced the inflammatory response when injected in hemisection spinal cord lesions in rats (Jain et al., 2006). The low

gelling temperature of agarose (SeaPrep®) necessitated the use of a cooling system to induce thermal gelation of *in vivo* after injection into the cord which is a drawback of this approach. This limitation was overcome by combining agarose with another thermosensitive polymer with opposite gelling behavior, methylcellulose, producing a blend that gels near physiological temperature (Martin et al., 2008). These blends are undergoing further investigation for neural tissue repair.

Alginate

Alginate (Figure 2-3) is a linear, anionic polysaccharide from brown algae that has been used for controlled drug delivery, cell encapsulation, wound dressings and other biomedical applications because of its many favorable properties which include being nontoxic, biocompatible, and able to form gels under mild conditions via ionic crosslinking with divalent ions (d'Ayala et al., 2008). A number of studies have examined the use of alginate for repair in both the PNS and CNS. Alginate hydrogels have been reported to support DRG neurite outgrowth *in vitro* with enhanced neuroregenerative properties when Schwann cells were incorporated (Mosahebi et al., 2001). Similarly, YIGSR peptide-modified alginate gels stimulated a significant increase in attachment of NB2a neuroblastoma cells as well as enhanced neuritie differentiation and outgrowth compared to unmodified alginate gels (Dhoot et al., 2004). In the cochlea, ionically crosslinked alginate beads were shown to be an effective matrix for delivery of NT-3 and afforded protection of auditory neurons after round window and intra-cochlear implantation in deafened guinea pigs (Noushi et al., 2005). Neural progenitor cells have also been cultured and expanded *in vitro* in enzymatically degradable alginate hydrogels containing poly(lactide-co-glycolide) (PLGA) microspheres loaded with alginate lyase (Ashton et al., 2007). The degradation rate of alginate was tunable by adjusting the concentration and release rate of the enzyme.

Suzuki and colleagues synthesized freeze-dried, covalently crosslinked alginate sponges via reaction of ethylenediamine and water soluble carbodiimide and demonstrated their usefulness for wound healing and peripheral nerve regeneration. In later studies freeze dried alginate sponges were implanted into the resected spinal cord and reportedly reduced glial scar formation and enhanced outgrowth of axons (Suzuki et al., 1999; Kataoka et al., 2001; Suzuki et al., 2002; Kataoka et al., 2004). Additionally, these alginate sponges were shown to be an effective matrix for transplantation of hippocampus-derived neurospheres which were injected into alginate sponge-filled spinal cord lesions (Wu et al., 2001). Extensive migration and differentiation of neurospheres were observed as well as good integration with host spinal cord tissue.

Self-assembling alginate anisotropic capillary hydrogels have been shown to promote directional axonal regeneration *in vitro* and after implantation into cervical spinal cord transection lesions (Prang et al., 2006). Enhanced regeneration was observed *in vitro* when the anisotropic alginate scaffolds were seeded with adult neural progenitor cells. Choi et al. prepared injectable alginate gels by dissolving covalently crosslinked alginate sponges in physiological saline (2006). When injected into acute spinal cord lesions in rats a reduction in CSPG expression was observed compared to untreated controls.

Chitosan

Chitosan (Figure 2-4) is a cationic polysaccharide derived from chitin. It is found in the exoskeleton of crustaceans and is the second most abundant natural polymer. Chitosan-based membranes have been reported to have good nerve cell affinity *in vitro* (Haipeng et al., 2000), which is enhanced by combining chitosan with gelatin (Cheng et al., 2003) or poly-L-lysine (Mingyu et al., 2004). Genipin-crosslinked chitosan scaffolds prevented cystic cavitation and promoted some functional recovery following acute SCI but produced a greater concentration of

inflammatory neutrophils compared to alginate scaffolds (Stopek, 2003). Minimal axonal regeneration was observed after delayed implantation of chitosan channels in spinal cord lesions. However extensive regeneration was obtained when the chitosan channels were filled with peripheral nerve grafts, but without evidence of functional recovery (Nomura et al., 2008). Similarly, axonal regeneration and partial locomotor functional recovery were observed after implantation of collagen-filled chitosan tubes after SCI, but not for chitosan tubes alone (Li et al., 2009). In situ-forming chitosan gels which form gels at physiological pH and temperature have been synthesized using β-glycerophosphate salt (Chenite et al., 2000; Chenite et al., 2001). In vitro studies indicated that these thermally-gelling chitosans supported limited growth of fetal mouse cortical cells which was enhanced by attachment of poly-D-lysine (Crompton et al., 2007). However after implantation in the brain these thermosensitive chitosan gels stimulated significant activation of macrophages which may limit their use for CNS repair (Crompton et al., 2006).

Collagen

Collagen is the most abundant protein in the human body and the primary component of the extracellular matrix and connective tissues. Collagen supports neuronal cell attachment and growth (Tomaselli et al., 1987) and is used as a substrate for neuronal cell culture (Letourneau, 2001). Collagen has also been used for peripheral nerve repair (Archibald et al., 1995; Navarro et al., 2001; Stang et al., 2005) and is the basis of commercial NeuroGen^{TM} nerve guides (Integra, 2005). In the injured spinal cord, corticospinal axons did not grow into collagen gels; however substantial ingrowth of axons was stimulated when the gels were combined with gray matter extracts from the cervical spinal cord (Joosten et al., 1995). Collagen grafts containing the neurotrophins BDNF and NT-3 increased locomotor function and stimulated axonal ingrowth in

the transected spinal cord (Houweling et al., 1998a; 1998b). Injured spinal axons regrew through implanted collagen tubes and reconnected with targets in the ventral root (Liu et al., 2001). Collagen filament scaffolds were reported to bridge spinal cord lesions and promote functional recovery in rats (Yoshii et al., 2003; 2004) and rabbits (Yoshii et al., 2009) when implanted parallel to the spinal cord axis. Collagen gels have also been used as a matrix for intrathecal delivery of growth factors to the spinal cord (Jimenez Hamann et al., 2003; 2005).

Hyaluronic Acid

Hyaluronic Acid (HA) is a non-sulfated glycosaminoglycan (GAG) that is ubiquitous in the body and found in abundance in the extracellular matrix (ECM) of most animal tissues. It is a linear anionic polysaccharide consisting of D-glucuronic acid and N-acetylglucosamine disaccharide repeat units (Figure 2-5). HA functions as a lubricant for all joints and interacts with the cell surface receptors CD44, RHAMM and ICAM-1 in the regulation of biological processes such as morphogenesis, wound healing and inflammation (Toole, 2001). Also, HA degradation products have been shown to stimulate angiogenesis (West et al., 1985) HA has been employed extensively in biomedical applications because it is biodegradable, biocompatible, and non-immunogenic in addition to its unique pseudoplastic rheological properties. Major uses of HA include viscosupplementation, ophthalmic viscosurgery, wound healing and drug delivery (Balazs and Denlinger, 1989) and for the prevention of post-surgical adhesions (Burns et al., 1995). Poor mechanical properties and rapid enzymatic degradation *in vivo* necessitate crosslinking or combination of HA with other polymers for tissue engineering applications (Segura et al., 2005).

In the CNS, HA is produced mostly by astrocytes and surrounds myelinated axons in white matter and neuronal cell bodies in grey matter of the spinal cord (Asher and Bignami, 1991; Bignami and Asher, 1992; Bignami et al., 1992). The functions of HA in the CNS are not fully

understood, however it has been associated with neuronal and glial cell migration, axonal guidance and synaptic modulation (Sherman et al., 2002). In the normal rat spinal cord, high molecular weight HA has been demonstrated to maintain astrocytes in a state of quiescence but is degraded after SCI which stimulates astrocyte proliferation (Struve et al., 2005). These findings suggest that degradation of HA plays a significant role in the formation of the glial scar following injury.

HA has been investigated as a matrix for cellular transplantation to the CNS. For example, attachment of OECs on HA thin films has been investigated *in vitro* (Mallek, 2006). Modification with the phospholipid 2-methacryloyloxyethyl phosphorylcholine (MPC) resulted in increased OEC attachment compared to unmodified films. In a recent study, HA-Polylysine hydrogels were shown to support survival and differentiation of neural stem cells into neurons and astrocytes in culture (Ren et al., 2009). DRGs cultured in 3-D crosslinked thiolated HA hydrogels exhibited enhanced survival and neurite extension *in vitro* when compared to DRGs cultured in fibrin matrices. However there was no difference in histological or functional outcome between rats implanted with the thiolated HA hydrogels following transection SCI and untreated control animals. HA has also been invesigated as a carrier for a Nogo-66 receptor (NgR) antibody to promote axonal regeneration (Tian et al., 2005). HA hydrogels coupled with PDL and the NgR antagonist were shown to support neural cell attachment and to induce DRG neurite outgrowth *in vitro* (Hou et al., 2006).

HA hydrogel scaffolds conjugated with bioactive molecules such as laminin (Hou et al., 2005), poly-D-lysine (PDL) (Tian et al., 2005), RGD (Cui et al., 2006) and IKVAV (Wei et al., 2007) have been implanted in the injured brain. The modified HA scaffolds were found to support cellular infiltration and angiogenesis, to reduce glial scarring and to improve DRG

neurite extension verses HA alone. HA has also been combined with methylcellulose (MC), a thermoreversible polymer that gels around 37 °C, to create a rapidly gelling matrix for localized, intrathecal drug delivery to the injured spinal cord (Gupta et al., 2006; Baumann et al., 2009; Kang et al., 2009).

Synthetic Polymers

PEG

Polyethylene glycol (PEG) (Figure 2-6) is a hydrophilic polymer with surfactant properties that is biocompatible and used in a number of products for human use. Several *in vitro* studies have been conducted to determine the suitability of PEG gels for delivery of cells and neurotrophins to the injured CNS. Photopolymerizable gels have been explored for their potential for minimally invasive delivery as they can be injected in the site of injury and cured *in vivo* by exposure to light. Photopolymerized PEG gels have been studied for controlled release of CNTF and were reported to enhance neurite outgrowth from retinal explants compared to PEG gels without CNTF (Burdick et al., 2006). Microspheres embedded within the photopolymerized PEG gels were also able to simultaneously deliver multiple neurotrophins with distinct release profiles. Photopolymerized PEG (Mahoney and Anseth, 2006) and poly-L-lysine-PEG (Hynes et al., 2007) gels have also been synthesized and supported *in vitro* survival of neural progenitor cells. *In vivo*, PEG solutions containing NT-3 were injected into the rat spinal cord following hemisection injury and subsequently polymerized by exposure to light (Piantino et al., 2006). The gels promoted axonal regeneration and improvement in open field BBB scoring and horizontal ladder walk tests. Injectable poly(N-isopropylacrylamide) (PNIPAAm)-PEG gels have also been synthesized for sustained release of BDNF and NT-3 in the injured CNS. These gels were reported to preserve neurotrophin bioactivity and support survival and attachment of BMSCs *in vitro* (Comolli et al., 2008).

Because of its fusogenic properties, PEG solutions have been investigated for topical application to the acutely inured spinal cord where they have been demonstrated to promote rapid functional recovery and restoration of axonal conduction through the lesion (Shi and Borgens, 1999; Borgens and Shi, 2000; Shi and Borgens, 2000; Borgens et al., 2002). Similar results have been obtained for subcutaneous (Borgens and Bohnert, 2001) and intravenous delivery of PEG (Laverty et al., 2004; Baptiste et al., 2009). The neuroprotective benefits of PEG are not fully understood but are believed to be due to its ability to rapidly restore integrity of damaged cells/membranes and to suppress secondary injury mechanisms such as the production of reactive oxygen species (Borgens et al., 2002; Luo et al., 2002; Liu-Snyder et al., 2007). PEG must be administered early after injury while , prior to glial scarring (Nisbet et al., 2008), and may be useful in combination with other approaches to SCI repair rather than as an independent treatment (Baptiste et al., 2009).

PHEMA

Poly(2-hydroxyethylmethacrylate) (PHEMA) (Figure 2-7) is a soft, hydrophilic, nonbiodegradable polymer and the most highly used hydrogel. PHEMA properties are highly tunable by varying the water content, degree of crosslinking and method of preparation (Peppas, 2009). Biomedical uses of PHEMA include soft contact lenses, drug delivery, wound healing, articulating surfaces for joint prostheses and artificial intervertebral discs (Meakin et al., 2003). PHEMA sponges with 85% water content have been engineered by Bakshi et al. to match the mechanical properties (compressive modulus) of the spinal cord (2004). When implanted into the hemisected cord the hydrogel scaffolds elicited a modest inflammatory response, had minimal scarring around the implant and supported considerable angiogenesis. Also, axonal regeneration was improved by soaking the PHEMA sponge in BDNF.

HEMA has been copolymerized with methyl methacrylate (MMA) to improve mechanical strength and application to spinal cord repair (Dalton et al., 2002). Unfilled guidance tubes synthesized PHEMA-PMMA implanted between the stumps of the transected rat spinal cord were found to promote regeneration of axons from brainstem motor nuclei with minimal inflammatory response and minimal scarring at the tube-spinal cord interface (Tsai et al., 2004). The PHEMA-PMMA channels collapsed over time due to inadequate mechanical strength and were subsequently reinforced with coils which increased the channel strength by seven times (Nomura et al., 2006). However, the coil-reinforced channels offered no regenerative improvement due to complications with syringomyelia and caudal migration of the rostral stump. Tsai et al. demonstrated that filling the PHEMA-PMMA channels with a matrix material, e.g. collagen, fibrin, Matrigel™, impacted the number of regenerating axons, the original of regenerating axons and also improved functional recovery (2006).

In recent studies, macroporous PHEMA scaffolds with positive charges were prepared by copolymerization with [2-(methacryloyloxy)ethyl] trimethylammonium chloride and implanted into the transected spinal cord (Hejčl et al., 2008). The positively-charged hydrogels adhered well to spinal cord tissue and permitted infiltration of blood vessels, neurofilaments and Schwann cells. Delayed implantation (1 week) was shown to result in a statistically significant decrease in cystic cavitation compared to implantation immediately following injury. PHEMA scaffolds of varying surface charges have also been compared in the same injury model (Hejčl et al., 2009). It was concluded that axonal regeneration within PHEMA hydrogels is promoted by charged functional groups, whether positive or negative, compared to uncharged scaffolds. However, regeneration was most significant in positively charged scaffolds.

PHPMA (Neurogel ™)

Poly(N-[2-hydroxypropyl methyacrylamide]) (PHPMA) (Figure 2-8) hydrogels with interconnected pores and viscoelastic properties similar to nervous tissue have been synthesized by Woerly et al. These hydrogels have been shown to support cellular ingrowth and axonal regeneration after acute implantation in the transected rat (Woerly et al., 1998; 1999) and cat (Woerly et al., 2001) spinal cord as well as in brain lesions (Woerly et al., 1999). PHPMA hydrogels also promoted tissue reconstruction and functional recovery following delayed implantation in compression lesions three months after injury (Woerly et al., 2001) and are reported to suppress glial scar formation (Woerly et al., 2004). RGD peptide-functionalized PHPMA hydrogels have also been synthesized under the trademark (NeuroGel™) and implanted into the injured spinal cord (Woerly et al., 2001). Schwann cells, astrocytes and embryonic neural cells entrapped within PHPMA had limited viability which was believed to be due to the polymerization conditions, e.g. monomer toxicity and heat production (Woerly et al., 1996a; 1996b), indicating that these hydrogels are not suitable for in situ cell immobilization. However, fibroblasts modified to express BDNF and ciliary neurotrophic factor (CNTF) have been infused into RGD-PHPMA hydrogels and reported to enhance axonal regeneration in the injured optic nerve (Loh et al., 2001).

PLA/PLGA

Poly(lactic acid) (PLA), poly(glycolic acid), PGA, and their copolymers (PLGA), are the most used synthetic, biodegradable. These polymers (Figure 2-9) are members of the poly(α-hydroxyacid) family and have been used in sutures, bone fixation devices, microspheres for drug delivery, and scaffolds for tissue engineering (Athanasiou et al., 1996). The mechanical properties and degradation rate (rate of hydrolysis) of PLGA copolymers can be easily

manipulated by adjusting molecular weight and monomer ratios, as well as the stereochemistry of PLA which exists in *D* and *L* isomeric forms (PDLA, PLLA).

The potential of poly(α-hydroxyacids) for spinal cord repair was first demonstrated by Gautier et al. who found that a PLGA copolymer and its degradation products did not adversely affect Schwann cell morphology and proliferation *in vitro* (1998). When implanted in the spinal cord PLGA cylinders had an inflammatory response similar to controls and showed evidence of axonal regeneration. Two types of PLA tubes containing Schwann cell cables were found to have inadequate mechanical properties and permeability for spinal cord repair (Oudega et al., 2001). Later, macroporous PLA foam scaffolds were synthesized which have been investigated for delivery of BDNF (Patist et al., 2004) and genetically-modified Schwann cells (Hurtado et al., 2006) to the injured cord . Porous PLGA scaffolds have be studied for Schwann cell delivery in recent studies (Chen et al., 2009). Also, PLGA nanoparticles have been shown to be effective for instraspinal delivery of the neurotrophic factor GDNF with enhanced neuronal survival and hindlimb locomotor recovery (Wang et al., 2008). The key natural and synthetic polymers investigated for CNS repair are summarized in Table 2-2 and Table 2-3, respectively.

Injectable Gels for Neural Tissue Repair

Gels derived from natural and synthetic polymers have been investigated as scaffolding for neural tissue repair as reviewed above because of their high water content, porous structure and soft, tissue-like mechanical properties (Woerly et al., 1999). For vinyl monomers such as HEMA, crosslinking is achieved with polyfunctional acrylic monomers such as the bisacrylates by free radical polymerization which results in covalently crosslinked molecular structures which are insoluble but readily swollen by water. Hydrogel properties (i.e. strength and water absorption) may be varied by adjusting the degree of crosslinking; i.e. the crosslink density. Gel

implants are frequently used in the form of sponges or soft, semi-solid jelly-like solids that may be cut to size for surgical implantation into the injured CNS tissues and organs such as the spinal cord. Because they are often synthesized with radical initiators and cytotoxic covalent crosslinking agents they must be extensively purified to be suitable for implantation. In addition, a number of studies have examined the use of gel implants in conjunction with cells, enzymes, or growth factors. However, incorporation of these agents during hydrogel synthesis subjects them to the free radical reaction chemistry which may be damaging or degrading.

It has been suggested that an ideal hydrogel scaffold for spinal cord regeneration should have the ability to be shaped in situ in addition to being biocompatible, biodegradable or bioresorbable, and permissive for cell migration and axonal outgrowth (Zhong and Bellamkonda, 2008). An in situ-forming gel has several advantages. The gel can be injected in a minimally-invasive procedure compared to sponge-like scaffolds which require lesioning the injured cord for implantation. Unlike foam or pre-formed gel scaffolds, an injectable gel can completely fill the irregular geometry of a contused lesion cavity (Figure 2-10) facilitating integration with host tissue. Also, multiple cells and substances can be easily dispersed within the material prior to gelation for simultaneous delivery in a single injection.

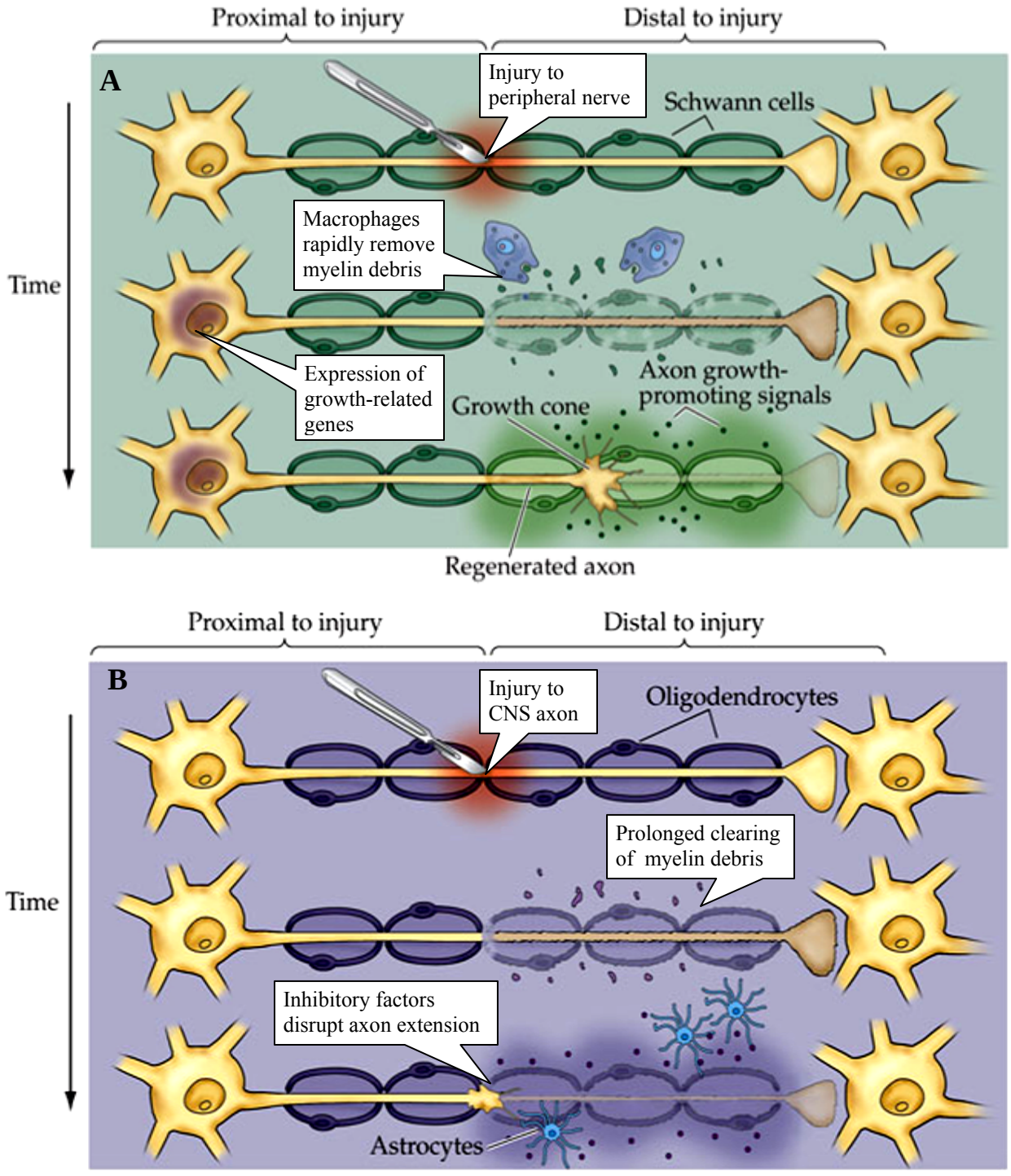

Figure 2-1. Cellular response to injury in the nervous system. A) Secretion of neurotrophins and other growth-promoting factors by Schwann cells in the PNS is essential to peripheral nerve regeneration. B) Myelin debris and inhibitory factors secreted by reactive astrocytes contribute to failure of CNS regeneration. [Reprinted with permission from Sinauer Associates, Inc. Purves, D., Augustine, G. J., Fitzpatrick, D., Hall, W. C., LaMantia, A.-S., McNamara, J. O., and White, L. E., 2008. Neuroscience. (Page 641, Figure 25.5; Page 648, Figure 25.10) Sinauer Associates, Inc., Sunderland, MA.]

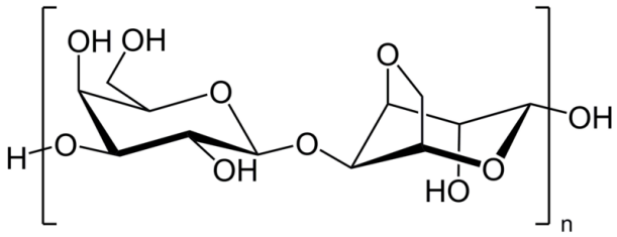

Figure 2-2. Chemical structure of agarose.

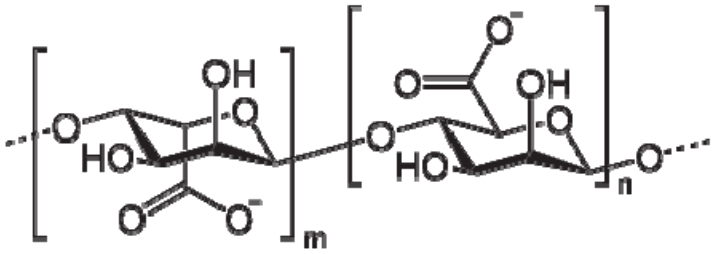

Figure 2-3. Chemical structure of alginate.

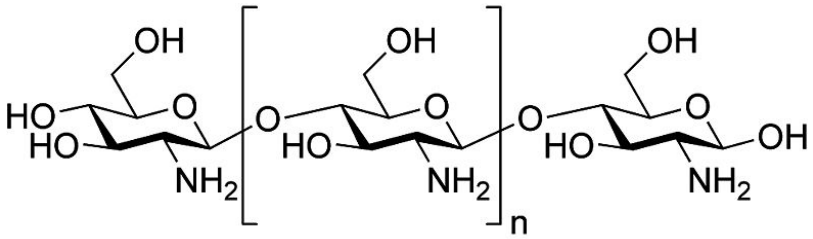

Figure 2-4. Chemical structure of chitosan.

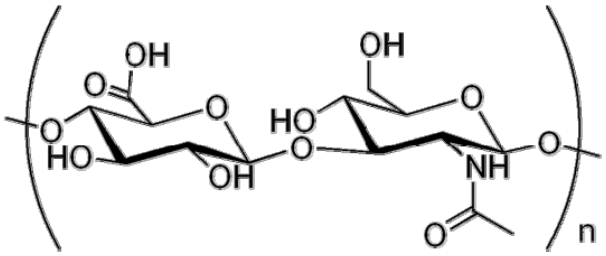

Figure 2-5. Chemical structure of hyaluronic acid.

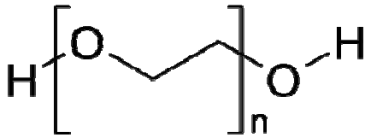

Figure 2-6. Chemical structure of polyethylene glycol (PEG).

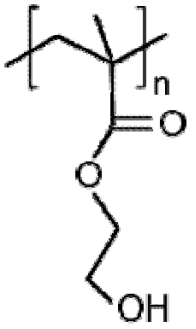

Figure 2-7. Chemical structure of poly(2-hydroxyethylmethacrylate) (PHEMA).

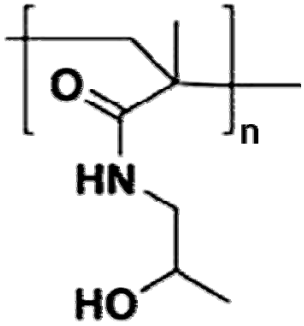

Figure 2-8. Chemical structure of poly(N-[2-hydroxypropyl methyacrylamide]) (PHPMA).

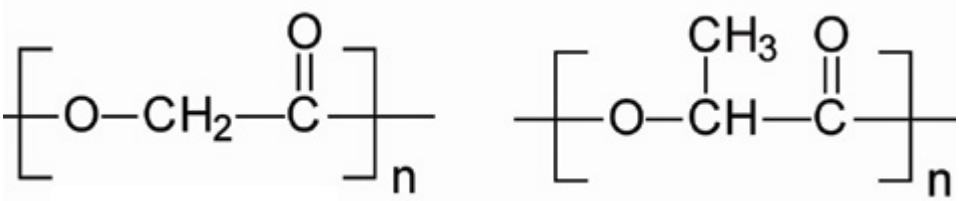

PGA PLA

Figure 2-9. Chemical structures of poly(glycolic acid) (PGA) and poly(lactic acid) (PLA).

Table 2-1. Summary of key natural biopolymers investigated for CNS repair

Polymer	Source	Advantages	Disadvantages
Agarose	Red algae	Thermoreversible gelation	Poor cell adhesion, cooling required to induce gelation
Alginate	Brown algae	Mild (ionic) crosslinking	Poor cell adhesion
Chitosan	Crustaceans	Cell adhesive (cationic)	Significant inflammatory response
Collagen	ECM	Supports cell attachment	Immunogenicity concerns
Hyaluronic acid	ECM	Bioactive	Poor cell adhesion, Poor mechanical properties

Table 2-2. Summary of key synthetic biopolymers investigated for CNS repair

Polymer	Degradable	Use in CNS repair
PEG	Yes	Injectable (photopolymerized) gels, topical application
PHEMA	No	Sponge-like scaffolds, tubular channels
PHPMA	No	Gel scaffolds
PLA/PLGA	Yes	Sponge-like scaffolds, tubular channels, nanoparticles

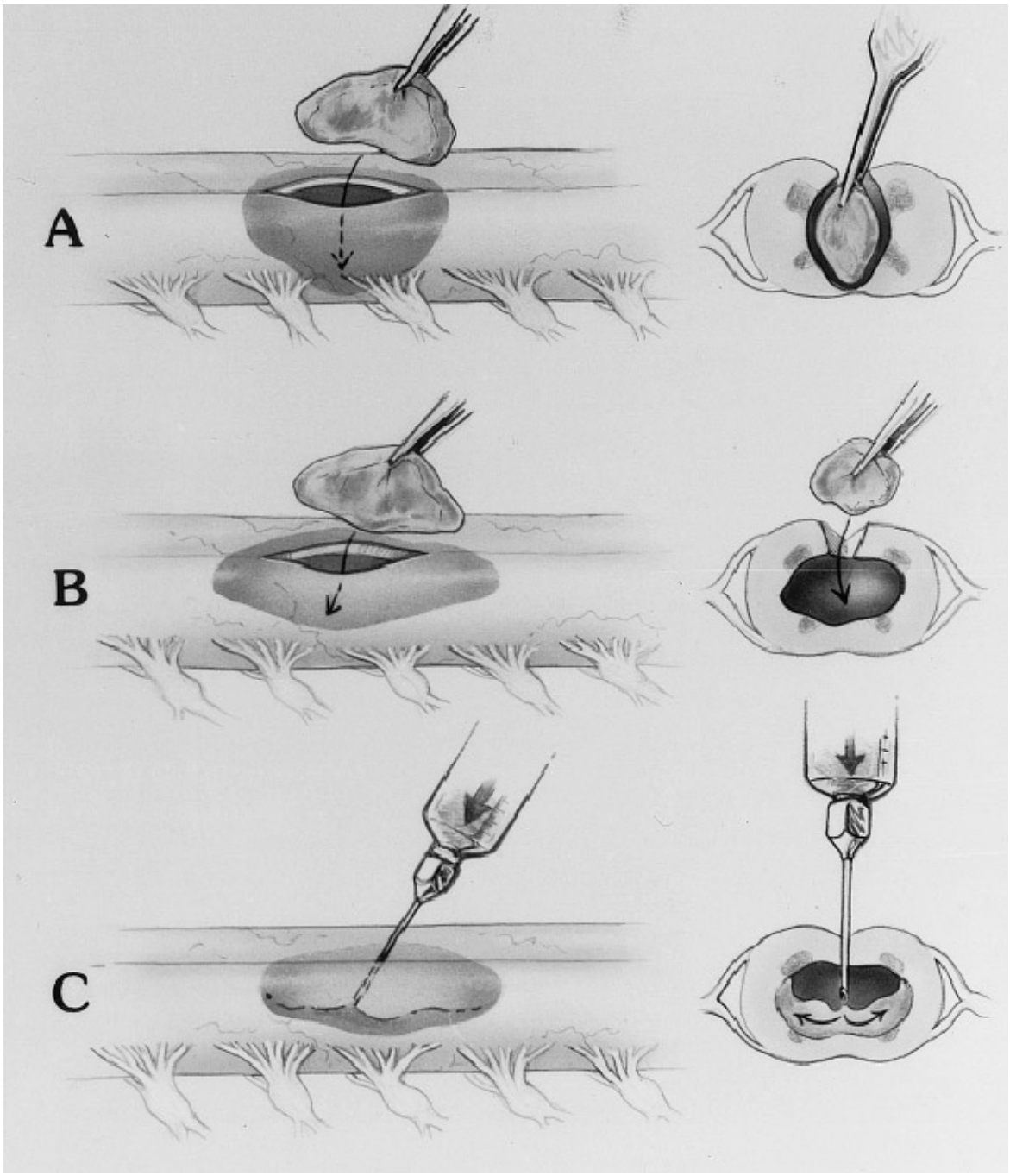

Figure 2-10. Methods of transplantation/implantation in the injured spinal cord. Scaffolds, pre-formed gels or whole pieces of tissue are inserted into A) resection or B) contusion lesions after making an incision in the spinal cord. C) Injectable gels or cellular suspensions may be injected into chronic contusions lesions directly through the dura. [Reprinted with permission from Elsevier: Giovanini, M. A., Reier, P. J., Eskin, T. A., Wirth, E., and Anderson, D. K., 1997. Characteristics of human fetal spinal cord grafts in the adult rat spinal cord: influences of lesion and grafting conditions. Exp. Neurol. 148, 523-543 (Page 524, Figure 1).]

CHAPTER 3
SYNTHESIS AND CHARACTERIZATION OF INJECTABLE CARBOXYMETHYLCELLULOSE-ALGINATE AND HYALURONIC ACID-ALGINATE GEL COMPOSITIONS

Introduction

Alginates are composed of β-D-mannuronic acid (M) and α-L-guluronic acid (G) residues (Figure 3-1) that are distributed in blocks of G, blocks of M and alternating GM sequences. The proportion and distribution of M, G and GM vary with the source from which alginate was obtained. These polymers are abundant in nature, non-toxic, biocompatible, bioresorbable and inexpensive, making them practical for a variety of food, pharmaceutical, cosmetic and biomedical applications. One of the key properties of alginate is the ability to form gels via ionic crosslinking with multivalent cations. Ca^{2+} ions for example conveniently fit in the cavity formed by blocks of G residues in adjacent polymer chains and form an "egg-box" structure (Grant et al., 1973) (Figure 3-2). Because the content and arrangement of G residues are responsible for gelling behavior of alginates, alginate source is a knob for varying properties (porosity, stiffness, swelling, and stability) of the final gel in addition to the selection and concentration of the crosslinking cation. For example, high G alginates form rigid, brittle gels compared to alginates with higher M content which form softer, deformable gels (ISP, 2000; Simpson et al., 2004).

Because of its mild ionic crosslinking conditions, alginate is considered an ideal matrix for encapsulating cells (Smidsrød and Skjåk-Bræk, 1990). For example, alginate gels have been extensively investigated for immobilization of a number of cell types, including chondrocytes for cartilage tissue engineering (Bonaventure et al., 1994; Marijnissen et al., 2000; Stevens et al., 2004; Xu et al., 2007) and pancreatic islet cells for treatment of type I diabetes (Soon-Shiong, 1999; Trivedi et al., 2001; Sambanis, 2003; Figliuzzi et al., 2006; Qi et al., 2008). Cells are typically entrapped by dripping alginate with dispersed cells into a solution of $CaCl_2$ or $CaSO_4$

(Smidsrød and Skjåk-Bræk, 1990; Tønnesen and Karlsen, 2002; d'Ayala et al., 2008). Crosslinking takes place from the outside in as the alginate solution contacts calcium ions which continue to diffuse into the gel bead over time. The resulting alginate beads are non-uniform as a result of depletion of alginate at the center of the gel (Skjåk-Bræk et al., 1989; Moe et al., 1995). Similarly, alginate gels have been prepared by diffusion of calcium ions into alginate solutions via the dialysis method, which also produces inhomogeneous gels (Skjåk-Bræk et al., 1989; Smidsrød and Skjåk-Bræk, 1990), which is not desirable for tissue engineering applications.

Draget et al. described an 'internal gelation' method for producing homogeneous alginate gels by employing a sparingly soluble calcium salt, $CaCO_3$, and glucono-δ-lactone (GDL) (Draget et al., 1989; Draget et al., 1990). GDL (Figure 3-3) is a non-toxic substance used in the food industry for curing, pickling, leavening, and pH control (FDA, 2002). GDL gradually hydrolyses to δ-gluconic acid (Pocker and Green, 1973), and Ca^{2+} ions are slowly liberated from $CaCO_3$ in an acid-base reaction with the formation of CO_2 gas and water (Equation 3-1). Subsequently, carboxyl groups (in G blocks) of two adjacent alginate chains are complexed by the Ca^{2+} ions (Equation 3-2) and a 3-D network is formed over time. Gels of neutral pH are obtained when equivalent amounts of $CaCO_3$ and GDL are used, i.e. when the molar ratio of GDL to $CaCO_3$ is equal to two (Draget et al., 1989). Crosslinking of alginate by $CaCO_3$-GDL is illustrated schematically in Figure 3-4.

$$CaCO_3 \xrightarrow{H^+} Ca^{2+} + HCO_3^- \xrightarrow{H^+} CO_2 \uparrow + H_2O \qquad (3\text{-}1)$$

$$Ca^{2+} + 2COO^- \rightarrow Ca(COO)_2 \text{ (complex)} \qquad (3\text{-}2)$$

Gradual crosslinking allows cells to be uniformly dispersed within the gel, making the internal gelation method an attractive approach to developing injectable, homogeneous alginate

gels suitable for spinal cord repair and other tissue engineering applications. These *in situ*-forming hydrogels are of interest as a novel matrix for spinal cord repair due to several key factors. First, these gels are comprised of natural polymers that are biocompatible, biodegradable/bioresorbable and can be modified via available functional groups to impart bioactivity. Second, an injectable matrix can be delivered directly into the cord through the dura minimizing the invasiveness of the procedure. Third, the gels can serve as a bridge for regenerating axons by filling and conforming to the irregular geometry of the cystic cavity in a contusion lesion. Finally, therapeutic cells and pro-regenerative substances can be easily incorporated simultaneously prior to gelation for a combined approach that targets multiple factors to create an environment favorable for repair and re-establishment of functional connections.

CMC (Figure 3-5) is an anionic, water-soluble derivative of cellulose whose properties are easy varied with the degree of carboxymethyl substitution (Hercules, 1999). CMC is used as a thickening agent in a number of food, cosmetic and pharmaceutical products and is also used for barriers for prevention of post-surgical adhesions (Peck et al., 1995; Guo et al., 1998; Zeng et al., 2007). CMC is considered to be a low cost alternative to HA (Ogushi et al., 2007); however it has not been significantly examined for CNS repair. This chapter focuses on the synthesis and characterization of ionically crosslinked ALG, ALG-CMC and ALG-HA gels. The primary goal was to synthesize injectable gel compositions via internal gelation of ALG combined with CMC or HA to modulate properties and to evaluate the suitability of these compositions as injectable cell-biopolymer matrices for neural tissue repair. This work is the first reported investigation of in situ-forming ALG, ALG-CMC and ALG-HA compositions for spinal cord repair. Aqueous ALG, CMC and HA solutions were prepared, mixed in varying ratios by volume and crosslinked

with Ca^{2+} ions released using the $CaCO_3$-GDL system. The effect of biopolymer composition, Ca^{2+} concentration and temperature on gelation time and mechanical properties was studied. Morphology of freeze-dried gels was also examined.

Materials and Methods

Polysaccharide Solution and Blend Preparation

Viscous (~1000 – 3000 cps) polysaccharide solutions were prepared with alginic acid sodium salt (high viscosity from *Macrocystis pyrifera*, MP Biomedical) and sodium carboxymethylcellulose (7HF PH, Hercules) using a procedure adapted from Mentak (Mentak, 1993). Ultrapure water (resistivity $\geq$ 17.4 MΩ), 600 mL, was vigorously stirred in a 1000 mL Pyrex® beaker at 1800 rpm using Caframo high speed mechanical mixers (Models BDC 6015 and BDC 1850) and 3-blade propellers. Powdered ALG (2.5% w/v) or CMC (1.5% w/v) was gently sifted into the vortex and stirred at 1800 rpm for the first 15 minutes. The propeller speed was reduced to 1000 rpm, and the solutions were covered with parafilm and allowed to mix for 12 hours. The moisture content of each powder was determined prior to solution preparation using a Mettler LJ16 moisture analyzer to determine the correct weight of each polymer needed to give the desired concentration.

ALG and CMC solutions were filtered into 250-mL Pyrex® bottles with screw caps using a stainless steel air pressure filtration funnel (Gelman Sciences) and 10 μm Spectra Mesh® nylon filters. The filtered solutions were allowed to remain at room temperature for 24 hours and were sterilized in a Tuttnauer 2540 EA autoclave on a programmed liquid cycle (20 minutes at 240°F). After sterilization ALG and CMC solutions were combined to give 75% ALG-25% CMC and 50% ALG-%-50% CMC compositions by volume. Appropriate volumes of each solution were

injected into in 100 mL Pyrex® bottles using 20 mL syringes and magnetically stirred for 1 hour to mix.

Hyaluronic acid solutions (0.5 % w/v) were prepared by adding HA powder (molecular weight 1.5 MDa, Genzyme) to ultrapure water and stirring magnetically for 12 hours. HA solutions were sterile-filtered through a 0.22 μm filter, and combined with ALG solutions to obtain 75% ALG-25% HA and 50% ALG-%-50% HA by volume. Final polysaccharide blend concentrations are shown in Table 3-1.

Crosslinked Gel Preparation

Crosslinked gels were prepared in 15 mL Nalgene containers. All mixture concentrations were based on a total volume of 10 mL. $CaCO_3$ was added to 1 mL of ultrapure water and sterilized by autoclaving. Sterile ALG, ALG-CMC or ALG-HA solutions, 8 mL, were added to the $CaCO_3$ suspension and magnetically stirred for 1 minute to mix. A freshly made solution of GDL (Sigma), 1 mL, was injected through a 1 cc syringe fitted with a 0.22 μm filter to initiate gelation, and the mixture was stirred for an additional 20 seconds. Low (6 mM) and high (8 mM) concentrations of Ca^{2+} were evaluated, and the concentration of GDL was adjusted for a $CaCO_3$ to GDL molar ratio of 1:1 to maintain neutral pH. The concentrations of ALG, CMC and HA in the final gels are given in Table 3-2.

Gelation Time

The rate of gel formation was determined by observing flow behavior of the gels as a function of time. A timer was started immediately after crosslinking was initiated by addition of GDL solution to polymer solution-$CaCO_3$ mixture. One mL of biopolymer blend solution was injected into 16 x 150 mm test tubes and allowed to gel. The tubes were tilted every 5 minutes to observe the change in flow of the polymer solutions. The time when the gel became too viscous

to flow was considered to be the gelation time. Sample flow was compared against a visual standard to minimize error since the same level of gelation was not achieved for all samples due to differences in composition. For gelation at physiological temperature, polymer solutions were equilibrated at 37 °C in a constant temperature bath for 2 hours prior to crosslinking. Samples were quickly returned to the bath after initiating gelation to maintain temperature.

Statistical Analysis

Average gelation times and standard error of the mean were calculated in Microsoft Excel. Statistical analysis was done using SigmaStat 3.1 software with assistance from Scott Cooper. A two-way ANOVA was conducted to determine the statistical influence of composition and Ca^{2+} concentration on gelation time at 37 °C. Tukey's test was used to determine which blends had a gelation rate different from that of pure ALG.

Rheological Characterization

The viscosity of each biopolymer solution and blend was measured with a Brookfield RVTDV-IICP cone-and-plate viscometer. Measurements were taken at room temperature as a function of different shear rates. Rheological evaluation of injectable gel compositions was carried out using a Paar-Physica UDS 200 rheometer with a cone-and-plate measuring system (MK226: diameter = 50 mm, angle = 1°). An amplitude sweep (γ = 0.01 to 100%, f = 1 Hz) was conducted at 37 °C to determine the region of near linear viscoelasticity (LVE) using the most viscous gel composition (ALG, high crosslink density). The ALG gel was injected onto the plate immediately after initiating crosslinking and was allowed to gel for 3 hours before initiating the test. Subsequently, time tests were performed on all biopolymer compositions at constant temperature (37 °C) using a frequency of 1 Hz and γ = 1% (below the LVE limit) to measure storage modulus (G') and loss modus (G") as a function of time. Each sample was freshly

prepared and injected onto the plate using a 10-mL syringe immediately after initiating crosslinking. To allow time to load the sample and lower the cone, each test was started exactly 5 minutes after GDL was mixed into the sample. G', and G" and were recorded every minute for a total of 2 hours.

Electron Microscopy

The morphology of freeze dried gels was examined by SEM with assistance from Paul Martin. One mL of biopolymer was injected into the wells of a 24-well cell culture plate immediately after initiating crosslinking and allowed to gel for 24 hours at 37 °C. The gels were then snap-frozen with liquid nitrogen and freeze-dried. Lyophilized gels were sectioned and mounted onto SEM stubs with conductive carbon adhesive tabs. A dusting of a gold/palladium alloy was applied to the samples (< 2 minutes) using a Technix Hummer V sputter coater. Images were aquired using the JEOL SEM-6400 scanning electron microscope with an accelerating voltage of 2 KeV, condenser lens setting of 8 to 10, and a 15 mm working distance.

Results and Discussion

Injectable ALG-CMC and ALG-HA Gel Compositions

In situ-forming gels based on ALG containing CMC or HA were prepared via internal gelation for the first time in this work. In this method, $CaCO_3$, a poorly soluble salt, was combined with GDL which slowly hydrolyzes to D-gluconic acid in aqueous solution. Slow release of calcium ions is triggered by the gradual decrease in pH associated with the hydrolysis of GDL. Neutral gels were obtained by maintaining a GDL to $CaCO_3$ molar ratio equal to 2. The gradual release of Ca^{2+} ions resulted in gradual crosslinking of ALG and produced uniform, transparent gels that visibly increased in stiffness over time (Figure 3-6). All compositions studied were injectable through a 22-gauge needle prior to crosslinking. The incorporation of

CMC or HA within the solution did not hinder the ability of ALG to gel in the presence of calcium ions.

Gelation rate was characterized by the time to solidify using the inverted tube method and was used a screening criteria to determine the appropriate range of compositions and crosslink densities (i.e. calcium ion concentrations) to consider for further study. In the screening studies ALG-CMC blends (25/75, 50/50, 75/25, 100/0 ALG/CMC by volume) were prepared from 2% ALG and 1.5% CMC (w/v) solutions. Three Ca^{2+} concentrations were initially examined: low (2 mM), medium (4 mM) and high (6 mM). Conditions under which observed gelation time exceeded 3 hours were excluded from further study. The ALG-CMC3 composition (25/75 ALG/CMC) did not produce gels when observed 24 hours after the addition GDL to initiate crosslinking but instead resulted in a non-uniform viscous fluid with gelatinous regions formed. It is believed that the concentration of ALG in the ALG-CMC3 composition (0.5% w/v) was below the critical gelling concentration and therefore a continuous gel did not form. This is consistent with observations by Straatmann et al. who prepared ALG gels (0.2 to 2 wt%) in a similar manner and reported gel formation when the ALG concentration was above 0.5 wt%. (2003). The results of our preliminary studies suggested that calcium ion concentration should be at least 6 mM and that ALG concentration should be above a minimum concentration of 0.5 % w/v in the final composition to obtain gels that solidified within 3 hours for the specific polymers used in this research.

Gelation Time

Gelation time was determined via the inverted tube method as a measure of gelation rate. This is important clinically as it is preferable that the gelling solution stiffen in a reasonable timeframe to maintain uniform distribution of incorporated cells, etc. dispersed within the gel once implanted. At the same time, gradual gelation affords injectability for an extended amount

of time after crosslinking has been initiated. Gelation time was generally observed to increase as the amount of ALG in the blend decreased for the compositions studied (Figure 3-7, 3-8). Also, gelation rate increased as the concentration of $CaCO_3$ increased. Two-way ANOVA indicated that the influence of biopolymer composition and Ca^{2+} concentration on gelation time at 37 °C were both statistically significant ($p<0.001$). Tukey's comparison test indicated that gelation rate of all blend compositions was significantly different ($p<0.05$) from ALG with the exception of ALG-HA1. This was true for both low (6 mM) and high (8 mM) Ca^{2+} concentrations.

Kuo and Ma prepared injectable ALG gels using the internal gelation method and demonstrated that the gelation rate, homogeneity and mechanical properties can be controlled by combining $CaCO_3$ with a more soluble calcium salt, specifically $CaSO_4$, and manipulating the ratio of the two salts (2001). Gelation rate increased as the proportion of $CaSO_4$ increased but the resulting gels were weaker and less homogeneous than those crosslinked with $CaCO_3$ alone. Osteoblasts were uniformly incorporated within the ALG gels *in vitro*, indicating the potential for the ALG-$CaCO_3$-GDL system to support cells. Kuo and Ma also observed more rapid gelation as the concentration of ALG decreased which was attributed to a decrease in viscosity. In our studies with ALG, ALG-CMC and ALG-HA gels, gelation rate decreased as ALG concentration decreased due to the decreasing proportion of ALG available for crosslinking relative to CMC or HA in solution. There did not appear to be a correlation between viscosity of the parent biopolymer solutions and gelation rate (Table 3-3).

Gelation rates for ALG and ALG-CMC were evaluated at both 25 °C and 37 °C and were observed to increase with increasing temperature for all compositions (Figure 3-8). This is also consistent with previously reported data (Kuo and Ma, 2001). The increased rate is due to acceleration of GDL hydrolysis with increasing temperature (Pocker and Green, 1973) which

results in a corresponding increased rate of Ca^{2+} release within the solutions. The compositional effect on gelation rate was more pronounced at lower temperature. Gelation rate is important clinically as it is preferable that the gelling solution stiffen in a reasonable timeframe to prevent leakage and ensure uniform distribution of incorporated cells, etc. dispersed within the gel. At the same time, gradual gelation affords injectability for an extended amount of time.

Rheology

Oscillatory testing in the linear viscoelastic region was conducted at 37 °C using a rheometer with a cone-and-plate attachment. The data revealed a gradual increase in storage (G') and loss moduli (G") of all compositions as a function of time (Figures 3-9 through 3-13). The storage modulus G' represents elastic behavior and is a measure of stiffness whereas the loss modulus G" represents the viscous behavior of the sample. As more alginate chains are complexed by calcium ions slowly liberated from $CaCO_3$, the resulting polymer network becomes more rigid.

A more rapid increase in G' was observed for compositions crosslinked with 8 mM $CaCO_3$ than with 6 mM $CaCO_3$ which is in agreement with the increase in gelation time observed with increasing calcium as discussed earlier. However, no relationship was observed between rheological behavior and gelation time measured by the inverted tube method. Instead the modulus G' remained fairly constant for all compositions in the region near the recorded gelation time. It was not expected that these data would correspond as the samples were subjected to different types and magnitudes of deformation in these tests. The modulus at test completion (120 minutes) was generally an order of magnitude greater for corresponding compositions at higher vs. lower calcium concentration. ALG gels were significantly stiffer for the initial 60 to 80 minutes of the oscillatory tests; however there was little difference between ALG and ALG-

CMC after 120 minutes. ALG-HA gels had the lowest modulus of all three compositions at both crosslink densities.

In oscillatory tests the intersection of G' and G", G'-G" crossover (green circles in Figures 3-9 through 3-11), is considered to be a measure of gel point (Tung and Dynes, 1982; Metzger, 2006). This point indicates the temperature or time (depending on the sample and test) at which there is a phase transition from viscous liquid behavior to elastic solid behavior at a critical extent of crosslinking reaction (Winter and Chambon, 1986). Beyond this point G' is greater than G" and the polymer behaves more like a viscous solid/gel than a fluid. The gel points for ALG, ALG-CMC and ALG-HA compositions ranged from 10 to 30 minutes (Table 3-4). The recorded values include five minutes added back to the observed G'-G" crossover times to compensate for the time delay during test startup. The gel points measured by rheometry were significantly lower than the gelation times observed by the inverted tube method. This is expected as the inverted tube method is not a measure of the actual onset of gelation but is rather an indication of the time at which the gel strength is sufficient enough that the gel no longer flows upon inversion. Strong gels have been reported to show permanent rupture and failure under large deformations whereas weak gels are able to flow without fracture and recover their solid, gel-like behavior (Ross-Murphy, 1995). This is consistent with observations from the inverted tube data, and it is believed that our compositions formed weak gels at the G'-G" crossover which were still deformable or pourable for an extended period of time beyond the gel point. Additional testing including replicates for each condition should be performed to get a more accurate representation of the rheological behavior of the ALG, ALG-CMC and ALG-HA compositions.

An adequate estimate of the stiffness of the spinal cord is needed to effectively design biomaterials for neural tissue engineering to avoid a mismatch in properties that can exert

physical stress on the cord. Also, it has been demonstrated *in vitro* that mechanical stiffness is inversely related to the rate of neurite extension within a gel (Balgude et al., 2001). Therefore implanted gels should be sufficiently compliant to permit axonal regneration. Mechanical properties are difficult to measure accurately due to the delicate nature of the tissue and significant stiffening of the cord even short times after death (Dalton et al., 2002). A number of mechanical tests have been employed to investigate the mechanical properties of the spinal cord under *in vitro* or *in vivo* conditions with great variability in the results. Despite the fact that tensile loading is not the primary mechanism of injury to the spinal cord, the majority of studies to estimate spinal cord modulus have been tensile tests with fewer studies devoted to compression testing or other techniques (Cheng et al., 2008).

The elastic modulus of the spinal cord including the pia mater has been estimated to be between ~200 and 600 kPa depending on the host species, method of measurement and elapsed time before measurement after death of the host (Dalton et al., 2002). The modulus of the feline spinal cord has been approximated at 230 kPa using an *in vivo* tensile test (Chang et al., 1988). In later studies by Ozawa et al., elastic moduli of both white and gray matter of rabbit spinal cord were estimated to be ~ 3 kPa using an in situ pipette aspiration technique developed for the assessment of soft biological tissue, and the pia was estimated to have a modulus of ~2000 kPa (2001; 2004). The compressive modulus of the spinal cord has been estimated at 5 kPa using an *in vivo* technique (Hung et al., 1982). These results demonstrate the diversity in published data on the properties of the cord. To date, oscillatory testing as performed in the present research has been reported for brain tissue but not for the spinal cord, and therefore we are unable to directly compare our results to published data (Cheng et al., 2008). It is recommended that compressive

modulus of the compositions studied here be measured under simulated physiological conditions in future studies to optimize the gel properties for use in the spinal cord.

Morphology

Pore structure is an important design consideration for materials used in tissue engineering applications. The implanted scaffold or gel must have high fractional porosity and sufficiently large pores for optimal cell attachment and growth and to allow infiltration of host constituents to promote ingrowth of regenerating tissue (Woerly et al., 1999). Scanning electron micrographs were taken of samples that were allowed to gel overnight in multi-well cell culture plates that were subsequently snap-frozen in liquid nitrogen and lyophilized. To get an accurate representation of the structure of a gel the morphology should be examined in a hydrated state under representative physiological conditions; however standard SEM was utilized to qualitatively examine pore size and morphology of the ALG, ALG-CMC and ALG-HA compositions. SEM of a representative ALG sample is shown in Figure 3-14. The freeze-dried compositions were observed to have a porous structure with fairly homogeneous pore sizes uniformly distributed throughout. The pore structure appeared to vary with gel composition but could not be confirmed due to distortion of some of the samples during sectioning. Further evaluation using a more appropriate technique for hydrated gels is recommended to elucidate the morphology and obtain quantifiable results.

Summary

Novel in situ-forming ALG-CMC and ALG-HA gels were prepared for the first time via gradual ionic crosslinking of ALG. Calcium ions were slowly released using the $CaCO_3$-GDL internal gelation technique. Gelation time was measured using the inverted tube method and ranged from ~1 to 2 hours at 37 °C for all compositions. The presence of CMC or HA in solution did not prevent crosslinking but did decrease gelation rate compared to pure ALG gels.

Increasing the calcium ion concentration resulted in an increased rate of gelation. Mechanical properties of the gels were evaluated using a cone-and-plate rheometer. The storage modulus G' of the biopolymer gels gradually increased with time and was on the order of 10^4 and 10^5 Pa for low and high crosslink densities, respectively, after two hours. The compositions were concluded to form weak gels at the gel point which ranged from 10 to 30 minutes as determined by the crossover of G' and G". SEMs of snap-frozen, freeze-dried gels revealed a fairly uniform pore structure but further study is required using an appropriate method to examine morphology in the hydrated state.

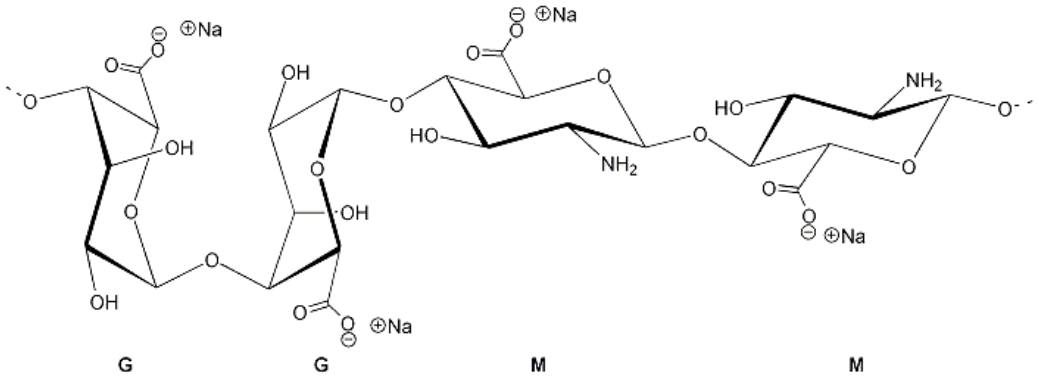

Figure 3-1. Structure of alginate showing guluronic acid (G) and mannuronic acid (M) residues. Consecutive G residues form a V-shaped cavity.

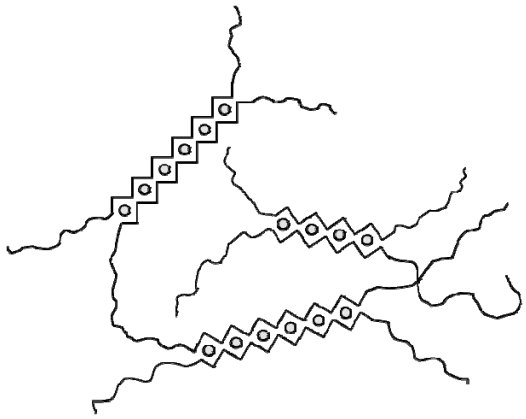

Figure 3-2. Egg-box model of ionic crosslinking of alginate. Divalent cations (circles) sit in V-shaped cavities formed by G blocks of adjacent chains.

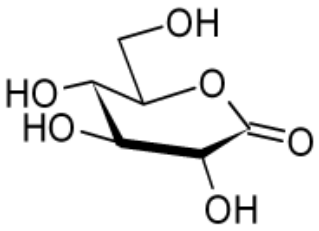

Figure 3-3. Chemical structure of glucono-δ-lactone (GDL).

Table 3-1. Concentration of polysaccharides in biopolymer solutions

Blend Designation	[ALG] wt%	[CMC] wt%	[HA] wt%
ALG	2.5%	-	-
ALG-CMC1	1.9%	0.4	-
ALG-CMC2	1.3%	0.8	-
ALG-HA1	1.9%	-	0.1
ALG-HA2	1.3%	-	0.3

Table 3-2. Concentration of polysaccharides in biopolymer gels

Gel Designation	[ALG] wt%	[CMC] wt%	[HA] wt%
ALG	2.0%	-	-
ALG-CMC1	1.5%	0.3	-
ALG-CMC2	1.0%	0.6	-
ALG-HA1	1.5%	-	0.1
ALG-HA2	1.0%	-	0.2

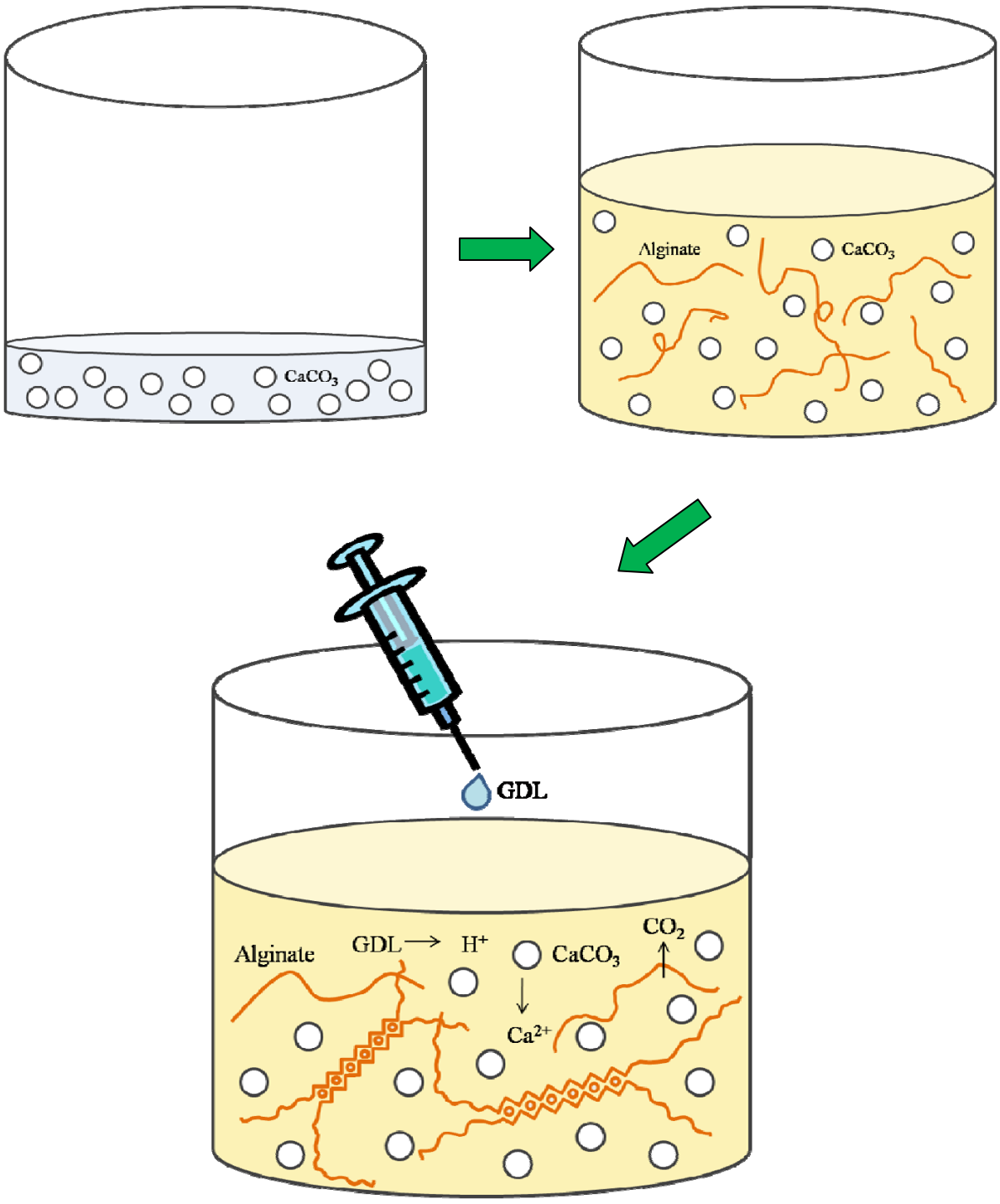

Figure 3-4. Schematic of alginate crosslinking procedure with GDL and $CaCO_3$.

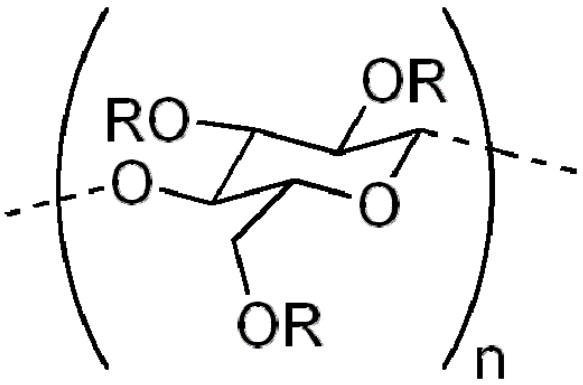

$$R = H \text{ or } CH_2CO_2H$$

Figure 3-5. Chemical structure of carboxymethylcellulose (CMC).

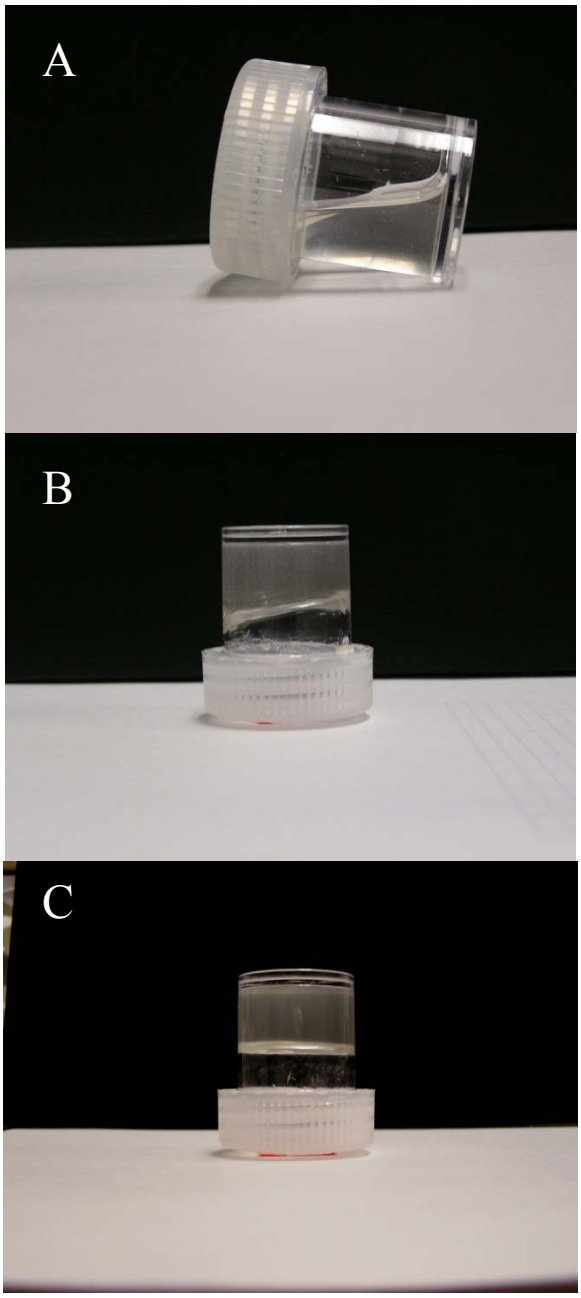

Figure 3-6. Photograph of ALG crosslinking progression by the internal gelation method. A) Initially the ALG solution is a viscous liquid. B) and C) The gel stiffens with time as calcium ions are released and complex with $-COO^-$ groups in G residues.

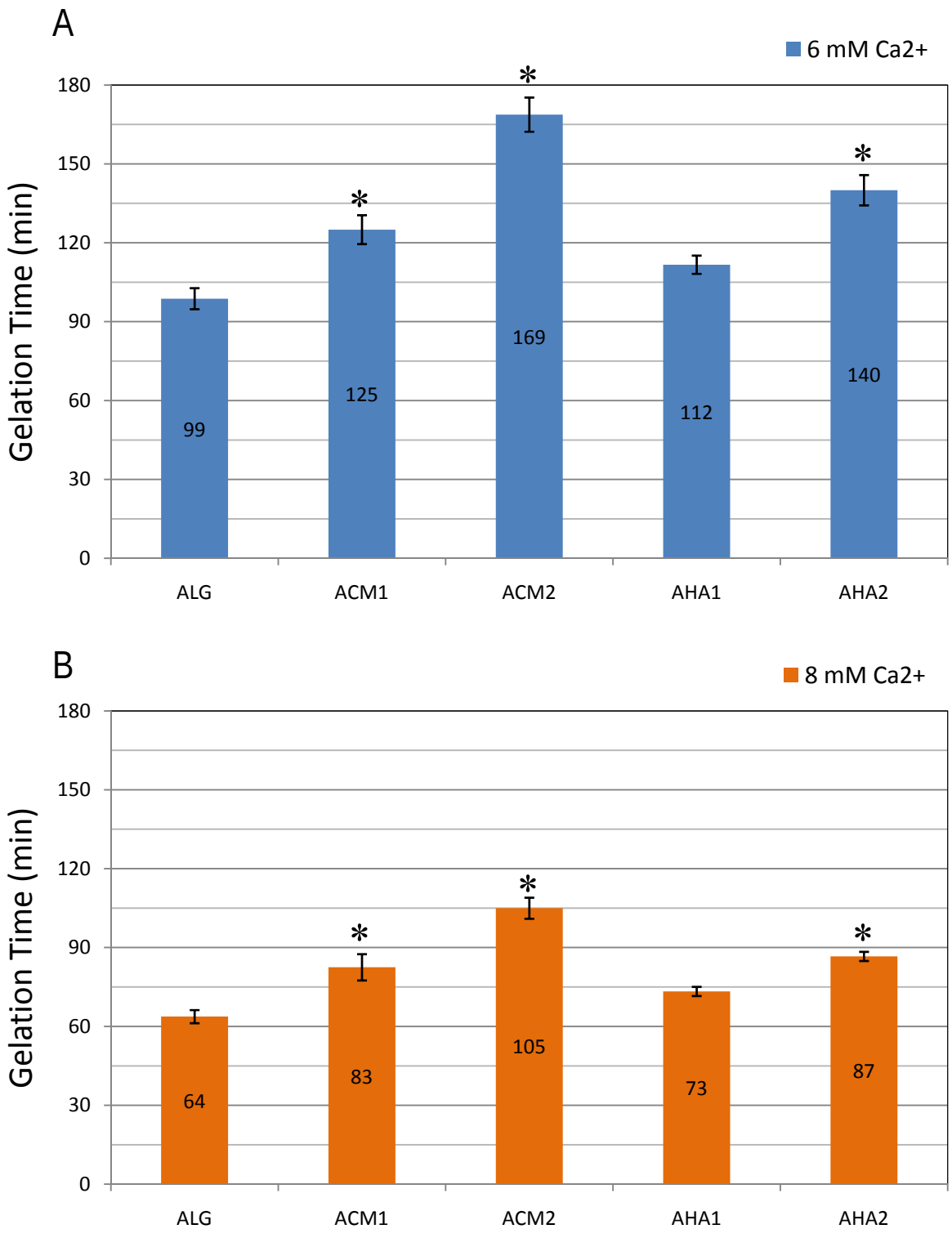

Figure 3-7. Gelation time at 37 °C as a function of biopolymer composition. A) low Ca^{2+} (6 mM) B) high Ca^{2+} (8 mM). Compositions with gelation time significantly different ($p<0.05$) from ALG are indicated by an asterisk.

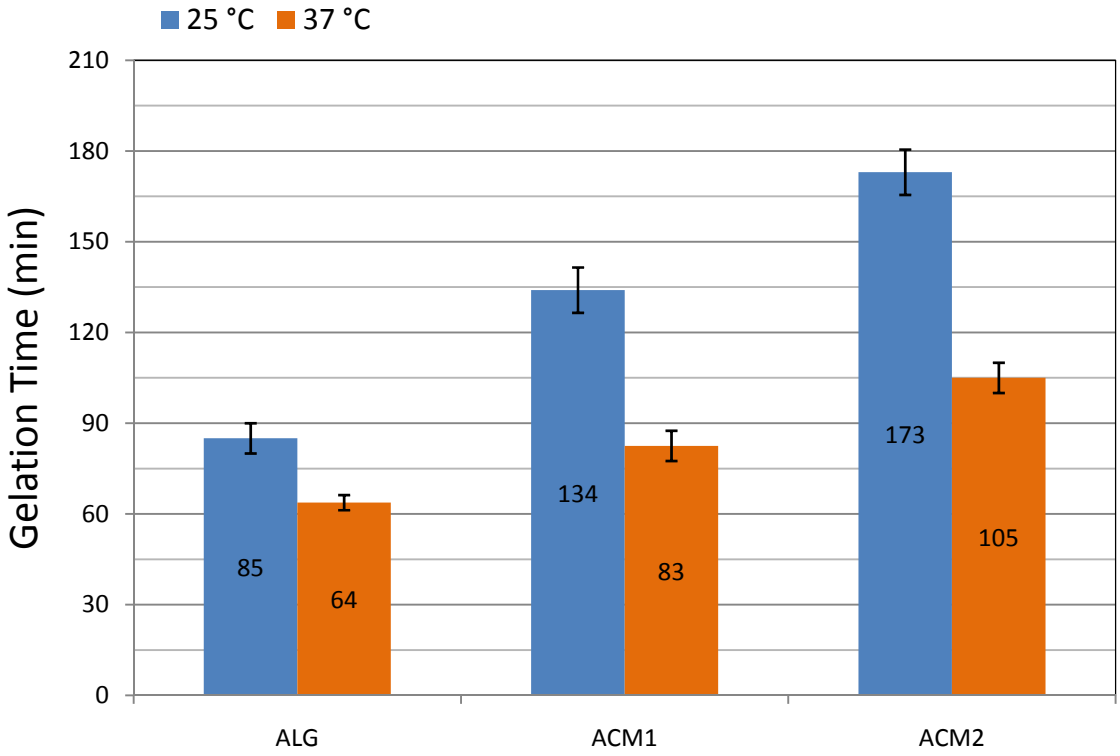

Figure 3-8. Effect of temperature on gelation time of ALG-CMC compositions at high crosslink density (8 mM Ca^{2+}).

Table 3-3. Viscosity and gelation times of ALG-CMC compositions at 25 °C

Solution	Viscosity at 25 °C (cps)	Gelation Time at 25 °C (min)
ALG	2860	85
ALG-CMC1	987	134
ALG-CMC2	1263	173

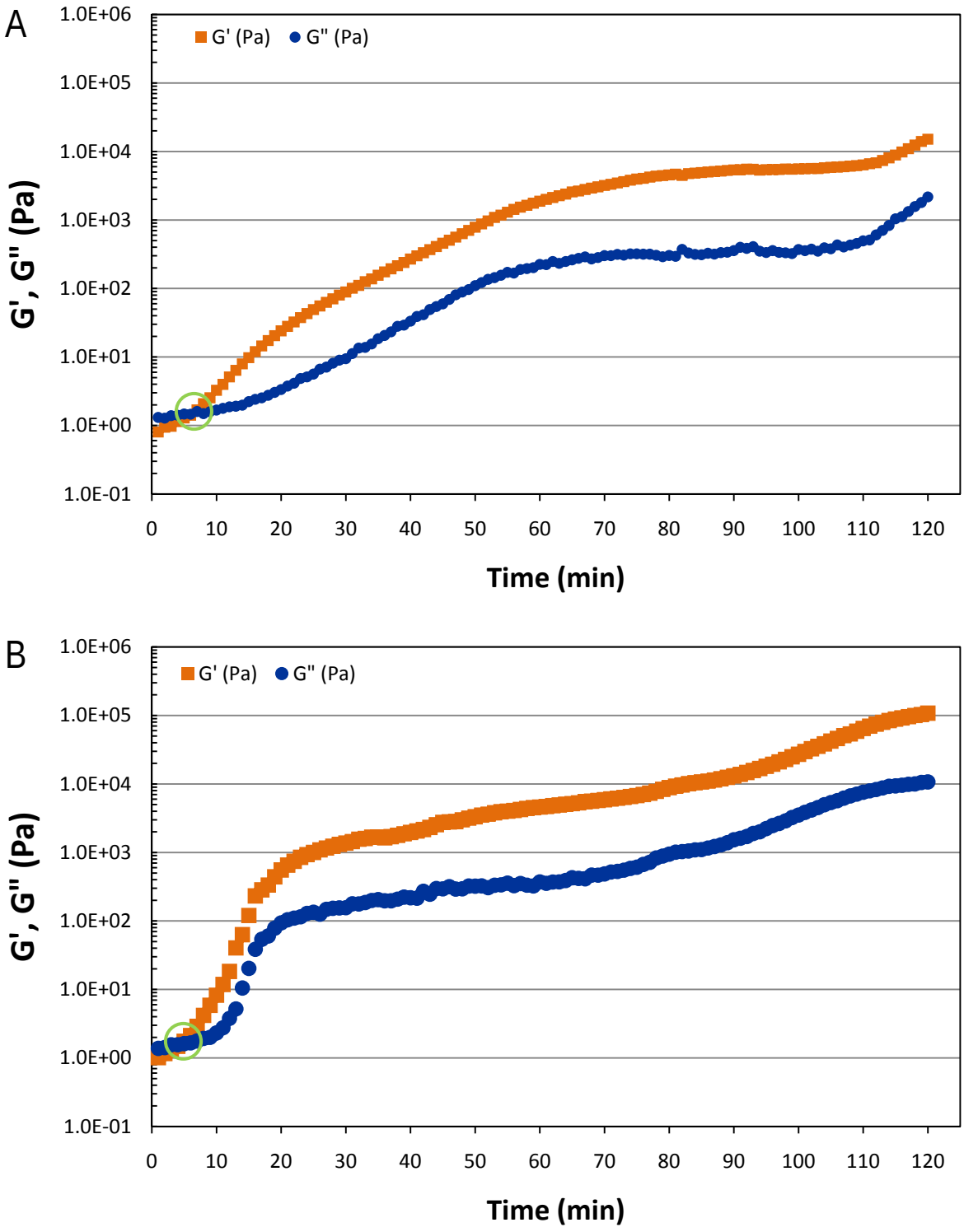

Figure 3-9. Modulus (G', G") of ALG gel as a function of time at 37 °C. A) Low Ca^{2+} (6 mM). B) High Ca^{2+} (8 mM).

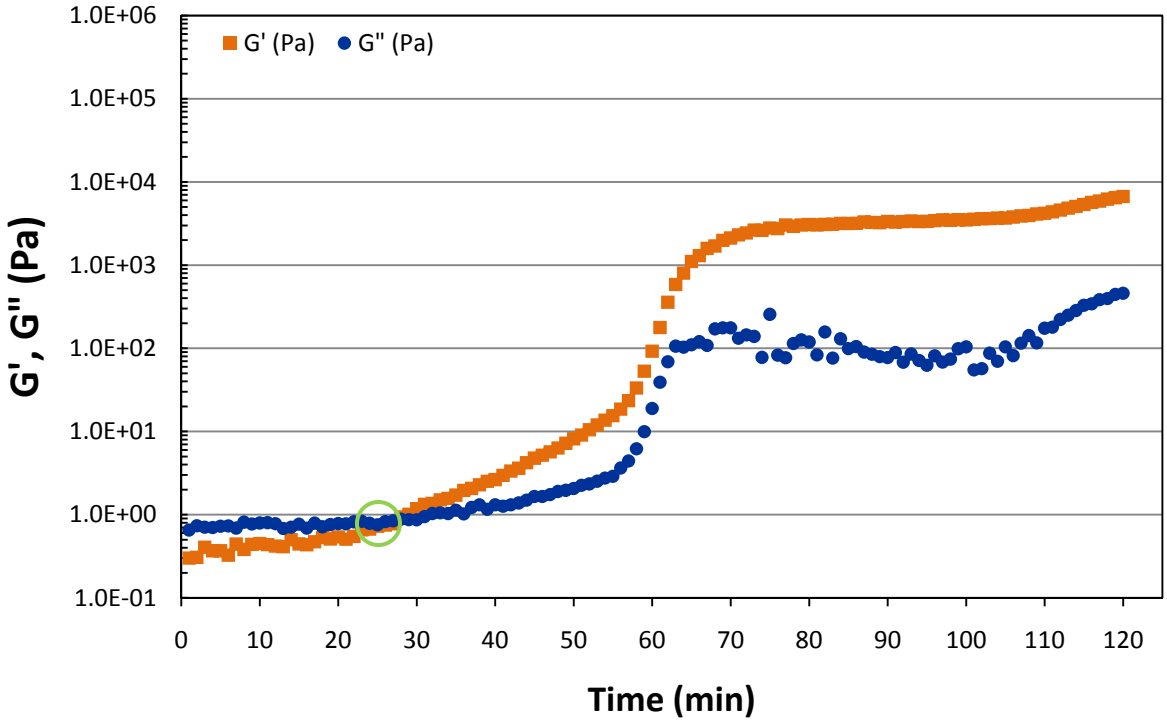

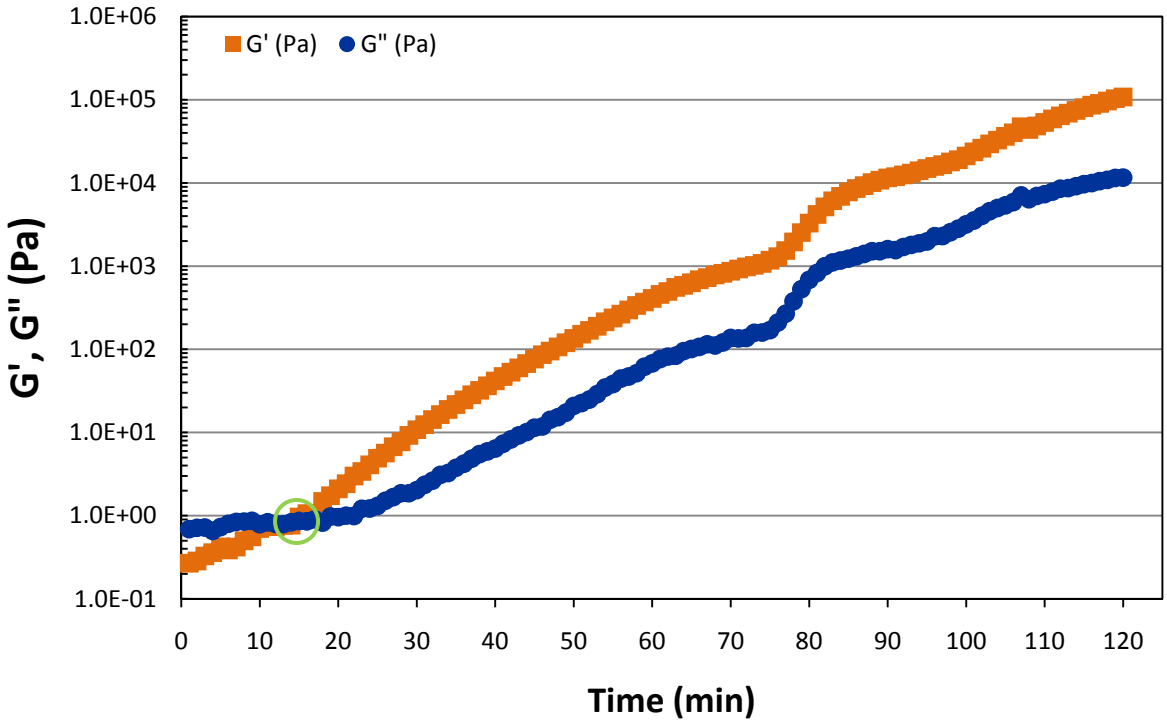

Figure 3-10. Modulus (G', G") of ALG-CMC gel as a function of time at 37 °C. A) Low Ca^{2+} (6 mM) B) High Ca^{2+} (8 mM)

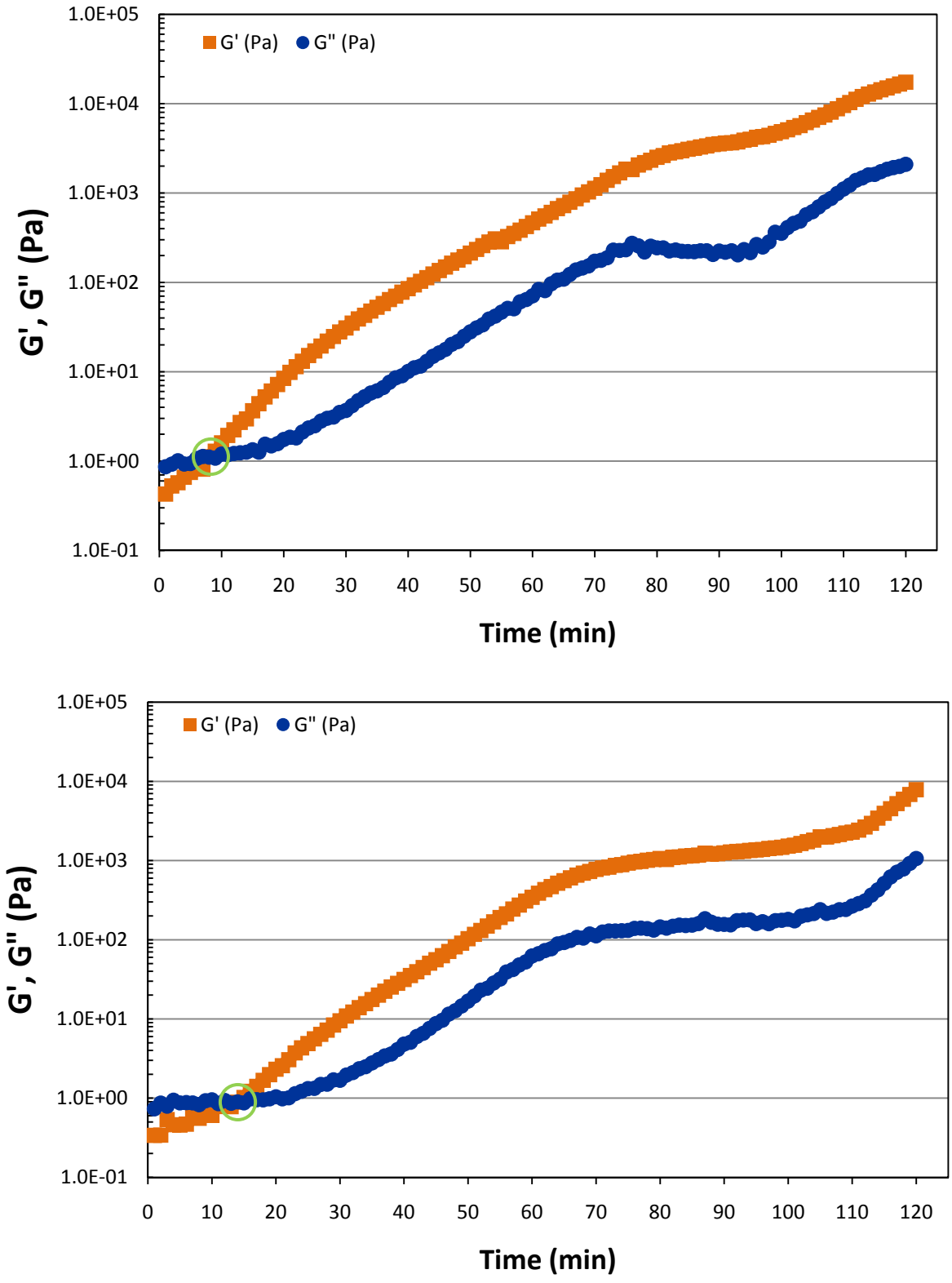

Figure 3-11. Modulus (G', G") of ALG-HA gel as a function of time at 37 °C. A) Low Ca^{2+} (6 mM). B) High Ca^{2+} (8 mM).

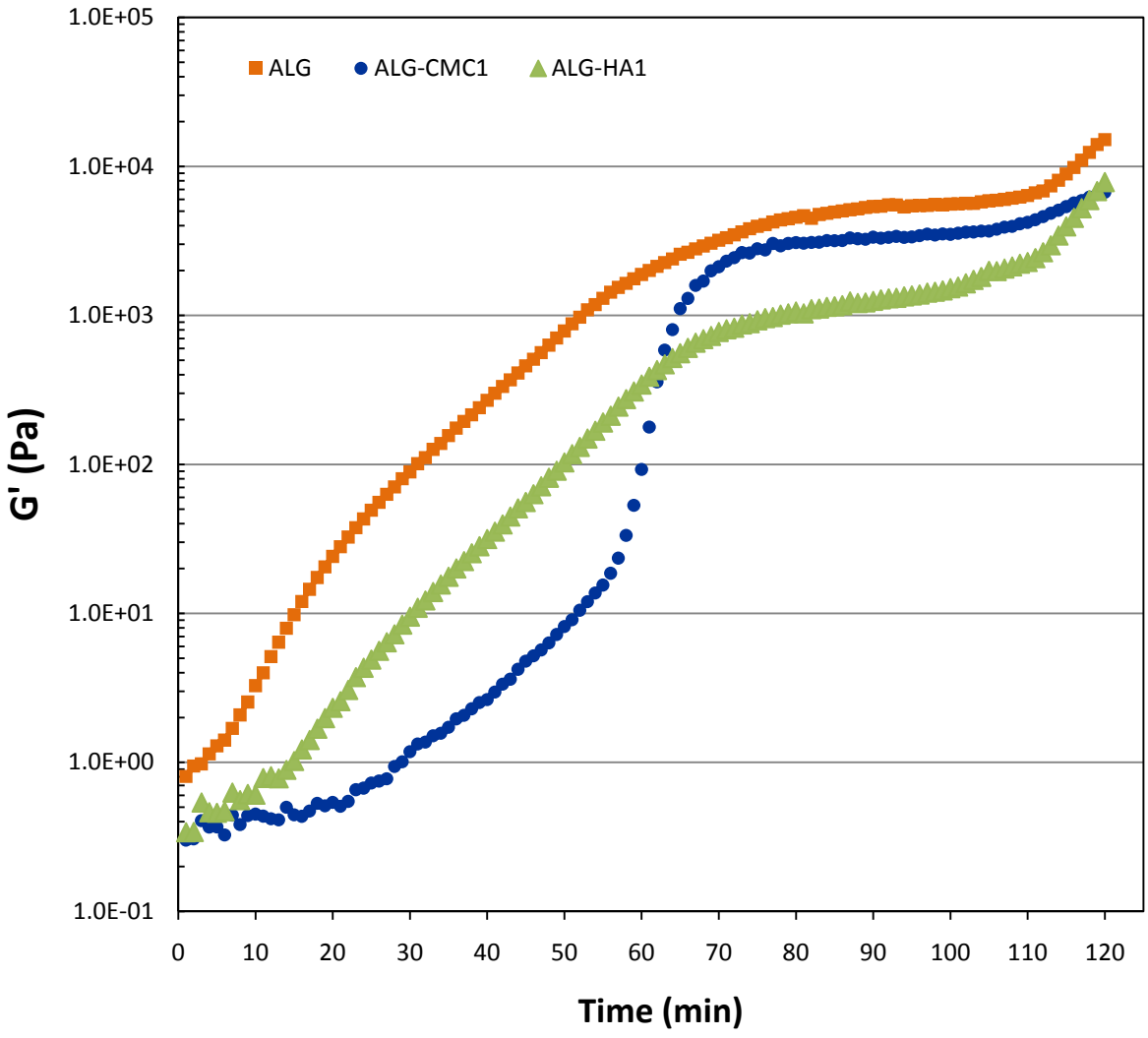

Figure 3-12. Storage modulus (G') of biopolymer compositions as a function of time at low crosslink density (6 mM Ca^{2+}) at 37 °C.

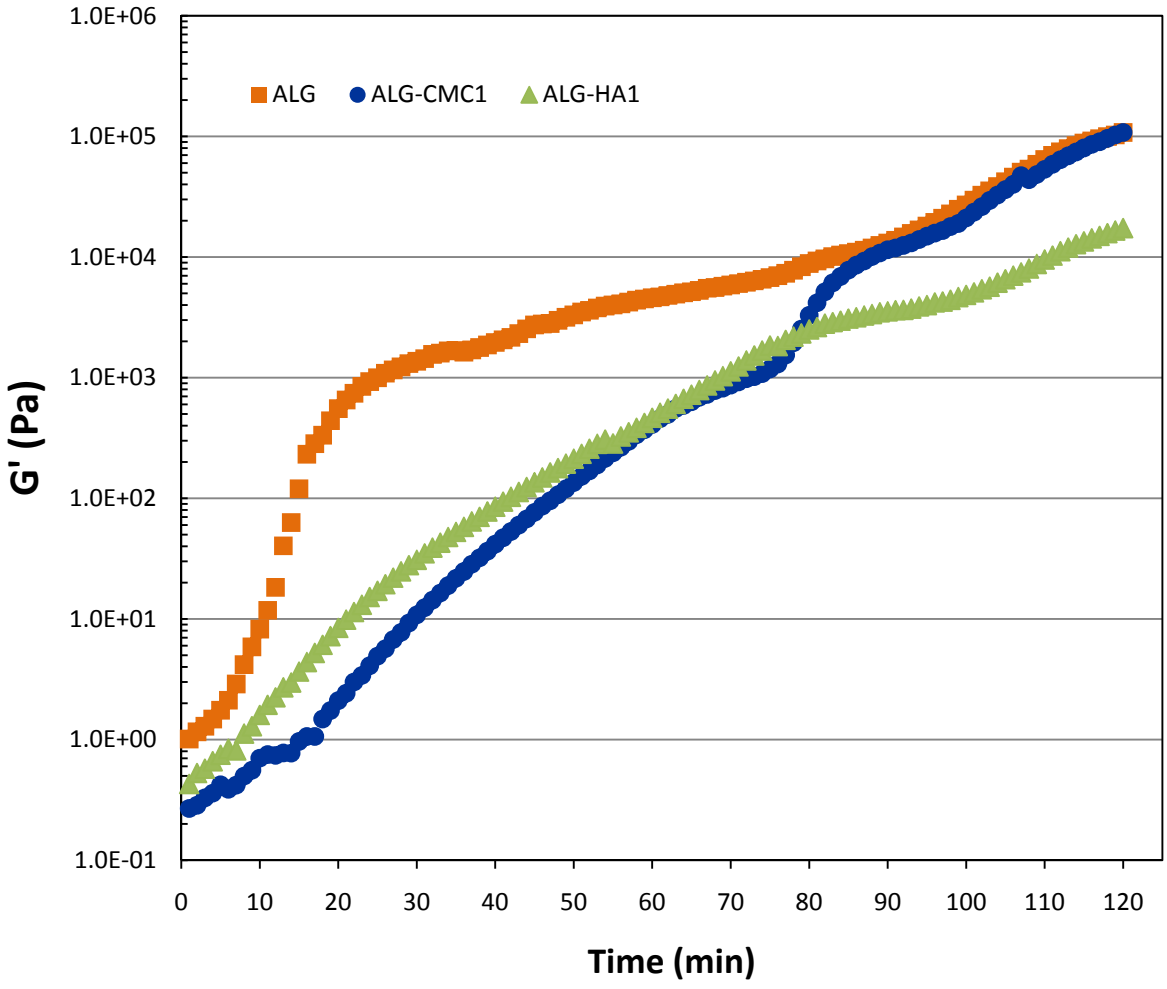

Figure 3-13. Storage modulus (G') of biopolymer compositions as a function of time at high crosslink density (8 mM Ca^{2+}) at 37 °C.

Table 3-4. Gel point (G'-G" crossover) and gelation time (inverted tube) for biopolymer compositions at 37 °C.

Solution	Ca^{2+} concentration (mM)	Gel point (min)	Gelation time (min)
ALG	6	11	99
ALG-CMC1	6	30	125
ALG-HA1	6	19	112
ALG	8	10	64
ALG-CMC1	8	20	83
ALG-HA1	8	13	73

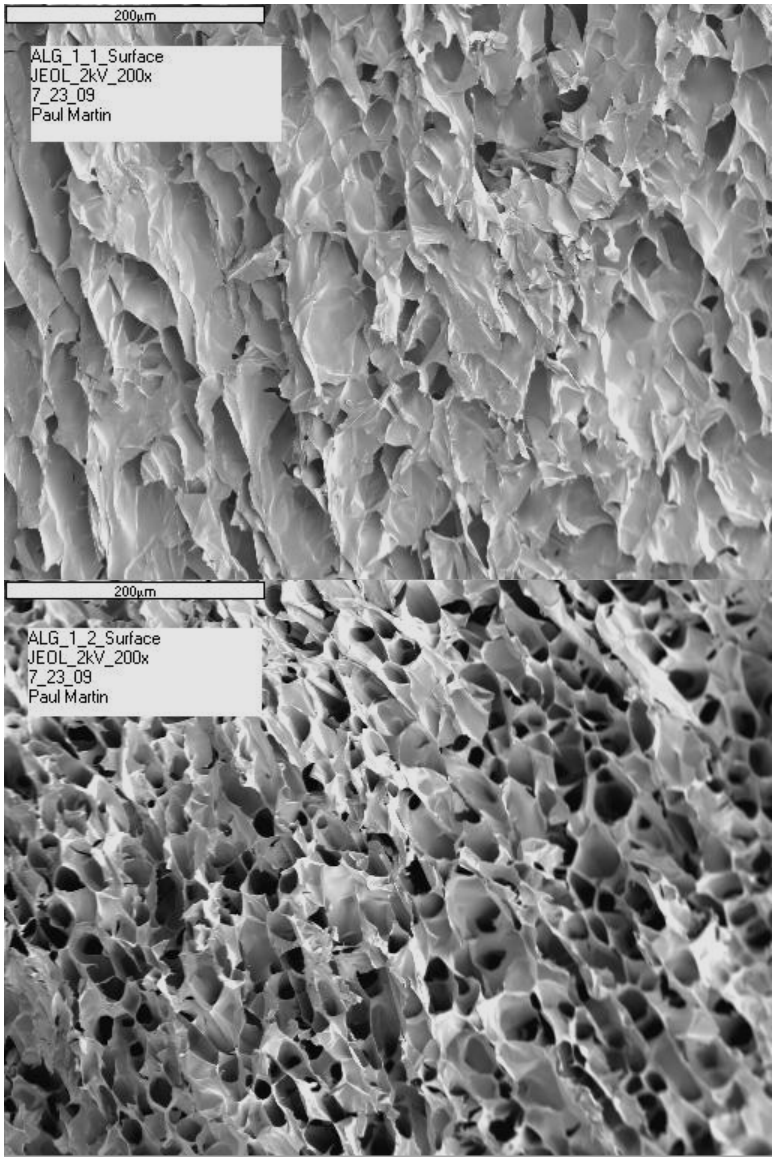

Figure 3-14. SEM micrographs of snap-frozen, freeze-dried ALG gel compositions. A) low (6 mM) Ca^{2+}. B) high (8 mM) Ca^{2+}.

CHAPTER 4
IN VITRO EVALUATION OF INJECTABLE GEL COMPOSITIONS AS A TRANSPLANTATION MATRIX FOR NEURAL TISSUE REPAIR

Introduction

When designing materials for biomedical applications, evaluating behavior and properties under physiological conditions is critical to ensure that the implant is non-toxic, will not elicit an adverse response in the body, and is adequate or effective for the intended application. It is not always feasible to conduct *in vivo* experiments, especially for screening or feasibility studies, therefore *in vitro* testing is an alternative for evaluating materials. It is important to match the experimental conditions to the actual *in vivo* environment as closely as possible to ensure reliability of the results.

This chapter focuses on in vitro evaluation of injectable alginate-based gel compositions as matrices for neural tissue repair. The primary objective was to characterize the properties of the gels under simulated physiological conditions to determine their suitability for use as an injectable matrix for repairing the injured spinal cord. Swelling and dissolution of gels were evaluated in artificial cerebrospinal fluid (aCSF) at 37 °C. The viability of Schwann cells dispersed in the gels was evaluated using an alamarBlue assay.

Materials and Methods

In Vitro Swelling and Dissolution

Swelling and dissolution of gels were evaluated in vitro in aCSF, ph 7.4 (Table 4-1) to mimic the physiological environment of the spinal cord. The weights of 144 empty micro-centrifuge tubes (1.5 mL) were measured and 0.5 mL of freshly prepared biopolymer composition was injected into each centrifuge tube (n = 3) immediately after crosslinking was initiated. The compositions were incubated overnight at 37 °C to ensure that gelation was complete, and the centrifuge tube weights with gel were determined. Initial wet gel weight, W_{wet}

(0), was determined by subtracting the weight of the tubes from the weight of tubes plus gel. A set of tubes were then frozen and lyophilized and used to determine the dry control gel weight, $W_{dry}(0)$. To the remaining tubes 0.5 mL of aCSF was added which was pre-equilibrated to 37 °C, and the tubes were placed in a biological cabinet. The fluid was changed daily, and the swollen gel weights, $W_{wet}(t)$, were determined by subtraction after 1, 4, 7, 14 and 28 days of incubation. The corresponding dry gel weights, $W_{dry}(t)$ were determined at the same timepoints on lyophilized gels. The degree of swelling and dissolution were determined as a function of time according to (4-1) and (4-2).

$$\% \text{ Swelling} = \frac{W_{wet}(t) - W_{wet}(0)}{W_{wet}(0)} \times 100 \qquad (4\text{-}1)$$

$$\% \text{ Dissolved} = \frac{W_{dry}(0) - W_{dry}(t)}{W_{dry}(0)} \times 100 \qquad (4\text{-}2)$$

Primary Schwann Cell Culture

Schwann cells were isolated from neonatal rats. P4 rat pups were sacrificed according to IACUC approved methods, and the sciatic nerves were dissected and dissociated according to established protocols (Notterpek et al., 1999). Nerves were dissected, stripped of connective tissue and epineurium, minced and digested at 37 °C in a humidified atmosphere of 5% CO_2 . The digestion medium consisted of Dulbecco's Modified Eagle's Medium (DMEM) (Gibco, Grand Island, NY), 15% fetal calf serum (FCS) (Hyclone, Logan, UT), penicillin streptomycin (Gibco) and an enzyme cocktail of 0.03% collagenase type III (Worthington, Lakewood, NJ), 0.1% hyaluronidase (Sigma), 1.25 units/mL dispase (Worthington). Cell suspensions were washed once and resuspended in culture medium (DMEM containing 10% FCS). Cells were then plated on poly-L-lysine (Sigma) coated plastic Petri-dishes in growth medium [DMEM with 10% FCS + 50 μL/5mL bovine pituitary extract (glial growth factor) (Biomedical Technologies, Inc.,

Stroughton, MA) + 1 μL/5mL forskolin (Calbiochem, La Jolla, CA)]. The medium was changed every other day. Cells were allowed to attach overnight and proliferate for 7 or 8 days.

Schwann cells were harvested by trypsinization. Culture medium was aspirated and plates were rinsed twice with DMEM. Trypsin/ethylenediaminetetraacetic acid (EDTA) was added to detach cells, and plates were incubated at 37 °C for 2 minutes. Proteolysis was stopped by adding 8 mL DMEM/10% fetal calf serum (FCS). Cell suspensions were transferred to 15 mL conical tubes and centrifuged for 5 minutes at 1200 rpm. Medium was aspirated, and the cell pellet was re-suspended in a known volume of Schwann cell growth medium. Cells were counted with a hemocytometer and adjusted to the desired final concentration.

Cell Viability

Sterile ALG, ALC-CMC and ALG-HA blends were prepared and combined with $CaCO_3$ and GDL to initiate gelation. Immediately after adding GDL, 400 μL of each biopolymer mixture was injected into the wells of a 24-well culture plate and allowed to gel overnight in a biological hood. Primary Schwann cells (pass 6) were harvested and re-suspended in growth medium at a concentration of 1×10^6cells in 25 mL. 400 μL of cell suspension was added on top of gels and onto poly-L-lysine-coated plates (controls) at a density of 2×10^4 cells/well (n = 6 per condition).

Viability of Schwann cells seeded on select biopolymer gels was determined using an alamarBlue assay (AbD Serotec, Oxford, UK) which incorporates a nontoxic oxidation-reduction (REDOX) indicator that changes color in response to reduction by metabolically active cells. The assay protocol was adapted from Novikova et al. (2006). 0Twenty four hours after cell seeding, medium from control wells was replaced with 300 μL of fresh growth medium containing 5% alamarBlue. Assay medium was added on top of gel compositions as the old medium was

absorbed by the gels and could not be removed. The plates were returned to the incubator for 4 hours, and 100 μL of the assay-containing medium was removed and transferred to a 96-well culture plate. Absorbance was measured at 570 nm and 600 nm using a Molecular Devices SpectraMax M5 muliplate reader, and viability was determined as percentage reduction of alamarBlue according to the supplier's protocol. Viability was assayed at 24 and 48 hours after seeding.

Cell Entrapment Feasibility Study

An experiment was conducted to determine the effects of culture medium on the gelling behavior of ALG gel. Four mL of sterile ALG solution and 4 mL of DMEM were added to $CaCO_3$ (1 mL) in a 15 mL Nalgene container and magnetically stirred for 1 minute. One mL of a fresh GDL solution was added to initiate crosslinking, and gelling behavior was visually observed by inverting tubes periodically.

To assess the feasibility of entrapping cells within gel compositions, an ALG composition was combined with a Schwann cell suspension and crosslinked under aseptic conditions. Four mL of sterile ALG solution and 4 mL of Schwann cells suspended in growth media were added to $CaCO_3$ (1 mL) and magnetically stirred for 1 minute. One mL of a fresh GDL solution was injected through a syringe fitted with a 0.22 μm filter to initiate crosslinking, and the Schwann cell-biopolymer mixture was stirred for 20 seconds. Four hundred μL of cell-gel mixture was injected into the wells of a 24 well culture plate and allowed to gel for 30 minutes in a biological cabinet at 37 °C. Fresh media was then added, and Schwann cells were examined the next day using an inverted microscope.

Results and Discussion

Swelling and Dissolution

Swelling and dissolution were examined at 37 °C for biopolymer gels that were covered with aCSF 24 hours after crosslinking was initiated. The fluid was changed at the same time daily, and samples were weighed after 1, 4, 7, 14 and 28 days. Swelling was apparent for many compositions as the gels expanded noticeably beyond their initial volume during the course of the experiment. The degree of swelling gradually increased over time (Figure 4-1) and was greatest for gels crosslinked with low (6 mM) $CaCO_3$. This behavior is consistent with what is expected for crosslinked polymers as the chains have greater flexibility when the crosslink density is low. As the degree of crosslinking increases, the gel becomes more rigid and the polymer network is less able to expand. This was also demonstrated by the rheological data presented in Chapter 3. After 28 days, swelling was greatest for ALG gels and decreased with decreasing ALG content. ALG-HA gels showed the lowest degree of swelling, and the ALG-HA2 gel showed a minimal degree of swelling. HA is known to have poor mechanical properties and may have contributed to this behavior. The mass of the gels was found to be stable during the course of the study and did not undergo significant dissolution.

For application in SCI repair, a minor degree of swelling is desirable as significant expansion of an implanted gel or scaffold can apply pressure to the cord that could potentially cause damage. Therefore the swelling behavior of the gel is an important factor to be considered in optimizing composition.

Cell Viability

Schwann cell viability was assayed using alamarBlue® (AB) at 24 and 48 hours after seeding onto biopolymer compositions. The AB assay is based on conversion of a non-fluorescent indicator dye, resazurin (blue), which is converted to a fluorescent dye, resorufin

(red), when reduced by metabolically active cells. The assay is non-toxic and therefore can be used to continuously monitor cell viability over time (Ahmed et al., 1994). Schwann cell viability was determined as % reduction of AB according to:

$$\% \text{ reduction of alamarBlue®} = \frac{(O2 \times A1) - (O1 \times A2)}{(R1 \times N2) - (R2 \times N1)} \times 100 \quad (4.1)$$

where O1 = molar extinction coefficient of oxidized AB at 570 nm (80586), O2 = molar extinction coefficient of oxidized AB at 600 nm (117216), A1 = absorbance of test wells at 570 nm, A2 = absorbance of test wells at 600 nm, R1 = molar extinction coefficient of reduced AB at 570 nm (155677), R2 = molar extinction coefficient of reduced AB at 600 nm (14652), N1 = absorbance of negative control well at 570 nm, and N2 = absorbance of negative control well at 600 nm. The coefficients O1, O2, R1 and R2 were obtained from the assay product literature.

The absorbances measured for the blank wells used as references in determining cell viability indicate that these well may have been contaminated with cells during the plating procedure. As a result, the calculated reduction of AB did not range from 0 to 100% as expected, and therefore Schwann cell viability could not be quantitatively determined. However, it could be determined from the data (Figure 4-2) that Schwann cells survived on all compositions and increased in number after 48 hours in culture. Viability appeared to be the same for all biopolymer compositions but definite conclusions cannot be drawn without repeating the experiment. The assay procedure should be further improved to take into account absorption of medium into the gels which can also skew the results.

Cell Entrapment Feasibility Study

The effect of cell culture medium on the gelling behavior of the ALG-$CaCO_3$-GDL system was investigated by mixing an ALG solution with DMEM prior to crosslinking. Crosslinking of ALG was observed to progress in a similar manner to previous experiments without culture

medium. The ALG composition did not flow after approximately one hour as reported for ALG gels prepared in water (Chapter 3). The DMEM formulation used (Gibco 11995) contains 1.8 mM $CaCl_2$, which is an additional source of calcium ions for crosslinking ALG. This Ca^{2+} concentration should be taken into account when formulating and optimizing the composition in future experiments.

ALG gels with dispersed Schwann cells had solidified when examined after 24 hours of incubation. A number of live Schwann cells were apparent by microscopy as well as a smaller number of dead cells which were clustered together (Figure 4-3). Previous *in vitro* studies have reported on the survival of Schwann cells incorporated within alginate gels prepared in DMEM containing 0.1 M $CaCl_2$ (Mosahebi et al., 2001; Novikova et al., 2006). Our results are consistent with these findings and indicate that ALG-based solutions can be mixed with cells suspended in culture medium prior to adding $CaCO_3$ and GDL to initiate crosslinking and that these compositions have the potential to support Schwann cells or other cells for transplantation in the injured CNS. Viability, proliferation and morphology of encapsulated cells should be examined in depth in future studies.

Summary

Swelling and stability of ALG, ALG-CMC, and ALG-HA gels were evaluated *in vitro* as a function of composition and calcium ion concentration. Compositions were allowed to gel in microcentrifuge tubes, covered with aCSF, and incubated at 37 °C for 28 days. The swollen and freeze-dried weights of each gel were determined in triplicate at 1, 4, 7, 14 and 28 days of incubation with aCSF changed daily. The gels were found to be stable during the course of the study. Maximum swelling was observed for ALG gels while the degree of swelling increased with increasing ALG content and decreasing crosslink density. Viability of Schwann cells seeded on top of biopolymer gels was examined using an AlamarBlue® assay. The potential for

injectable ALG-$CaCO_3$-GDL gels as transplantation matrices was demonstrated by survival of encapsulated Schwann cells *in vitro*; however viability could not be quantified. Future studies should investigate the viability, proliferation and morphology of Schwann cells or other cells of interest encapsulated within the gels.

Table 4-1. Artificial cerebrospinal fluid formulation

Component	Concentration	Unit
NaCl	148.0	mM
KCl	3.0	mM
$CaCl_2 \bullet 2H_20$	1.4	mM
$MgCl_2$	0.8	mM
Na_2HPO_4	1.5	mM
NaH_2PO_4	0.2	mM
BSA	0.1	mg/mL

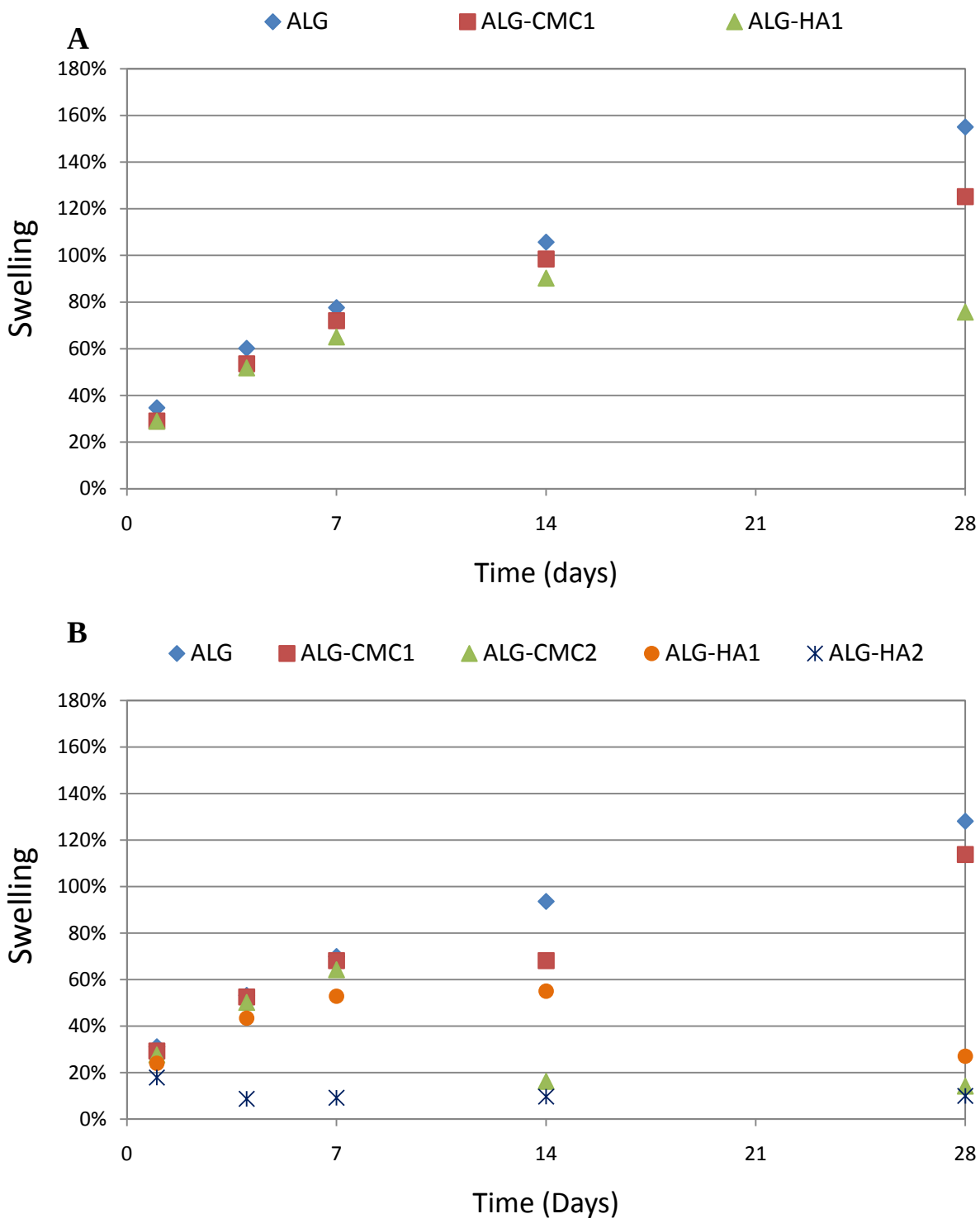

Figure 4-1. Swelling of biopolymer compositions in artificial cerebrospinal fluid at 37 °C. A) low (6 mM) Ca^{2+}. B) high (8mM) Ca^{2+}.

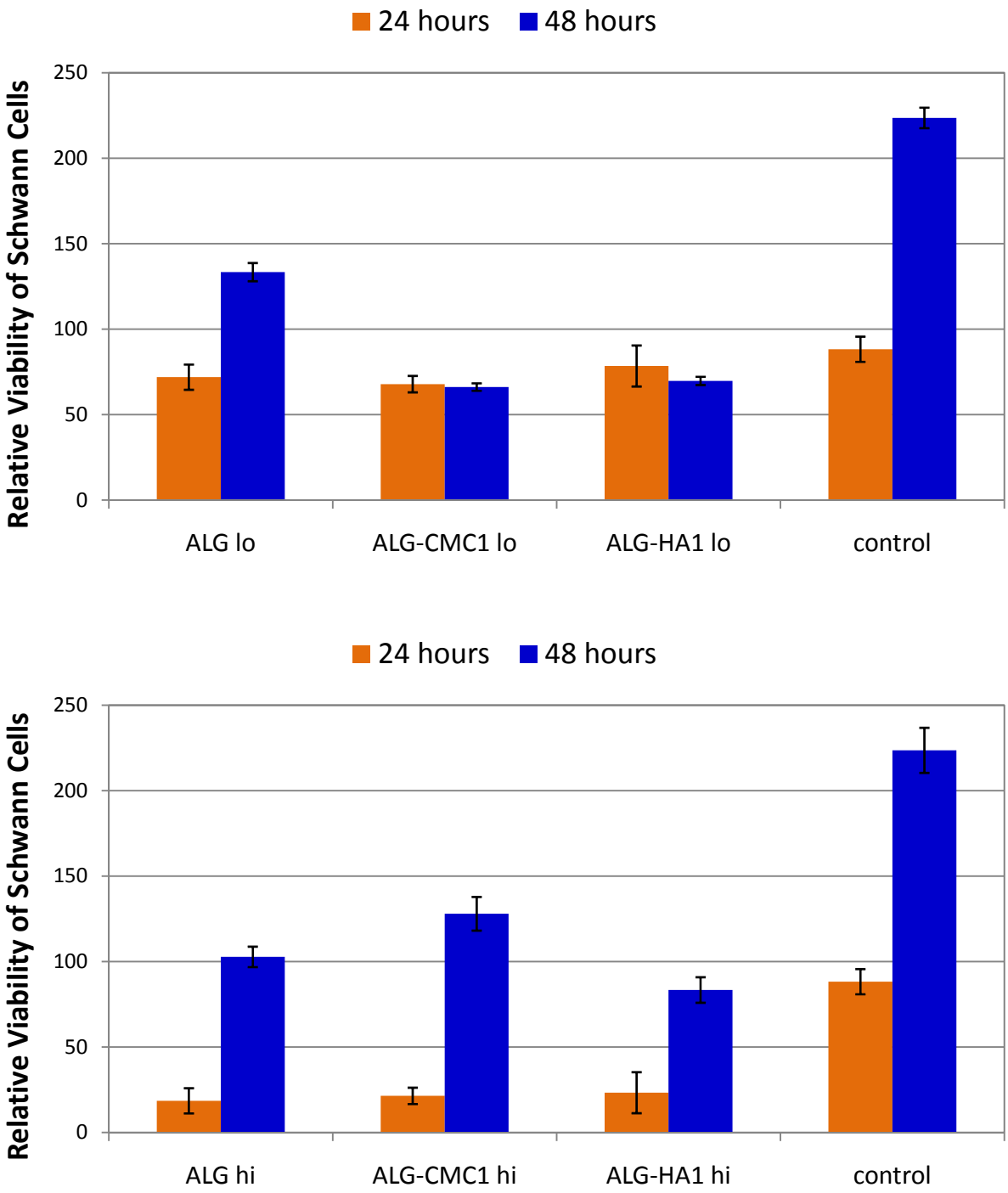

Figure 4-2. Relative viability of Schwann cells after 24 and 48 hours. A) low (6 mM) Ca^{2+}. B) high (8mM) Ca^{2+}.

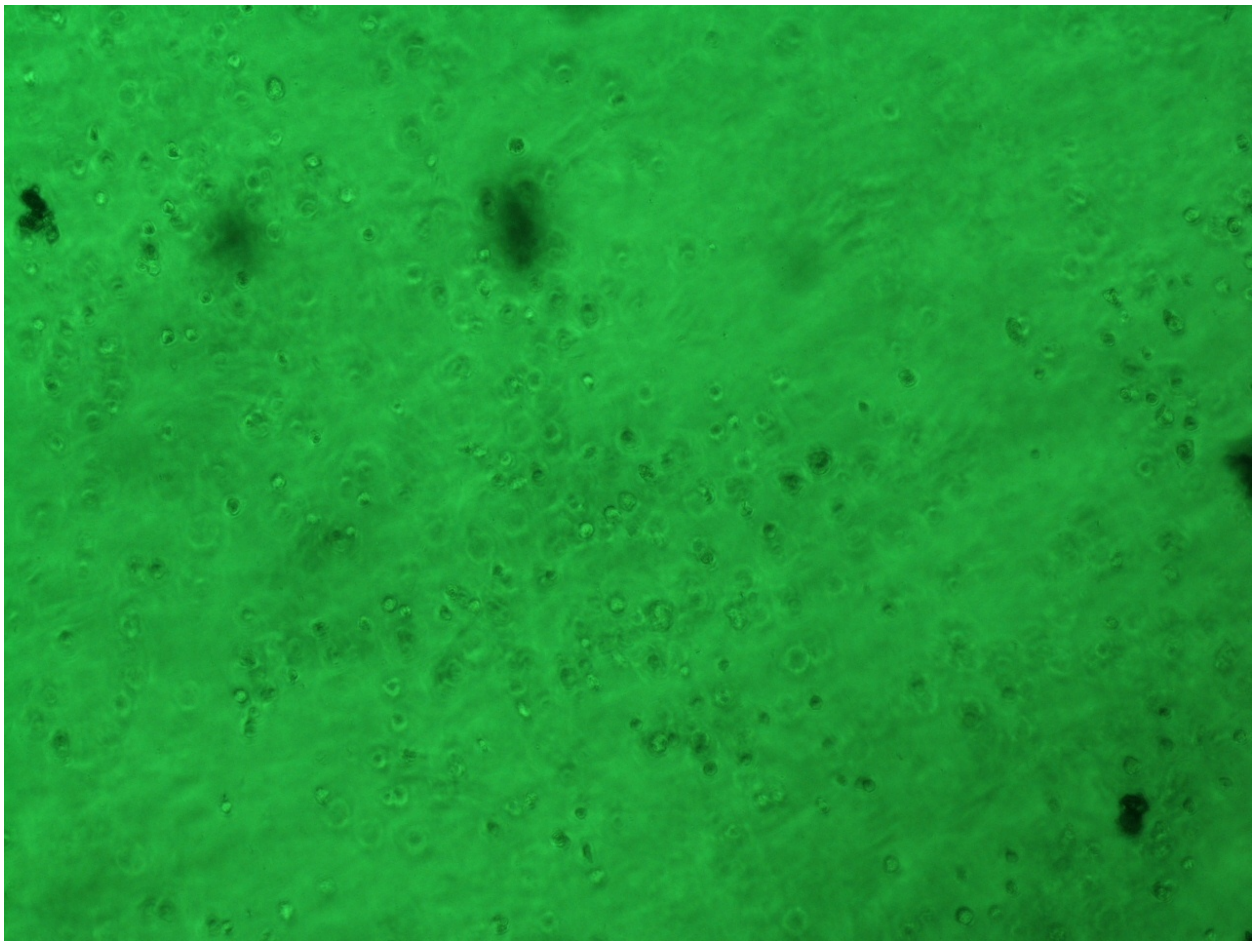

Figure 4-3. Inverted microscope image of Schwann cells encapsulated within an ALG gel. A number of live cells are visible as well as a clusters of dead cells (black).

.

CHAPTER 5
IN VIVO EVALUATION OF AN INJECTABLE ALGINATE-BASED GEL COMPOSITION IN A CERVICAL SPINAL CORD CONTUSION INJURY MODEL

Introduction

There are approximately 12,000 new cases of SCI in the United States each year, primarily affecting young adults between the ages of 16 and 30 (NSCISC, 2008). The majority of SCIs are caused by contusion or compression of the cord due to impingement by the vertebral column and most frequently occur at the cervical level. Respiratory impairment and associated complications are some of the most severe consequences of SCI, especially for upper- to mid-cervical spinal cord trauma, and are the leading causes of SCI mortality and morbidity (Zimmer et al., 2007). This makes evaluation of potential treatments for SCI in cervical injury models with application to respiratory function recovery of utmost importance.

A number of *in vivo* studies evaluating biopolymer substrates for SCI repair have utilized transection type models in which an incision is made to partially or completely sever the spinal cord or to remove an entire section. A polymeric scaffold typically in the form of a sponge or pre-formed gel is subsequently implanted into the lesion. The nature of hemisection and transection injuries make them ideal models for assessing transplantation of pre-formed gels and scaffolds that can be placed into the lesion. Furthermore, given the precision of these lesions, they serve as valuable proof-of-principles models for studies aimed at promoting and evaluating axonal regeneration (Steward et al., 2003; Talac et al., 2004). However, this type of injury rarely occurs in human SCI. Compression or contusion injuries more closely resemble those injuries seen in humans, but few studies have investigated the use of biomatrices in such injuries. (Woerly et al., 2001; Borgens et al., 2002; Tysseling-Mattiace et al., 2008).

The objective of this study was to evaluate the potential of injectable ALG-based compositions as a matrix for neural tissue repair *in vivo* using a clinically relevant SCI model

with important practical implications. Proof-of-concept was demonstrated by injecting ALG-CMC1 biopolymer gel into the contused adult rat cervical spinal cord. Animals received contusion injuries using an Infinite Horizon (IH) Impactor at C3/C4 and were treated with gel one week later. Animals were allowed to recover for one week post-implantation, and tissue was examined after cresyl violent staining.

Materials and Methods

Biopolymer Gel Preparation

ALG-CMC1 composition was prepared as previously described. Briefly, ALG (2.5% w/v) and CMC (1.5% w/v) solutions were prepared in ultrapure water by high speed mechanical mixing at 1000 rpm for 12 hours. The moisture content of each powder was determined beforehand to determine the correct weight of each polymer needed to give the desired concentration. ALG and CMC solutions were filtered into 250-mL Pyrex® bottles using an air pressure filtration funnel and 10 μm nylon filters. The filtered solutions were allowed to remain at room temperature for 24 hours and were sterilized in an autoclave on a programmed liquid cycle (20 minutes at 240°F).

Under sterile conditions in a biological hood, ALG (30 mL) and CMC (10 mL) solutions were combined by injecting into a 100 mL Pyrex® bottle using 20 mL syringes and magnetically stirred for 1 hour to mix. A suspension of $CaCO_3$ (8 mg) in 1 mL of ultrapure water was prepared in a 15 mL Nalgene container and sterilized by autoclaving. All materials were stored at room temperature and kept sealed to maintain sterility.

On the day of animal surgery ALG-CMC1 solution and $CaCO_3$ suspension were equilibrated to 37 °C for 2 hours in a water bath. All procedures were carried out in a biological hood. The polysaccharide solution, 8 mL, was added to the $CaCO_3$ suspension using a 10 mL syringe and magnetically stirred for 1 minute. A fresh solution of GDL (28 mg in 1 mL ultrapure

water) was prepared and added by syringe filtration (0.22 μm filter) to initiate gelation, and the mixture was stirred for an additional 20 seconds. The sterile ALG-CMC1 biopolymer composition was then immediately transported to the surgery suite for implantation.

Contusion Injuries

All procedures involving animals were conducted following NIH guidelines and with approval from the Institutional Animal Care and Use Committee at the University of Florida. All animal surgeries and histology were conducted with assistance from Barbara O'Steen, Alex Jones and Drs. Paul Reier and Michael Lane (College of Medicine, Department of Neuroscience). Adult Female Sprague-Dawley rats (230 to 250g; n = 3) were obtained from Harlan-Scientific and housed in the Animal Care Facility at the McKnight Brain Institute, University of Florida. Animals were anesthetized for all surgical procedures by injection of xylazine (3 mg subcutaneous; Phoenix Pharmaceutical, Inc., St. Joseph, MO) and ketamine (90 mg/kg intraperitoneal; Fort Dodge Animal Health, Fort Dodge, IA).

Following anesthesia, the surgical site was shaved and sterilized. All animals were then laid in the prone position on a heat-pad (maintained at 36 °C). A dorsal incision was made from approximately the first to fifth cervical segment (C1-C5) and muscle overlying the vertebral column retracted. A laminectomy was then performed to remove the entire C3 vertebral segment and most of C4. A contusion was subsequently made at C3/C4 using the Infinite Horizon Pneumatic Impactor (Precision Systems & Instrumentation, Lexington, KY) (Figure 5-1). Animals were secured in sterile clamps to position the exposed cord beneath the impactor probe and the probe was raised approximately 5mm above the intact dura. Spinal cord contusions were then made in air at a preset force of 150 kilodynes with zero dwell time. The resulting impact force ranged from 151 to 159 kdynes. Following contusion, the muscle layers overlying the

exposed cord were sutured with 4-0 Vicryl (Ethicon, Inc., Somerville, NJ), and the skin was closed with wound clips. Each rat was given subcutaneous injections of Lactated Ringers (5 ml) to prevent dehydration, yohimbine (0.4 mg; Lloyd Laboratories, Shenandoah, IA) to reverse the action of xylazine, and buprenorphine (0.012 mg; Reckitt Benckiser Pharmaceutical, Inc., Richmond, VA) to reduce any post-operative pain. Rats were evaluated daily for overall post-operative health and well-being.

Biopolymer Gel Injection

One week following, animals were again anesthetized and the injury site re-exposed. The site of injury and cavitation was identified by bruising at the laminectomy site. A sterile, freshly prepared ALG-CMC1 gelling mixture was drawn into a 1 mL Tuberculin syringe and backfilled into a Hamilton syringe with a 30-gauge needle. The filled syringe was mounted above the animal in a micromanipulator, and approximately 40-50 μL of the biopolymer gelling composition was injected through the dura into the injury site of each animal. The needle was retracted when reflux was observed. The muscles were then re-sutured and the skin closed with would clips. Animals were left to recover for 1 week at which time they received a lethal dose of anesthetic.

Tissue Resection and Histology

Two weeks post injury (one week post-gel injection) the rats were euthanized with 0.4 ml of Beuthanasia-D Special euthanasia solution (78 mg pentobarbital sodium and 10 mg phenytoin sodium; Schering-Plough Animal Health Corp., Union, NJ). Spinal cord tissue taken from each rat was processed in a different manner to investigate the best method for obtaining a quality section without loss of the gel. The methods were as follows:

Animal 1) Tissue was cryoprotected through a series of sucrose steps without fixation. The animal was intracardially perfused with 15% sucrose, dissected and stored in 15% sucrose for 24

hours, then transferred into 30% sucrose. Once the tissue began to sink in the sucrose solution, it was considered ready to be frozen for sectioning. The tissue was frozen by immersion in cooled isopentane in a beaker on dry-ice.

Animal 2) Tissue was dissected immediately following euthanasia and snap-frozen by immersion in cooled isopentane, without fixation or cryoprotection.

Animal 3) Tissue was processed by perfusion with paraformaldehyde (4% w/v in 0.1 M PBS). The fixed tissue was subsequently dissected and stored in the same solution until ready for cryoprotections. The tissue was then cryoprotected by immersion in a series of sucrose solutions (as described above) and frozen in isopentane.

Histology

Frozen tissue was mounted in O.C.T. (Optimal Cutting Temperature, TissueTek) and sectioned (20 μm thick, either transverse or longitudinal as indicated) at -20 °C in a cryostat. Sections were immediately slide mounted and air dried. All sections were subsequently stained with cresyl violet. Following brief immersion in distilled water, the sections were incubated in cresyl violet for 2 minutes. Sections were then rinsed in distilled water, dehydrated in a series of alcohols, followed by xylene (2-5 minutes in each). Upon completion all slides were coverslipped with permanent mounting medium (Richard-Allen Scientific). To assess the appearance of the gel stained with Cresyl Violet, some gel material was applied directly to clean microscope slides and processed for staining as described above.

Microscopy

All tissue was examined by brightfield microscopy using a Zeiss AxioPhot microscope. All images were taken with a Zeiss AxioCam digital camera connected to a PC. Images were color corrected for white balance only. No other color correction profiles were used at any stage. Sections from each animal were qualitatively reviewed for the presence of scaffold material.

Results and Discussion

Contusion Injuries

In this study, injuries were introduced in the cervical spinal cord of adult rats at C3/C4 using an Infinite Horizon (IH) impactor. The IH impactor is a computer-controlled device that applies a set force to the exposed spinal cord of an immobilized subject, resulting in damage to both white and grey matter (Scheff et al., 2003; Scheff and Roberts, 2009). This device has the demonstrated ability to produce consistent contusion injuries in small rodents and can impose graded degrees of damage by adjusting user-defined force settings. The type of injuries produced by the IH impactor and similar devices, rapid application of force to produce a contusion, are reported to accurately mimic injuries seen in humans (Stokes and Jakeman, 2002). The cervical contusion injury model used in this study has been well characterized in the laboratory of Dr. P. J. Reier (Department of Neuroscience at the University of Florida) and has proven useful for quantitative evaluation of respiratory dysfunction following cervical SCI (El-Bohy et al., 1998; Lane et al., 2008). Because most incidents of spinal cord trauma are contusion/compression injuries, and over half of these injuries occur at cervical levels, the model used in this work closely matches the majority of human cases of SCI and has significant clinical relevance and translational potential.

Biopolymer Gel Injection

This study represents the first reported study of injectable, in situ-forming ALG-based biopolymer compositions in the injured spinal cord. Three rats received injections of ALG-CMC1 gel crosslinked with 8 mM Ca^{2+} one week post-injury. Immediately after incorporating a fresh GDL solution, the ALG-CMC1 gel was brought into the surgical suite, and the first rat was treated within 15 minutes. Although the biopolymer solutions exhibit pseudoplastic behavior, the viscosity was too high to allow aspiration directly into a Hamilton syringe fitted with a 33-gauge

needle. Therefore the solution was loaded into a 1-mm syringe attached to a 20-gauge needle. The gel was then backfilled into the Hamilton syringe and injected through the dura until reflux was observed. The remaining animals were treated approximately 10 minutes apart using the same ALG-CMC1 sample. Pseudoplastic behavior and gradual increase in viscosity (see chapter 4) facilitated injection for at least 30 minutes after crosslinking was initiated, which allowed sufficient time to load the syringe before treating each animal. This flexibility in working time may prove critical in surgical situations where unexpected delays could arise.

The gels used in this study are also advantageous for treating actual human cases of SCI because they are able to completely fill the irregularly shaped volume of contusion lesions and can be delivered in a minimally invasive procedure. Scaffolds and semi-solid gels require sizing before implantation and cannot conform to the shape of the lesion which can affect integration with host tissue (Stabenfeldt et al., 2006). Minimizing mismatch between the scaffold and host tissue may also be important for reducing the inflammatory response (Hanson et al., 1996; Jain et al., 2006; Anderson, 2008).

Histology

In contrast to the deep violet appearance of cells within the spinal cord stained with cresyl violet, ALG-CMC1 gel was labeled a distinctive pink color (Figure 5-2). Tissue from Animal 1 was cryoprotected by a series of sucrose steps without fixation. This histological technique preserved and allowed clear visualization of the gel which was differentiated from host tissue due to color of stain, confirming that the gel was successfully delivered to the injured spinal cord. ALG-CMC1 gel appeared to intermingle with host tissue and completely fill the contusion cavity (Figure 5-3). No rigid boundary between implant and host spinal cord tissue was apparent and evidence of gel was visible in sections rostral to the lesion epicenter (Figure 5-4). This is likely due to prolonged liquid-like behavior of the ALG-CMC1 composition which would have

allowed flow throughout the lesion before extensive crosslinking immobilized the gel. Also, the gel did not appear to elicit a significant inflammatory response as there was no noticeable accumulation of cells along gel-tissue interfaces.

Tissue from Animal 2 underwent the least amount of histological processing whereby the tissue was snap-frozen immediately after the animal was euthanized. ALG-CMC1 gel was not visible in this animal (Figure 5-5). Animal 3 tissue was cryoprotected and fixed with paraformaldehyde. There was no gross evidence of gel in the lesion, however pink fragments were visible at higher magnifications indicating that gel was present in the lesion and most likely dissolved during the fixation process (Figure 5-6).

Previous studies in the laboratory of Dr. Paul Reier demonstrated the development of a significant cystic cavity one week post-injury in rats subjected to cervical contusion injury model used in this research (Figure 5-6, Figure 5-7). In this work, cystic cavitation appeared to be minimal in animals treated with ALC-CMC1 gel. This suggests that the gel may have suppressed cavity progression; however this cannot be determined conclusively without further study.

Summary

Contusion injuries represent the most common cases of human SCI, and the majority of these injuries occur at cervical levels. However, most neural tissue engineering studies have focused on thoracic level injuries and have utilized transection lesions which are convenient for implantation of sponges or semi-solid gel scaffolds. This work is the first reported use of injectable ALG-based gel compositions for CNS repair. Feasibility of this approach was demonstrated in a clinically-relevant SCI model by successful injection of an ALG-CMC composition into cervical spinal cord contusion injuries in adult rats one week post-injury. Injectability allowed the gels to be delivered into the injured cord through the dura, minimizing the invasiveness of the procedure. The biopolymer composition integrated well with host tissue

and did not appear to stimulate a significant inflammatory response. Also, treatment with the ALG-CMC gel appeared to suppress cystic cavitation. The results of this study indicate that in-situ forming ALG-based compositions have significant potential for CNS tissue repair and should undergo further investigation.

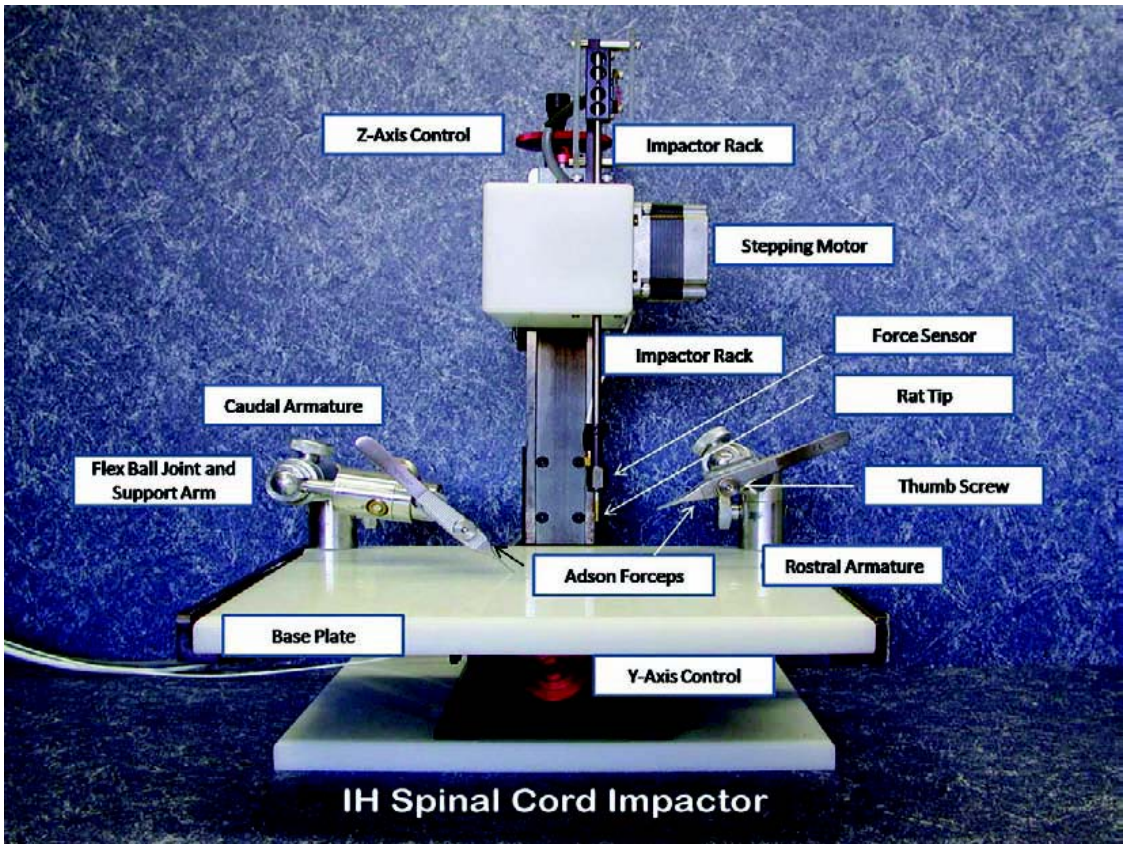

Figure 5-1. Infinite Horizon spinal cord impactor. [Reprinted with permission from Springer Science + Business Media: Scheff, S., and Roberts, K. N., 2009. Infinite horizon spinal cord contusion model. In: Chen, J., Xu, X.-M., Xu, Z. C., and Zhang, J. H., (Eds.), Animal models of acute neurological injuries (Page 424, Figure 1). Humana Press, New York.]

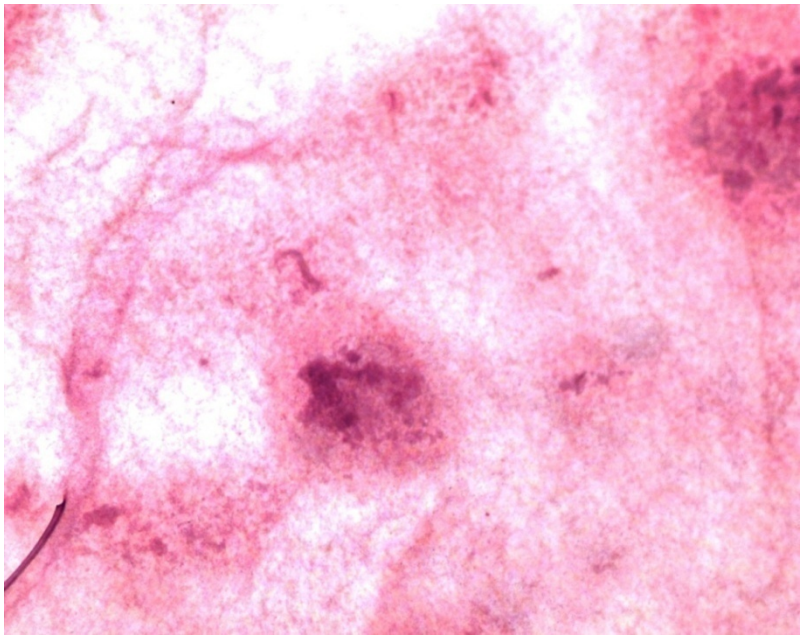

Figure 5-2. Cresyl violet stain of ALG-CMC1 gel showing pink coloration.

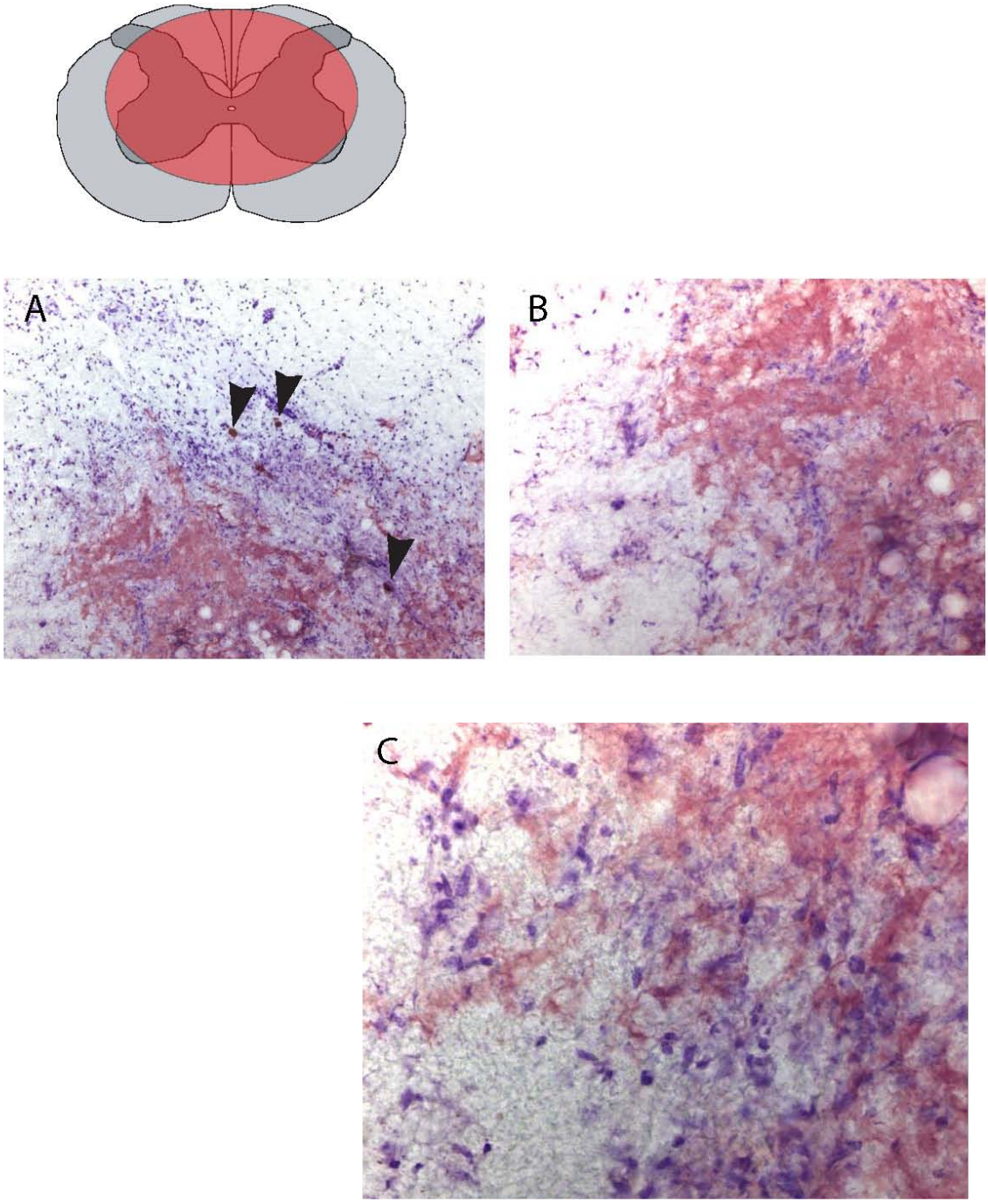

Figure 5-3. Tissue near the lesion epicenter stained with cresyl violet one week post-treatment with ALG-CMC1 gel (A). Panels (B) and (C) are details. Tissue was cryoprotected, but not fixed. Gel implants integrated well with host tissue.

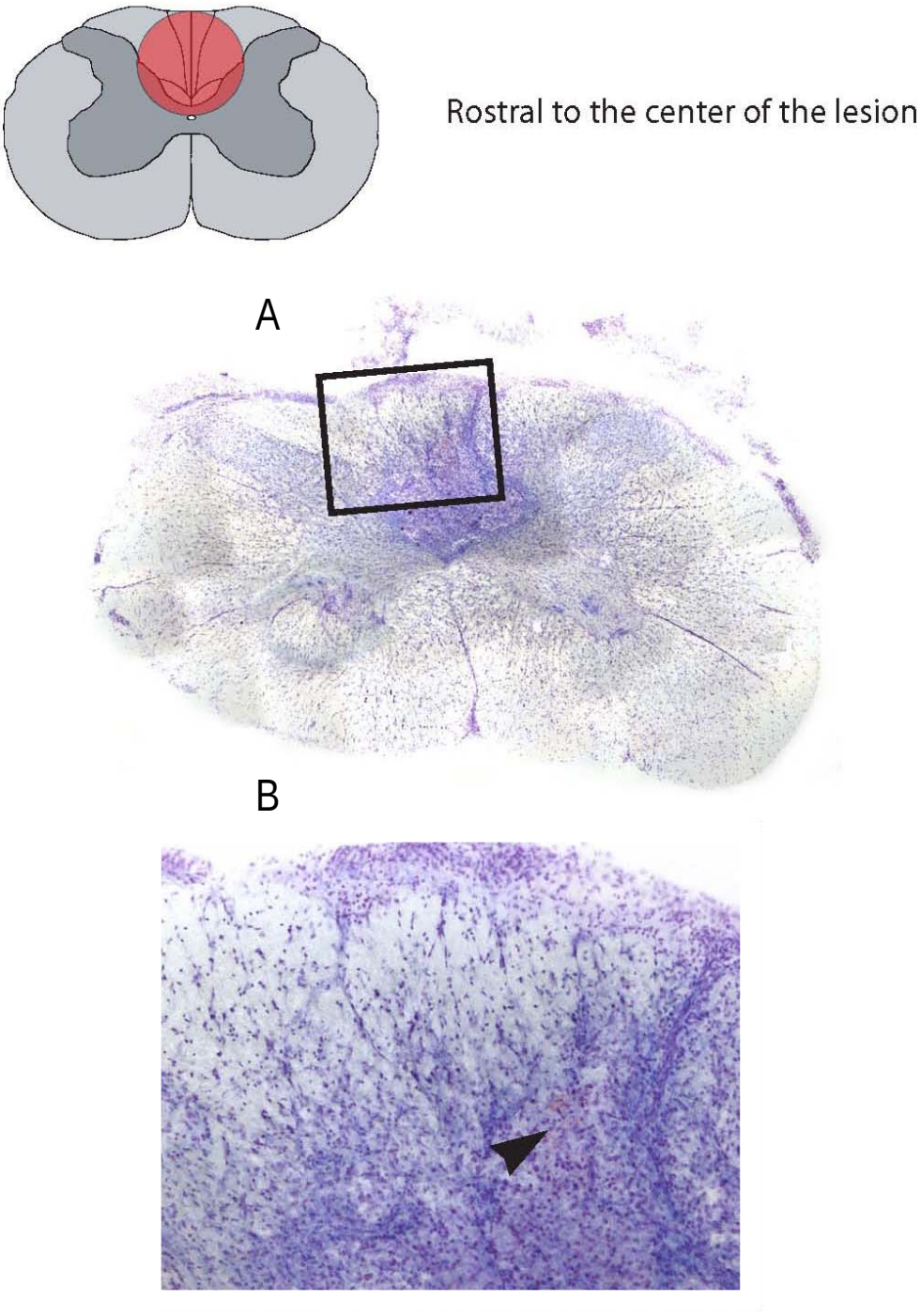

Figure 5-4. Tissue rostral to lesion epicenter stained with cresyl violet one week post-treatment with ALG-CMC1 gel (A). Panel (B) is a detail showing a fragment of the gel (arrow). Tissue was cryoprotected, but not fixed.

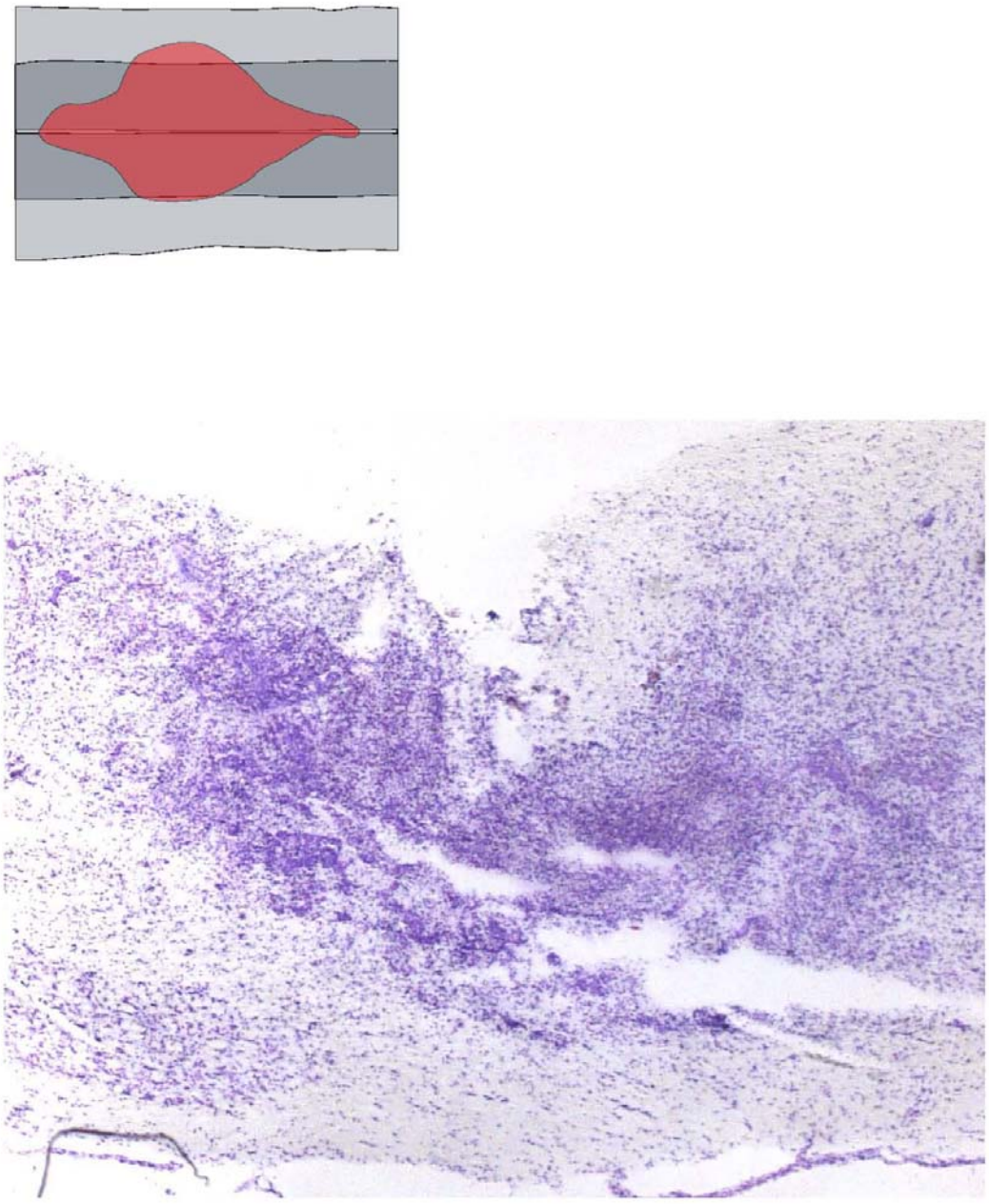

Figure 5-5. Tissue near lesion epicenter stained with cresyl violet one week post-treatment with ALG-CMC1 gel. Tissue was not cryoprotected or fixed.

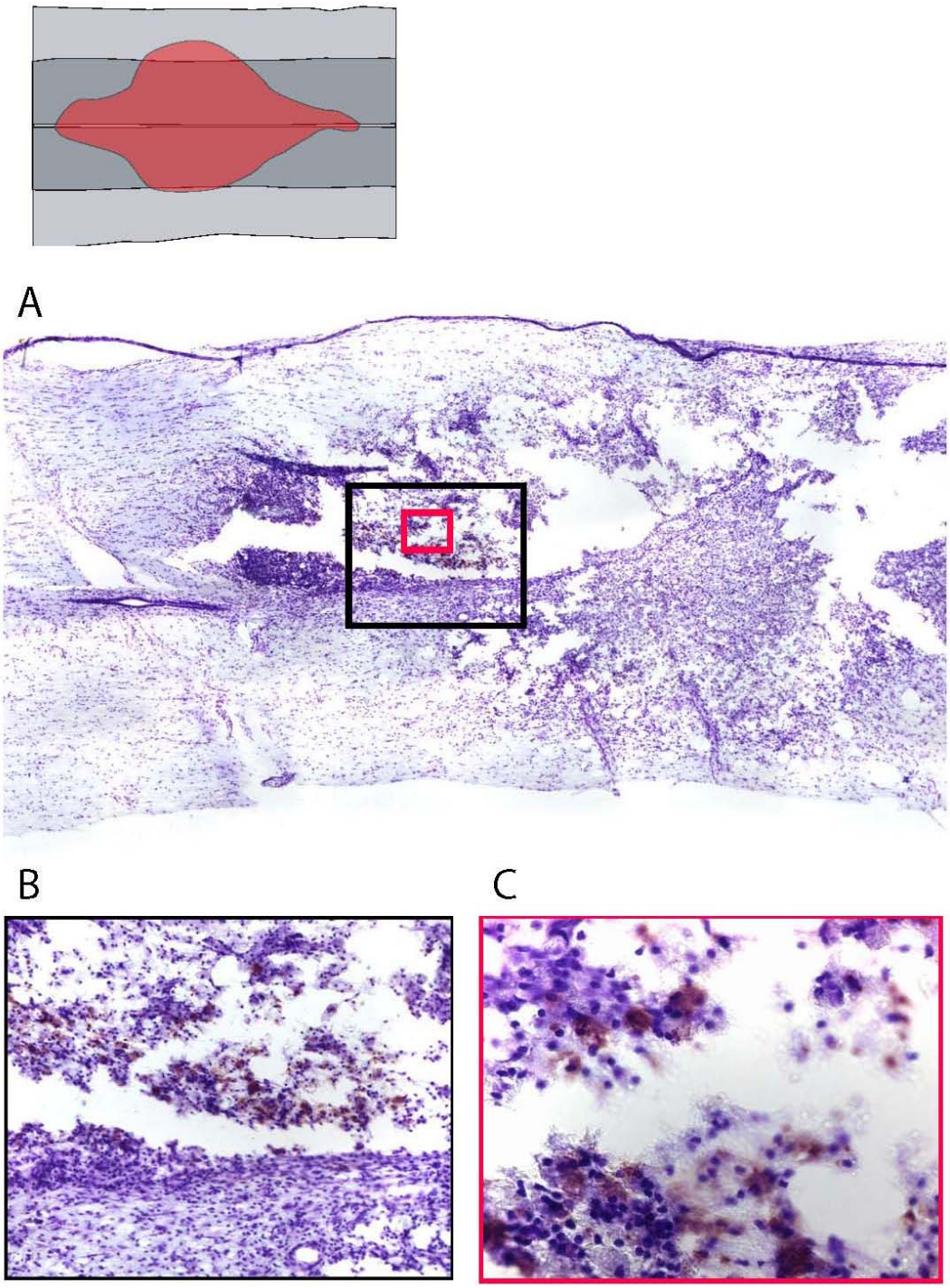

Figure 5-6. Tissue near lesion epicenter stained via cresyl violet one week post-treatment with ALG-CMC1 gel. Tissue was fixed with paraformaldye and subsequently cryoprotected. Evidence of gel (pink) is not apparent (A) except under higher magnification (B) and (C).

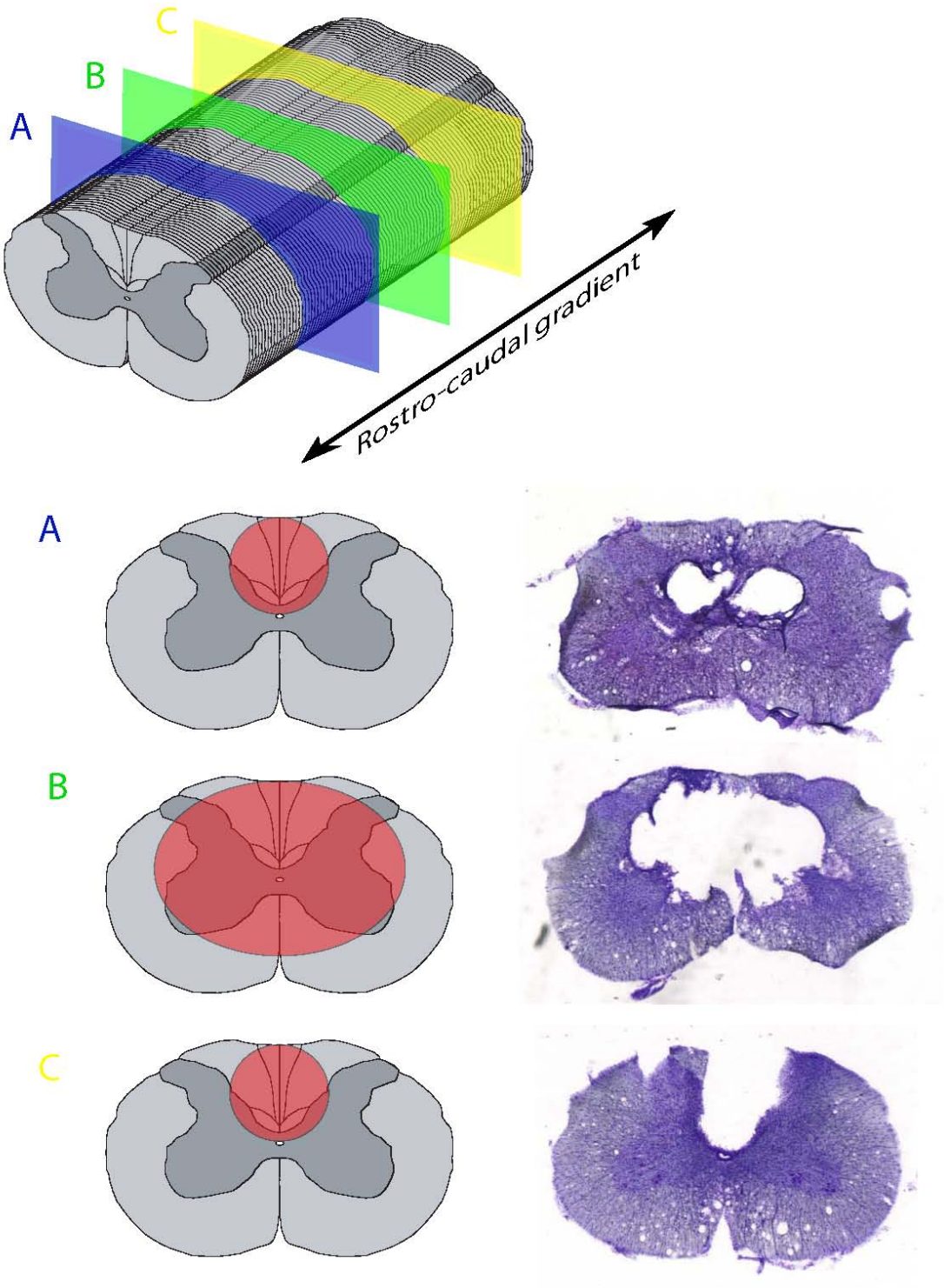

Figure 5-7. Cresyl violet staining of contusion lesion tissue from an untreated subject one week post-injury (from a prior study). Substantial tissue loss is apparent at the lesion epicenter (B) and in rostral (A) and caudal (C) directions.

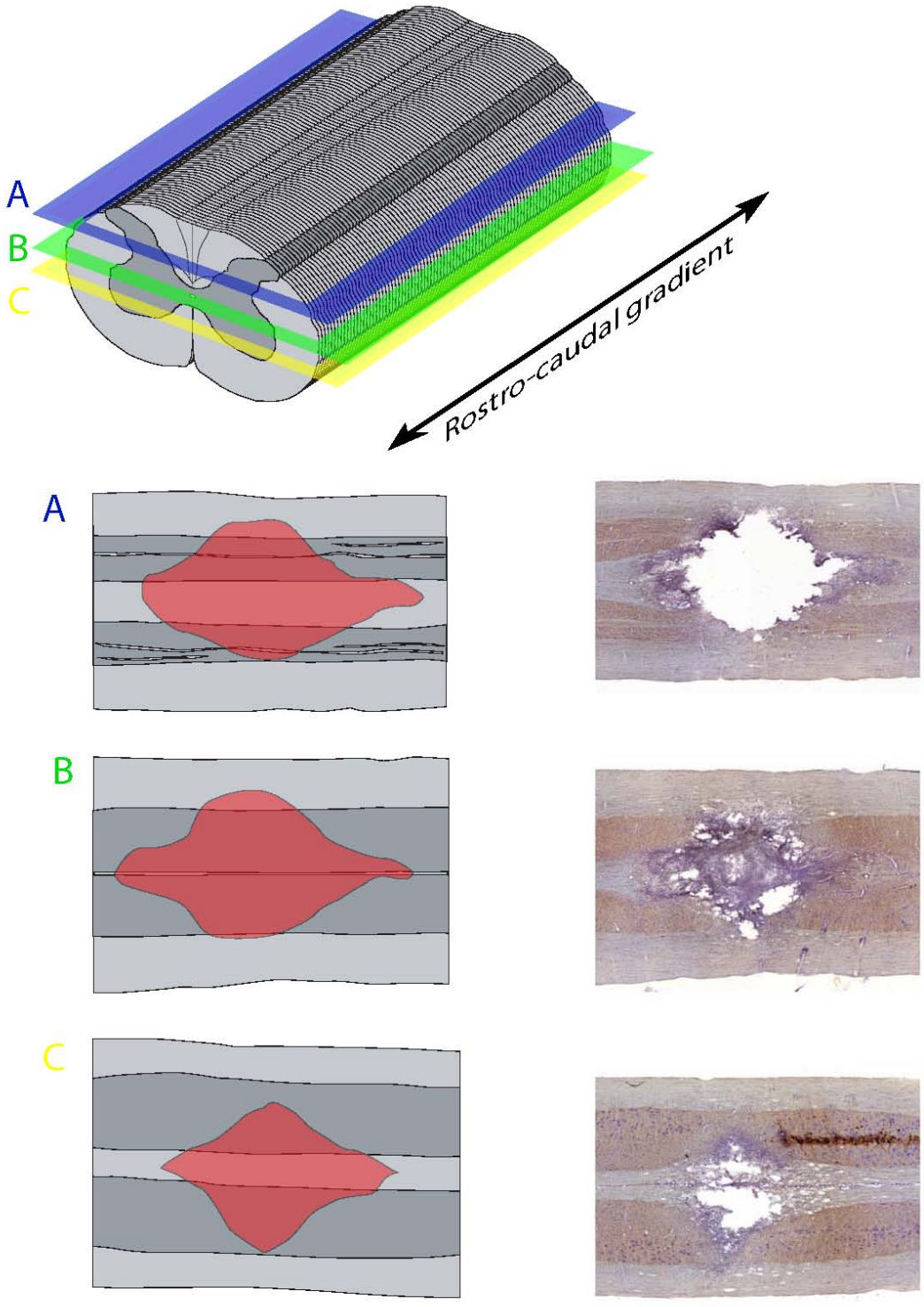

Figure 5-8. Cresyl violet staining of longitudinal section from an untreated subject one week post-contusion injury in a prior study. Significant tissue loss is apparent close to the injured surface (A) which declines moving ventrally through the cord (B) and (C).

CHAPTER 6
CONCLUSIONS

A variety of biomaterials constructs have been investigated for neural tissue repair mostly in the form of sponge-like scaffolds or pre-formed gels which must be cut to size and require incision of the spinal cord for implantation. The purpose of this research was to develop and characterize biopolymer gel compositions for minimally-invasive delivery to injured CNS tissue. The primary goal was to prepare injectable ALG-based gels that can be combined with viable cells, bioactive molecules or drugs and bridge the lesion, prevent or reduce cystic cavitation and provide a favorable terrain for axonal regeneration. The following conclusions were drawn:

- In situ-forming ALG, ALG-CMC and ALG-HA gels suitable for soft tissue engineering were synthesized via gradual ionic crosslinking of ALG with $CaCO_3$ and GDL. The compositions studied were injectable through a 22-gauge needle prior to crosslinking.
- Gelation was studied using the inverted tube method as a function of composition, calcium ion concentration, and temperature.
- Gelation time was extended as the amount of alginate in the gel decreased ($p<0.05$).
- Increasing the concentration of Ca^{2+} from 6 mM to 8 mM resulted in a significant decrease in gelation time ($p<0.05$).
- Gelation rate at 37 °C was faster than at room temperature (25 °C).
- Swelling behavior in artificial cerebrospinal fluid varied by composition and increased with increasing ALG content and decreasing concentration of $CaCO_3$.
- Potential for cellular transplantation was shown by survival of encapsulated Schwann cells *in vitro*.
- Proof of concept was demonstrated by injection of ALG-CMC1 gel into the contused cervical spinal cord of adult rats one week post-injury. The compositions integrated well with host tissue and do not stimulate a significant inflammatory response.
- In situ-forming gels based on ALG-$CaCO_3$-GDL are promising candidates for neural tissue repair and should undergo further investigation.

CHAPTER 7
FUTURE WORK

The focus of this work was to explore the suitability and feasibility of utilizing injectable, in situ-forming ALG, ALC-CMC and ALG-HA gels for repair of injured nervous system tissue. The promising results of the current studies suggest that these biopolymer compositions should undergo further investigation. The following are possible future research directions for consideration:

- **Extended *in vivo* studies of gel compositions.** Pilot studies have shown that ALG-based gel compositions can be injected into the injured spinal cord and integrate well with host tissue. More extensive studies implanting gels with and without Schwann cells should be conducted. Immunohistochemical analysis and evaluation of functional outcomes at several time points are necessary for fully evaluating the suitability of these gels.

- **Attachment of bioactive peptides.** Covalent attachment of bioactive peptides, e.g. laminin, fibronectin, or peptide sequences, e.g. IKVAV, to biopolymer compositions should be explored to enhance cellular adhesion within the gel environment.

- **Incorporation of porous $CaCO_3$ microparticles.** Porous $CaCO_3$ microparticles embedded within alginate solutions have recently been shown to be an effective carrier for sustained release of ibuprofen *in vitro* (Wang et al., 2008). These porous microparticles could potentially be utilized as a reservoir for controlled delivery of neurotrophins, chondroitinase ABC to degrade inhibitory CSPGs, or drugs (e.g. methylprednisolone) while simultaneously serving as a source of calcium ions for in situ gelation of alginate.

LIST OF REFERENCES

Agudo, M., Woodhoo, A., Webber, D., Mirsky, R., Jessen, K. R., and Mcmahon, S. B., 2008. Schwann cell precursors transplanted into the injured spinal cord multiply, integrate and are permissive for axon growth. Glia 56**,** 1263-1270.

Ahmed, S. A., R. M. Gogal, J., and Walsh, J. E., 1994. A new rapid and simple non-radioactive assay to monitor and determine the proliferation of lymphocytes: an alternative to [3H]thymidine incorporation assay. J. Immunol. Methods 170**,** 211-224.

Alper, J., 2009. Geron gets green light for human trial of ES cell-derived product. Nat. Biotechnol. 27**,** 213-214.

Anderson, J. M., 2008. Biocompatibility and bioresponse to biomaterials. In: Atala, A., Lanza, R., Nerem, R., and Thomson, J. A., (Eds.), Principles of regenerative medicine. Academic Press, New York, pp. 704-723.

Archibald, S. J., Shefner, J., Krarup, C., and Madison, R. D., 1995. Monkey median nerve repaired by nerve graft or collagen nerve guide tube. J. Neurosci. 15**,** 4109-4123.

Asher, R., and Bignami, A., 1991. Localization of hyaluronate in primary glial cell cultures derived from newborn rat brain. Exp. Cell Res. 195**,** 401-411.

Ashton, R. S., Banerjee, A., Punyani, S., Schaffer, D. V., and Kane, R. S., 2007. Scaffolds based on degradable alginate hydrogels and poly(lactide-co-glycolide) microspheres for stem cell culture. Biomaterials 27**,** 5518-5525.

Athanasiou, K. A., Niederauer, G. G., and Agrawal, C. M., 1996. Sterilization, toxicity, biocompatibility and clinical applications of polylactic acid/ polyglycolic acid copolymers. Biomaterials 17**,** 93-102.

Bakshi, A., Fisher, O., Dagci, T., Himes, B. T., Fischer, I., and Lowman, A., 2004. Mechanically engineered hydrogel scaffolds for axonal growth and angiogenesis after transplantation in spinal cord injury. J. Neurosurg. Spine 1**,** 322-329.

Balazs, E. A., and Denlinger, J. L., 1989. Clinical uses of hyaluronan. In: Evered, D., and Whelan, J., (Eds.), The biology of hyaluronan. Wiley, New York, pp. 265-280.

Balgude, A. P., Yu, X., Szymanski, A., and Bellamkonda, R. V., 2001. Agarose gel stiffness determines rate of DRG neurite extension in 3D cultures. Biomaterials 22**,** 1077-1084.

Ban, D.-X., Kong, X.-H., Feng, S.-Q., Ning, G.-Z., Chen, J.-T., and Guo, S.-F., 2009. Intraspinal cord graft of autologous activated Schwann cells efficiently promotes axonal regeneration and functional recovery after rat's spinal cord injury. Brain Res. 1256**,** 149-161.

Baptiste, D. C., Austin, J. W., Zhao, W., Nahirny, A., Sugita, S., and Fehlings, M. G., 2009. Systemic polyethylene glycol promotes neurological recovery and tissue sparing in rats after cervical spinal cord injury. J. Neuropathol. Exp. Neurol. 68**,** 661-676.

Baptiste, D. C., and Fehlings, M. G., 2006. Pharmacological approaches to repair the injured spinal cord. J. Neurotrauma 23**,** 318-334.

Bareyre, F. M., 2008. Neuronal repair and replacement in spinal cord injury. J. Neurol. Sci. 265**,** 63-72.

Barnett, S. C., and Chang, L., 2004. Olfactory ensheathing cells and CNS repair: going solo or in need of a friend? Trends Neurosci. 27**,** 54-60.

Bartolomei, J. C., and Greer, C. A., 2000. Olfactory ensheathing cells: bridging the gap in spinal cord injury. Neurosurgery 47**,** 1057–1069.

Baumann, M. D., Kang, C. E., Stanwick, J. C., Wang, Y., Kim, H., Lapitsky, Y., and Shoichet, M. S., 2009. An injectable drug delivery platform for sustained combination therapy. J. Controlled Release 138**,** 205-213.

Bellamkonda, R., Ranieri, J. P., Bouche, N., and Aebischer, P., 1995. Hydrogel-based three-dimensional matrix for neural cells. J. Biomed. Mater. Res. 29**,** 663-671.

Benfey, M., and Aguayo, A. J., 1982. Extensive elongation of axons from rat brain into peripheral nerve grafts. Nature 296**,** 150-152.

Bignami, A., and Asher, R., 1992. Some observations on the localization of hyaluronic acid in adult, newborn and embryonal rat brain. Int. J. Dev. Neurosci. 10**,** 45-57.

Bignami, A., Asher, R., and Perides, G., 1992. The extracellular matrix of rat spinal cord: a comparative study on the localization of hyaluronic acid, glial hyaluronate-binding protein, and chondroitin sulfate proteoglycan. Exp. Neurol. 117**,** 90-93.

Bonaventure, J., Kadhom, N., Cohen-Solal, L., Ng, K. H., Bourguignon, J., Lasselin, C., and Freisinger, P., 1994. Reexpression of cartilage-specific genes by dedifferentiated human articular chondrocytes cultured in alginate beads. Exp. Cell Res. 212**,** 97-104.

Borgens, R. B., and Bohnert, D., 2001. Rapid recovery from spinal cord injury after subcutaneously administered polyethylene glycol. J. Neurosci. Res. 66**,** 1179-1186.

Borgens, R. B., and Shi, R., 2000. Immediate recovery from spinal cord injury through molecular repair of nerve membranes with polyethylene glycol. FASEB J. 14**,** 27-35.

Borgens, R. B., Shi, R., and Bohnert, D., 2002. Behavioral recovery from spinal cord injury following delayed application of polyethylene glycol. J. Exp. Biol. 205**,** 1-10.

Bracken, M., 2002. Steroids for acute spinal cord injury, Cochrane Database of Systematic Reviews CD001046. John Wiley & Sons, Ltd.

Bracken, M. B., Collins, W. F., Freeman, D. F., Shepard, M. J., Wagner, F. W., Silten, R. M., Hellenbrand, K. G., Ransohoff, J., Hunt, W. E., Perot, P. L., Jr., and et, a., 1984. Efficacy of methylprednisolone in acute spinal cord injury. JAMA 251**,** 45-52.

Bracken, M. B., Shepard, M. J., Collins, W. F., Holford, T. R., Young, W., Baskin, D. S., Eisenberg, H. M., Flamm, E., Leo-Summers, L., Maroon, J., and et al., 1990. A randomized, controlled trial of methylprednisolone or naloxone in the treatment of acute spinal-cord injury. Results of the Second National Acute Spinal Cord Injury Study. N. Engl. J. Med. 322**,** 1405-1411.

Bracken, M. B., Shepard, M. J., Holford, T. R., Leo-Summers, L., Aldrich, E. F., Fazl, M., Fehlings, M., Herr, D. L., Hitchon, P. W., Marshall, L. F., Nockels, R. P., Pascale, V., Perot, P. L., Jr., Piepmeier, J., Sonntag, V. K., Wagner, F., Wilberger, J. E., Winn, H. R., and Young, W., 1997. Administration of methylprednisolone for 24 or 48 hours or tirilazad mesylate for 48 hours in the treatment of acute spinal cord injury. Results of the Third National Acute Spinal Cord Injury Randomized Controlled Trial. National Acute Spinal Cord Injury Study. JAMA 277**,** 1597-1604.

Bunge, M. B., 2008. Novel combination strategies to repair the injured mammalian spinal cord. J. Spinal Cord Med. 31**,** 262-269.

Burdick, J. A., Ward, M., Liang, E., Young, M. J., and Langer, R., 2006. Stimulation of neurite outgrowth by neurotrophins delivered from degradable hydrogels. Biomaterials 27**,** 452-459.

Burns, J. W., Skinner, K., Colt, J., Sheidlin, A., Bronson, R., Yaacobi, Y., and Goldberg, E. P., 1995. Prevention of tissue injury and postsurgical adhesions by precoating tissues with hyaluronic acid solutions. J. Surg. Res. 59**,** 644-652.

Busch, S. A., and Silver, J., 2007. The role of extracellular matrix in CNS regeneration. Curr. Opin. Neurobiol. 17**,** 120-127.

Chang, G.-L., Hung, T.-K., and Feng, W. W., 1988. An in-vivo measurement and analysis of viscoelastic properties of the spinal cord of cats. J. Biomech. Eng. 110**,** 115-122.

Chau, C. H., Shum, D. K. Y., Li, H., Pei, J., Lui, Y. Y., Wirthlin, L., Chan, Y. S., and Xu, X. M., 2004. Chondroitinase ABC enhances axonal regrowth through Schwann cell-seeded guidance channels after spinal cord injury. FASEB J. 18**,** 194-196.

Chen, B. K., Knight, A. M., de Ruiter, G. C. W., Spinner, R. J., Yaszemski, M. J., Currier, B. L., and Windebank, A. J., 2009. Axon regeneration through scaffold into distal spinal cord after transection. J. Neurotrauma In Press.

Cheng, M., Deng, J., Yang, F., Gong, Y., Zhao, N., and Zhang, X., 2003. Study on physical properties and nerve cell affinity of composite films from chitosan and gelatin solutions. Biomaterials 24**,** 2871-2880.

Cheng, S., Clarke, E. C., and Bilston, L. E., 2008. Rheological properties of the tissues of the central nervous system: a review. Med. Eng. Phys. 30**,** 1318-1337.

Chenite, A., Buschmann, M., Wang, D., Chaput, C., and Kandani, N., 2001. Rheological characterisation of thermogelling chitosan/glycerol-phosphate solutions. Carbohydr. Polym. 46**,** 39-47.

Chenite, A., Chaput, C., Wang, D., Combes, C., Buschmann, M. D., Hoemann, C. D., Leroux, J. C., Atkinson, B. L., Binette, F., and Selmani, A., 2000. Novel injectable neutral solutions of chitosan form biodegradable gels in situ. Biomaterials 21**,** 2155-2161.

Choi, G.-H., Youn, Y.-H., Kim, D.-Y., Son, H.-S., Kim, H.-T., and Kim, J.-K., 2006. Alginate gel decreases chondroitin sulfate proteoglycan immunoreactivity following spinal cord injury: preliminary study. Tissue Eng. Reg. Med. 3**,** 472-477.

Comolli, N., Neuhuber, B., Fischer, I., and Lowman, A., 2008. In vitro analysis of PNIPAAm-PEG, a novel, injectable scaffold for spinal cord repair. Acta Biomater. 5**,** 1046-1055.

Coutts, M., and Keirstead, H. S., 2008. Stem cells for the treatment of spinal cord injury. Exp. Neurol. 209**,** 368-377.

Crompton, K. E., Goud, J. D., Bellamkonda, R. V., Gengenbach, T. R., Finkelstein, D. I., Horne, M. K., and Forsythe, J. S., 2007. Polylysine-functionalised thermoresponsive chitosan hydrogel for neural tissue engineering. Biomaterials 28**,** 441-449.

Crompton, K. E., Tomas, D., Finkelstein, D. I., Marr, M., Forsythe, J. S., and Horne, M. K., 2006. Inflammatory response on injection of chitosan/GP to the brain. J. Mater. Sci. Mater. Med. 17**,** 633-639.

Cui, F. Z., Tian, W. M., Hou, S. P., Xu, Q. Y., and Lee, I.-S., 2006. Hyaluronic acid hydrogel immobilized with RGD peptides for brain tissue engineering. Journal of Materials Science - Materials in Medicine 17**,** 1393–1401.

d'Ayala, G. G., Malinconico, M., and Laurienzo, P., 2008. Marine derived polysaccharides for biomedical applications: chemical modification approaches. Molecules 13**,** 2069-2106.

Dalton, P. D., Flynn, L., and Shoichet, M. S., 2002. Manufacture of poly(2-hydroxyethyl methacrylate-co-methyl methacrylate) hydrogel tubes for use as nerve guidance channels. Biomaterials 23**,** 3843-3851.

Dalton, P. D., Flynn, L., and Shoichet, M. S., 2002. Manufacture of poly(2-hydroxyethyl methacrylate-co-methyl methacrylate) hydrogel tubes for use as nerve guidance channels. Biomaterials 23**,** 3843-3851.

Darian-Smith, C., 2009. Synaptic plasticity, neurogenesis, and functional recovery after spinal cord injury. Neuroscientist 15**,** 149-165.

David, S., and Aguayo, A. J., 1981. Axonal elongation into peripheral nervous system "bridges" after central nervous system injury in adult rats. Science 214**,** 931-933.

Deshpande, D. M., Kim, Y. S., Martinez, T., Carmen, J., Dike, S., Shats, I., Rubin, L. L., Drummond, J., Krishnan, C., Hoke, A., Maragakis, N., Shefner, J., Rothstein, J. D., and Kerr, D. A., 2006. Recovery from paralysis in adult rats using embryonic stem cells. Ann. Neurol. 60**,** 32-55.

Dezawa, M., 2002. Central and peripheral nerve regeneration by transplantation of Schwann cells and transdifferentiated bone marrowstromal cells. Anat. Sci. Int. 77**,** 12-25.

Dhoot, N. O., Tobias, C. A., Fischer, I., and Wheatley, M. A., 2004. Peptide-modified alginate surfaces as a growth permissive substrate for neurite outgrowth. J. Biomed. Mater. Res. A 71A**,** 191-200.

Dillon, G. P., Xiaojun, Y., Sridharan, A., Ranieri, J. P., and Bellamkonda, R. V., 1998. The influence of physical structure and charge on neurite extension in a 3D hydrogel scaffold. J. Biomater. Sci. Polym. Ed. 9**,** 1049-1069.

Dougherty, K. D., Dreyfus, C. F., and Black, I. B., 2000. Brain-derived neurotrophic factor in astrocytes, oligodendrocytes, and microglia/macrophages after spinal cord injury. Neurobiol. Dis. 7**,** 574-585.

Draget, K. I., Østgaard, K., and Smidsrød, O., 1989. Alginate-based solid media for plant-tissue culture. Appl. Microbiol. Biotechnol. 31**,** 79-83.

Draget, K. I., Østgaard, K., and Smidsrød, O., 1990. Homogeneous alginate gels: A technical approach. Carbohydr. Polym. 14**,** 159-178.

El-Bohy, A. A., Schrimsher, G. W., Reier, P. J., and Goshgarian, H. G., 1998. Quantitative assessment of respiratory function following contusion injury of the cervical spinal cord. Exp. Neurol. 150**,** 143-152.

Fawcett, J. W., and Asher, R. A., 1999. The glial scar and central nervous system repair. Brain Res. Bull. 49**,** 377-391.

FDA, 2002. 21CFR184.1318 Title 21 - food and drugs, pp. 502.

Feron, F., Perry, C., Cochrane, J., Licina, P., Nowitzke, A., Urquhart, S., Geraghty, T., and Mackay-Sim, A., 2005. Autologous olfactory ensheathing cell transplantation in human spinal cord injury. Brain 128**,** 2951-2960.

Figliuzzi, M., Plati, T., Cornolti, R., Adobati, F., Fagiani, A., Rossi, L., Remuzzi, G., and Remuzzi, A., 2006. Biocompatibility and function of microencapsulated pancreatic islets. Acta Biomater. 2**,** 221-227.

Franssen, E. H. P., de Bree, F. M., and Verhaagen, J., 2007. Olfactory ensheathing glia: their contribution to primary olfactory nervous system regeneration and their regenerative potential following transplantation into the injured spinal cord. Brain Res. Rev. 56**,** 236-258.

Friedman, J. A., Windebank, A. J., Moore, M. J., Spinner, R. J., Currier, B. L., and Yaszemski, M. J., 2002. Biodegradable polymer grafts for surgical repair of the injured spinal cord. Neurosurgery 51**,** 742-752.

García-Alías, G., Lin, R., Akrimi, S. F., Story, D., Bradbury, E. J., and Fawcett, J. W., 2008. Therapeutic time window for the application of chondroitinase ABC after spinal cord injury. Exp. Neurol. 210**,** 331-338.

García-Alías, G., López-Vales, R., Forés, J., Navarro, X., and Verdú, E., 2004. Acute transplantation of olfactory ensheathing cells or Schwann cells promotes recovery after spinal cord injury in the rat. J. Neurosci. Res. 75**,** 632-641.

Gautier, S. E., Oudega, M., Fragoso, M., Chapon, P., Plant, G. W., Bunge, M. B., and Parel, J.-M., 1998. Poly(alpha-hydroxyacids) for application in the spinal cord: resorbability and biocompatibility with adult rat Schwann cells and spinal cord. J. Biomed. Mater. Res. 42**,** 642-654.

Geller, H. M., and Fawcett, J. W., 2002. Building a bridge: engineering spinal cord repair. Exp. Neurol. 174**,** 125-136.

Gerndt, S. J., Rodriguez, J. L., Pawlik, J. W., Taheri, P. A., Wahl, W. L., Micheals, A. J., and Papadopoulos, S. M., 1997. Consequences of high-dose steroid therapy for acute spinal cord injury. J. Trauma 42**,** 279-284.

Giovanini, M. A., Reier, P. J., Eskin, T. A., Wirth, E., and Anderson, D. K., 1997. Characteristics of human fetal spinal cord grafts in the adult rat spinal cord: influences of lesion and grafting conditions. Exp. Neurol. 148**,** 523-543.

Grandpre, T., and Strittmatter, S. M., 2001. Nogo: a molecular determinant of axonal growth and regeneration. Neuroscientist 7**,** 377-386.

Grant, G. T., Morris, E. R., Rees, D. A., Smith, P. J. C., and Thom, D., 1973. Biological interactions between polysaccharides and divalent cations: the egg-box model. FEBS Lett. 32**,** 195-198.

Guest, J. D., Herrera, L., Margitich, I., Oliveria, M., Marcillo, A., and Casas, C. E., 2008. Xenografts of expanded primate olfactory ensheathing glia support transient behavioral recovery that is independent of serotonergic or corticospinal axonal regeneration in nude rats following spinal cord transection. Exp. Neurol. 212**,** 261-274.

Guest, J. D., Rao, A., Olson, L., Bunge, M. B., and Bunge, R. P., 1997. The ability of human Schwann cell grafts to promote regeneration in the transected nude rat spinal cord. Exp. Neurol. 148**,** 502-522.

Guo, J.-H., Skinner, G. W., Harcum, W. W., and Barnum, P. E., 1998. Pharmaceutical applications of naturally occurring water-soluble polymers. Pharm. Sci. Tech. Today 1**,** 254-261

Guo, J., Su, H., Zeng, Y., Liang, Y.-X., Wong, W. M., Ellis-Behnke, R. G., So, K.-F., and Wu, W., 2007. Reknitting the injured spinal cord by self-assembling peptide nanofiber scaffold. Nanomed. Nanotechnol. Biol. Med. 3**,** 311-321.

Gupta, D., Tator, C. H., and Shoichet, M. S., 2006. Fast-gelling injectable blend of hyaluronan and methylcellulose for intrathecal, localized delivery to the injured spinal cord. Biomaterials 27**,** 2370-2379.

Haipeng, G., Yinghui, Z., Jianchun, L., Yandao, G., Nanming, Z., and Xiufang, Z., 2000. Studies on nerve cell affinity of chitosan-derived materials. J. Biomed. Mater. Res. A 52**,** 285-295.

Hall, E. D., 1992. The neuroprotective pharmacology of methylprednisolone. J. Neurosurg. 76**,** 13-22.

Hall, E. D., and Springer, J. E., 2004. Neuroprotection and acute spinal cord injury: a reappraisal. NeuroRX 1**,** 80-100.

Hall, S., 2001. Nerve repair: a neurobiologist's view. J. Hand Surg. B. 26**,** 129-136.

Hanson, S., Lalor, P. A., Niemi, S. M., Northup, S. J., Ratner, B. D., Spector, M., Vale, B. H., and Willson, J. E., 1996. Testing biomaterials. In: Ratner, B. D., Hoffman, A. S., Schoen, F. J., and Lemons, J. E., (Eds.), Biomaterials science: an introduction to materials in medicine. Academic Press, San Diego, pp. 215-242.

Harvey, A. R., 2000. Use of cell/polymer hybrid structures as conduits for regenerative growth in the central nervous system. In: Saunders, N., and Dziegielewska, K. M., (Eds.), Degeneration and regeneration in the nervous system Harwood Academic Publishers, Amsterdam, pp. 191-203.

Hejčl, A., Lesný, P., Přádný, M., Šedý, J., Zámečník, J., Jendelová, P., Michálek, J., and Syková, E., 2009. Macroporous hydrogels based on 2-hydroxyethyl methacrylate. part 6: 3D hydrogels with positive and negative surface charges and polyelectrolyte complexes in spinal cord injury repair J. Mater. Sci. Mater. Med. 20**,** 1571-1577.

Hejčl, A., Urdzikova, L., Šedý, J., Lesný, P., Přádný, M., Michálek, J., Burian, M., Hajek, M., Zámečník, J., Jendelová, P., and Syková, E., 2008. Acute and delayed implantation of positively charged 2-hydroxyethyl methacrylate scaffolds in spinal cord injury in the rat. J. Neurosurg. Spine 8**,** 67-73.

Hercules, 1999. Aqualon(R) sodium carboxymethylcellulose: physical and chemical properties. Wilmington, DE.

Hou, S., Tian, W., Xu, Q., Cui, F., Zhang, J., Lu, Q., and Zhao, C., 2006. The enhancement of cell adherence and inducement of neurite outgrowth of dorsal root ganglia co-cultured with hyaluronic acid hydrogels modified with Nogo-66 receptor antagonist in vitro. Neuroscience 137**,** 519-529.

Hou, S., Xu, Q., Tian, W., Cui, F., Cai, Q., Ma, J., and Lee, I.-S., 2005. The repair of brain lesion by implantation of hyaluronic acid hydrogels modified with laminin. J. Neurosci. Methods 148**,** 60-70.

Houweling, D. A., Lankhorst, A. J., Gispen, W. H., Bär, P. R., and Joosten, E. A. J., 1998. Collagen containing neurotrophin-3 (NT-3) attracts regrowing injured corticospinal axons in the adult rat spinal cord and promotes partial functional recovery. Exp. Neurol. 153**,** 49-59.

Houweling, D. A., van Asseldonk, J. T. H., Lankhorst, A. J., Hamers, F. P. T., Martin, D., Bär, P. R., and Joosten, E. A. J., 1998. Local application of collagen containing brain-derived neurotrophic factor decreases the loss of function after spinal cord injury in the adult rat. Neurosci. Lett. 251**,** 193-196.

Hugenholtz, H., 2003. Methylprednisolone for acute spinal cord injury: not a standard of care. CMAJ 168**,** 1145-1146.

Hung, T. K., Lin, H. S., Bunegin, L., and Albin, M. S., 1982. Mechanical and neurological response of cat spinal cord under static loading. Surg. Neurol. 17**,** 213-217.

Hurtado, A., Moon, L. D. F., Maquet, V., Blits, B., Jerome, R., and Oudega, M., 2006. Poly (d,l-lactic acid) macroporous guidance scaffolds seeded with Schwann cells genetically modified to secrete a bi-functional neurotrophin implanted in the completely transected adult rat thoracic spinal cord. Biomaterials 27**,** 430-442.

Hynes, S. R., McGregor, L. M., Rauch, M. F., and Lavik, E. B., 2007. Photopolymerized poly(ethylene glycol)/poly(L-lysine) hydrogels for the delivery of neural progenitor cells. J. Biomater. Sci.-Polym. Ed. 18**,** 1017-1030.

Ikegami, T., Nakamura, M., Yamane, J., Katoh, H., Okada, S., Iwanami, A., Watanabe, K., Ishii, K., Kato, F., Fujita, H., Toyomi, T., Okano, H. J., Toyama, Y., and Okano, H., 2005. Chondroitinase ABC combined with neural stem/progenitor cell transplantation enhances graft cell migration and outgrowth of growth-associated protein-43-positive fibers after rat spinal cord injury. Eur. J. Neurosci. 22**,** 3036-3046.

Integra, 2005. NeuraGen™ nerve guide: advanced solutions for peripheral nerve repair. Integra LifeSciences Corp., Plainsboro, NJ, pp. 1-4.

ISP, 2000. Alginates: products for scientific water control. International Specialty Products, San Diego, CA.

Jain, A., Kim, Y.-T., McKeon, R. J., and Bellamkonda, R. V., 2006. In situ gelling hydrogels for conformal repair of spinal cord defects, and local delivery of BDNF after spinal cord injury. Biomaterials 27**,** 497-504.

Ji, B., Li, M., Budel, S., Pepinsky, R. B., Walus, L., Engber, T. M., Strittmatter, S. M., and Relton, J. K., 2005. Effect of combined treatment with methylprednisolone and soluble Nogo-66 receptor after rat spinal cord injury. Eur. J. Neurosci. 22**,** 587-594.

Jimenez Hamann, M. C., Tator, C. H., and Shoichet, M. S., 2005. Injectable intrathecal delivery system for localized administration of EGF and FGF-2 to the injured rat spinal cord. Exp. Neurol. 194**,** 106-119.

Jimenez Hamann, M. C., Tsai, E. C., Tator, C. H., and Shoichet, M. S., 2003. Novel intrathecal delivery system for treatment of spinal cord injury. Exp. Neurol. 182**,** 300-309.

Joosten, E. A. J., Bär, P. R., and Gispen, W. H., 1995. Directional regrowth of lesioned corticospinal tract axons in adult rat spinal cord. Neuroscience 69**,** 619-626.

Kakulas, B. A., 2004. Neuropathology: the foundation for new treatments in spinal cord injury. Spinal Cord 42**,** 549-563.

Kang, C. E., Poon, P. C., Tator, C. H., and Shoichet, M. S., 2009. A new paradigm for local and sustained release of therapeutic molecules to the injured spinal cord for neuroprotection and tissue repair. Tissue Eng. Part A 15**,** 595-604.

Kataoka, K., Suzuki, Y., Kitada, M., Hashimoto, T., Chou, H., Bai, H., Ohta, M., Wu, S., Suzuki, K., and Ide, C., 2004. Alginate enhances elongation of early regenerating axons in spinal cord of young rats. Tissue Eng. 10**,** 493-504.

Kataoka, K., Suzuki, Y., Kitada, M., Ohnishi, K., Suzuki, K., Tanihara, M., Ide, C., Endo, K., and Nishimura, Y., 2001. Alginate, a bioresorbable material derived from brown seaweed, enhances elongation of amputated axons of spinal cord in infant rats. J. Biomed. Mater. Res. 54**,** 373-384.

Kim, Y.-t., Caldwell, J.-M., and Bellamkonda, R. V., 2009. Nanoparticle-mediated local delivery of methylprednisolone after spinal cord injury. Biomaterials 30**,** 2582-2590.

Kitamura, Y., Yanagisawa, D., Takata, K., and Taniguchi, T., 2009. Neuroprotective function in brain microglia. Curr. Anaesthesia & Crit. Care 20**,** 142-147.

Kocsis, J. D., Lankford, K. L., Sasaki, M., and Radtke, C., 2009. Unique in vivo properties of olfactory ensheathing cells that may contribute to neural repair and protection following spinal cord injury. Neurosci. Lett. 456**,** 137-142.

Kuo, C. K., and Ma, P. X., 2001. Ionically crosslinked alginate hydrogels as scaffolds for tissue engineering: part 1. structure, gelation rate and mechanical properties. Biomaterials 22**,** 511-521.

Kwon, B. K., Tetzlaff, W., Grauer, J. N., Beiner, J., and Vaccaro, A. R., 2004. Pathophysiology and pharmacologic treatment of acute spinal cord injury. The Spine Journal 4**,** 451-464.

Lakatos, A., Barnett, S. C., and Franklin, R. J. M., 2003. Olfactory ensheathing cells induce less host astrocyte response and chondroitin sulphate proteoglycan expression than schwann cells following transplantation into adult cns white matter. Exp. Neurol. 184**,** 237-246.

Lakatos, A., Franklin, R. J. M., and Barnett, S. C., 2000. Olfactory ensheathing cells and Schwann cells differ in their in vitro interactions with astrocytes. Glia 32**,** 214-225.

Lane, M. A., Fuller, D. D., White, T. E., and Reier, P. J., 2008. Respiratory neuroplasticity and cervical spinal cord injury: translational perspectives. Trends Neurosci. 31**,** 538-547.

Lavdas, A. A., Papastefanaki, F., Thomaidou, D., and Matsas, R., 2008. Schwann cell transplantation for CNS repair. Curr. Med. Chem. 15**,** 151-160.

Laverty, P. H., Leskovar, A., Breur, G. J., Coates, J. R., Bergman, R. L., Widmer, W. R., Toombs, J. P., Shapiro, S., and Borgens, R. B., 2004. A preliminary study of intravenous surfactants in paraplegic dogs: polymer therapy in canine clinical SCI. J. Neurotrauma 21**,** 1767–1777.

Letourneau, P. C., 2001. Preparation of substrata for in vitro culture of neurons. In: Fedoroff, S., and Richardson, A., (Eds.), Protocols for neural cell culture. Humana Press, Totowa, NJ, pp. 245-254.

Li, S., Kim, J.-E., Budel, S., Hampton, T. G., and Strittmatter, S. M., 2005. Transgenic inhibition of Nogo-66 receptor function allows axonal sprouting and improved locomotion after spinal injury. Mol. Cell. Neurosci. 29**,** 26-39.

Li, X., Yang, Z., Zhang, A., Wang, T., and Chen, W., 2009. Repair of thoracic spinal cord injury by chitosan tube implantation in adult rats. Biomaterials 30**,** 1121-1132.

Li, Y., Field, P. M., and Raisman, G., 1997. Repair of adult rat corticospinal tract by transplants of olfactory ensheathing cells. Science 277**,** 2000-2002.

Li, Y., Field, P. M., and Raisman, G., 1998. Regeneration of adult rat corticospinal axons induced by transplanted olfactory ensheathing cells. J. Neurosci. 18**,** 10514-10524.

Li, Y., Li, D., Khaw, P. T., and Raisman, G., 2008. Transplanted olfactory ensheathing cells incorporated into the optic nerve head ensheathe retinal ganglion cell axons: Possible relevance to glaucoma. Neurosci. Lett. 440**,** 251-254.

Li, Y., Sauve, Y., Li, D., Lund, R. D., and Raisman, G., 2003. Transplanted olfactory ensheathing cells promote regeneration of cut adult rat optic nerve axons. J. Neurosci. 23**,** 7783-7788.

Lima, C., Pratas-Vital, J., Escada, P., Hasse-Ferreira, A., Capucho, C., and Peduzzi, J. D., 2006. Olfactory mucosa autografts in human spinal cord injury: a pilot clinical study. J. Spinal Cord Med. 29**,** 191–203.

Liu-Snyder, P., Logan, M. P., Shi, R., Smith, D. T., and Borgens, R. B., 2007. Neuroprotection from secondary injury by polyethylene glycol requires its internalization. J. Exp. Biol. 210**,** 1455-1462.

Liu, S., Said, G., and Tadie, M., 2001. Regrowth of the rostral spinal axons into the caudal ventral roots through a collagen tube implanted into hemisected adult rat spinal cord. Neurosurgery 49**,** 143-151.

Loh, N. K., Woerly, S., Bunt, S. M., Wilton, S. D., and Harvey, A. R., 2001. The regrowth of axons within tissue defects in the CNS is promoted by implanted hydrogel matrices that contain BDNF and CNTF producing fibroblasts. Exp. Neurol. 170**,** 72-84.

López-Vales, R., Forés, J., Navarro, X., and Verdú, E., 2006. Olfactory ensheathing glia graft in combination with FK506 administration promote repair after spinal cord injury. Neurobiol. Dis. 24**,** 443-454.

López-Vales, R., Forés, J., Verdú, E., and Navarro, X., 2006. Acute and delayed transplantation of olfactory ensheathing cells promote partial recovery after complete transection of the spinal cord. Neurobiol. Dis. 21**,** 57-68.

Louro, J., and Pearse, D. D., 2008. Stem and progenitor cell therapies: recent progress for spinal cord injury repair. Neurol. Res. 30**,** 5-16.

Luo, J., Borgens, R., and Shi, R., 2002. Polyethylene glycol immediately repairs neuronal membranes and inhibits free radical production after acute spinal cord injury. J. Neurochem. 83**,** 471-480.

Mackay-Sim, A., Féron, F., Cochrane, J., Bassingthwaighte, L., Bayliss, C., Davies, W., Fronek, P., Gray, C., Kerr, G., Licina, P., Nowitzke, A., Perry, C., Silburn, P. A. S., Urquhart, S., and Geraghty, T., 2008. Autologous olfactory ensheathing cell transplantation in human paraplegia: a 3-year clinical trial. Brain 131**,** 2376–2386.

Mahoney, M. J., and Anseth, K. S., 2006. Three-dimensional growth and function of neural tissue in degradable polyethylene glycol hydrogels. Biomaterials 27**,** 2265–2274.

Mallek, J. D., 2006. Hyaluronic acid-olfactory ensheathing cell compositions for spinal cord injury nerve regeneration, (Thesis), University of Florida, Gainesville, FL.

Marijnissen, W. J. C. M., van Osch, G. J. V. M., Aigner, J., Verwoerd-Verhoef, H. L., and Verhaar, J. A. N., 2000. Tissue-engineered cartilage using serially passaged articular chondrocytes. Chondrocytes in alginate, combined in vivo with a synthetic (E210) or biologic biodegradable carrier (DBM). Biomaterials 21**,** 571-580.

Martin, B. C., Minner, E. J., Wiseman, S. L., Klank, R. L., and Gilbert, R. J., 2008. Agarose and methylcellulose hydrogel blends for nerve regeneration applications. Journal of Neural Engineering 5**,** 221-231.

Martin, D., Robe, P., Franzen, R., Delrée, P., Schoenen, J., Stevenaert, A., and Moonen, G., 1996. Effects of Schwann cell transplantation in a contusion model of rat spinal cord injury. J. Neurosci. Res. 45**,** 588-597.

McDonald, J. W., Liu, X.-Z., Qu, Y., Liu, S., Mickey, S. K., Turetsky, D., Gottlieb, D. I., and Choi, D. W., 1999. Transplanted embryonic stem cells survive, differentiate and promote recovery in injured rat spinal cord. Nat. Med. 5**,** 1410-1412.

McGraw, J., Hiebert, G. W., and Steeves, J. D., 2001. Modulating astrogliosis after neurotrauma. J. Neurosci. Res. 63**,** 109-115.

Meakin, J. R., Hukins, D. W. L., Aspden, R. M., and Imrie, C. T., 2003. Rheological properties of poly(2-hydroxyethyl methacrylate) (pHEMA) as a function of water content and deformation frequency Journal of Materials Science - Materials in Medicine 14**,** 783-787.

Mentak, K., 1993. Tissue-protective hydrophilic polymer solutions and surface modifications, (Dissertation), University of Florida, Gainesville, FL.

Metzger, T. G., 2006. The rheology handbook: for users of rotational and oscillatory rheometers. Vincentz Network GmbH & Co. KG, Hannover, Germany.

Miller, S. M., 2008. Methylpredisolone in acute spinal cord injury: a tarnished standard. J. Neurosurg. Anesthesiol. 20**,** 140-142.

Mingyu, C., Kai, G., Jiamou, L., Yandao, G., Nanming, Z., and Xiufang, Z., 2004. Surface modification and characterization of chitosan film blended with poly-L-lysine. J. Biomater. Appl. 19**,** 59-75.

Moe, S. T., Draget, K. I., Skjak-Braek, G., and Smidsrod, O., 1995. Alginates. In: Stephen, A. M., (Ed.), Food polysaccharides and their applications. Marcel Dekker, New York, pp. 245-286.

Mosahebi, A., Simon, M., Wiberg, M., and Terenghi, G., 2001. A novel use of alginate hydrogel as Schwann cell matrix. Tissue Eng. 7**,** 525-534.

Navarro, X., Verdú, E., Rodríguez, F. J., and Ceballos, D., 2001. Artificial nerve graft for the repair of peripheral nerve injuries. Neurol. Sci. 22**,** S7-S13.

Nisbet, D. R., Crompton, K. E., Horne, M. K., Finkelstein, D. I., and Forsythe, J. S., 2008. Neural tissue engineering of the CNS using hydrogels. J. Biomed. Mater. Res. B 87B**,** 251-263.

Nisbet, D. R., Moses, D., Gengenbach, T. R., Forsythe, J. S., Finkelstein, D. I., and Horne, M. K., 2009. Enhancing neurite outgrowth from primary neurones and neural stem cells using thermoresponsive hydrogel scaffolds for the repair of spinal cord injury. J Biomed Mater Res A 89**,** 24-35.

Nomura, H., Baladie, B., Katayama, Y., Morshead, C. M., Shoichet, M. S., and Tator, C. H., 2008. Delayed implantation of intramedullary chitosan channels containing nerve grafts promotes extensive axonal regeneration after spinal cord injury. Neurosurgery 63**,** 127-143.

Nomura, H., Katayama, Y., Shoichet, M. S., and Tator, C. H., 2006. Complete spinal cord transection treated by implantation of a reinforced synthetic hydrogel channel results in syringomelia and caudal migration of the rostral stump. Neurosurgery 59**,** 183-192.

Nomura, H., Tator, C. H., and Shoichet, M. S., 2006. Bioengineered strategies for spinal cord repair. J. Neurotrauma 23**,** 496-507.

Notterpek, L., Snipes, G. J., and Shooter, E. M., 1999. Temporal expression pattern of peripheral myelin protein 22 during in vivo and in vitro myelination. Glia 25**,** 358-369.

Noushi, F., Richardson, R. T., Hardman, J., Clark, G., and O'Leary, S., 2005. Delivery of neurotrophin-3 to the cochlea using alginate beads. Otology & Neurotology 26**,** 528-533.

Novikova, L. N., Mosahebi, A., Wiberg, M., Terenghi, G., Kellerth, J.-O., and Novikov, L. N., 2006. Alginate hydrogel and matrigel as potential cell carriers for neurotransplantation. J. Biomed. Mater. Res. A 77A**,** 242-252.

Novikova, L. N., Novikov, L. N., and Kellerth, J.-O., 2003. Biopolymers and biodegradable smart implants for tissue regeneration after spinal cord injury. Curr. Opin. Neurol. 16**,** 711-715.

NSCISC, 2007. The 2007 annual statistical report for the spinal cord injury model systems. University of Alabama at Birmingham, Birmingham, AL.

NSCISC, 2008. Spinal cord injury facts and figures at a glance. University of Alabama at Birmingham, Birmingham, AL, (http://images.main.uab.edu/spinalcord/pdffiles/Facts08.pdf), accessed August 2008.

Ogushi, Y., Sakai, S., and Kawakami, K., 2007. Synthesis of enzymatically-gellable carboxymethylcellulose for biomedical applications. J. Biosci. Bioeng. 104**,** 30-33.

Oudega, M., Gautier, S. E., Chapon, P., Fragoso, M., Bates, M. L., Parel, J.-M., and Bartlett Bunge, M., 2001. Axonal regeneration into Schwann cell grafts within resorbable poly([alpha]-hydroxyacid) guidance channels in the adult rat spinal cord. Biomaterials 22**,** 1125-1136.

Oudega, M., Moon, L. D. F., and de Almeida Leme, R. J., 2005. Schwann cells for spinal cord repair. Braz. J. Med. Biol. Res. 38**,** 825-835.

Ozawa, H., Matsumoto, T., Ohashi, T., Sato, M., and Kokubun, S., 2001. Comparison of spinal cord gray matter and white matter softness: measurement by pipette aspiration method. J. Neurosurg. Spine 2 95**,** 221–224.

Ozawa, H., Matsumoto, T., Ohashi, T., Sato, M., and Kokubun, S., 2004. Mechanical properties and function of the spinal pia mater. J. Neurosurg. Spine 1 1**,** 122–127.

Patist, C. M., Mulder, M. B., Gautier, S. E., Maquet, V., Jérôme, R., and Oudega, M., 2004. Freeze-dried poly(D,L-lactic acid) macroporous guidance scaffolds impregnated with brain-derived neurotrophic factor in the transected adult rat thoracic spinal cord. Biomaterials 25**,** 1569-1582.

Peck, L. S., Quigg, J. M., Fossum, G. T., and Goldberg, E. P., 1995. Evaluation of CMC and HA solutions for adhesiolysis. J. Invest. Surg. 8**,** 337-348.

Peppas, N. A., 2009. Hydrogels. In: Ratner, B. D., Dyro, J., Grimnes, S. J., and Schoen, F. J., (Eds.), Biomedical engineering desk reference. Academic Press, pp. 188-195.

Piantino, J., Burdick, J. A., Goldberg, D., Langer, R., and Benowitz, L. I., 2006. An injectable, biodegradable hydrogel for trophic factor delivery enhances axonal rewiring and improves performance after spinal cord injury. Exp. Neurol. 201**,** 359-367.

Pocker, Y., and Green, E., 1973. Hydrolysis of D-glucono-delta-lactone I. general acid-base catalysis, solvent deuterium isotope effects, and transition state characterization. J. Am. Chem. Soc. 95**,** 113-119.

Prang, P., Müller, R., Eljaouhari, A., Heckmann, K., Kunz, W., Weber, T., Faber, C., Vroemen, M., Bogdahn, U., and Weidner, N., 2006. The promotion of oriented axonal regrowth in the injured spinal cord by alginate-based anisotropic capillary hydrogels. Biomaterials 27**,** 3560-3569.

Prewitt, C. M. F., Niesman, I. R., Kane, C. J. M., and Houlé, J. D., 1997. Activated macrophage/microglial cells can promote the regeneration of sensory axons into the injured spinal cord. Exp. Neurol. 148**,** 433-443.

Profyris, C., Cheema, S. S., Zang, D., Azari, M. F., Boyle, K., and Petratos, S., 2004. Degenerative and regenerative mechanisms governing spinal cord injury. Neurobiol. Dis. 15**,** 415-436.

Purves, D., Augustine, G. J., Fitzpatrick, D., Hall, W. C., LaMantia, A.-S., McNamara, J. O., and White, L. E., 2008. Neuroscience. Sinauer Associates, Inc., Sunderland, MA.

Qi, M., Strand, B. L., Morch, Y., Lacik, I., Wang, Y., Salehi, P., Barbaro, B., Gangemi, A., Kuechle, J., Romagnoli, T., Hansen, M. A., Rodriguez, L. A., Benedetti, E., Hunkeler, D., Skjak-Brajk, G., and Oberholzer, J., 2008. Encapsulation of human islets in novel inhomogeneous alginate-Ca2+/Ba2+ Microbeads: in vitro and in vivo function. Artif. Cells. Blood Substit. Immobil. Biotechnol. 36**,** 403-420.

Qian, T., Guo, X., Levi, A. D., Vanni, S., Shebert, R. T., and Sipski, M. L., 2005. High-dose methylprednisolone may cause myopathy in acute spinal cord injury patients. Spinal Cord 43**,** 199-203.

Rabchevsky, A. G., Fugaccia, I., Sullivan, P. G., Blades, D. A., and Scheff, S. W., 2002. Efficacy of methylprednisolone therapy for the injured rat spinal cord. J. Neurosci. Res. 68**,** 7-18.

Rabchevsky, A. G., and Streit, W. J., 1997. Grafting of cultured microglial cells into the lesioned spinal cord of adult rats enhances neurite outgrowth. J. Neurosci. Res. 47**,** 34-48.

Ramer, L., Ramer, M., and Steeves, J., 2005. Setting the stage for functional repair of spinal cord injuries: a cast of thousands. Spinal Cord 43**,** 134-161.

Ramer, L. M., Au, E., Richter, M. W., Liu, J., Tetzlaff, W., and Roskams, A. J., 2004. Peripheral olfactory ensheathing cells reduce scar and cavity formation and promote regeneration after spinal cord injury. J. Comp. Neurol. 473**,** 1-15.

Ramón-Cueto, A., and Avila, J., 1998. Olfactory ensheathing glia: properties and function. Brain Res. Bull. 46**,** 175-187.

Ramón-Cueto, A., Cordero, M. I., Santos-Benito, F. F., and Avila, J., 2000. Functional recovery of paraplegic rats and motor axon regeneration in their spinal cords by olfactory ensheathing glia. Neuron 25**,** 425-435.

Ramón-Cueto, A., and Nieto-Sampedro, M., 1994. Regeneration into the spinal cord of transected dorsal root axons is promoted by ensheathing glia transplants. Exp. Neurol. 127**,** 232-244

Rasouli, A., Bhatia, N., Suryadevara, S., Cahill, K., and Gupta, R., 2006. Transplantation of Preconditioned Schwann Cells in Peripheral Nerve Grafts After Contusion in the Adult Spinal Cord. Improvement of Recovery in a Rat Model. J. Bone Joint Surg. Am. 88**,** 2400-2410.

Reier, P. J., 2004. Cellular transplantation strategies for spinal cord injury and translational neurobiology. NeuroRX 1**,** 424-451.

Reier, P. J., 2004. Cellular transplantation strategies for spinal cord injury and translational neurobiology. NeuroRx 1**,** 424-451.

Reier, P. J., and Lane, M. A., 2008. Degeneration, regeneration, and plasticity in the nervous system In: Conn, P. M., (Ed.), Neuroscience in medicine. Humana Press, Totowa, NJ, pp. 691-727.

Ren, Y.-J., Zhou, Z.-Y., Cui, F.-Z., Ying, W., Zhao, J.-P., and Xu, Q.-Y., 2009. Hyaluronic acid/polylysine hydrogel as a transfer system for transplantation of neural stem cells. J. Bioact. Compatible Polym. 24**,** 56-62.

Richardson, P. M., McGuinness, U. M., and Aguayo, A. J., 1980. Axons from CNS neurons regenerate into PNS grafts. Nature 284**,** 264-265.

Ronsyn, M. W., Berneman, Z. N., Van Tendeloo, V. F. I., Jorens, P. G., and Ponsaerts, P., 2008. Can cell therapy heal a spinal cord injury? Spinal Cord 46**,** 532-539.

Ross-Murphy, S. B., 1995. Structure-property relationships in food biopolymer gels and solutions. J. Rheol. 39**,** 1451-1463.

Saberi, H., Moshayedi, P., Aghayan, H.-R., Arjmand, B., Hosseini, S.-K., Emami-Razavi, S.-H., Rahimi-Movaghar, V., Raza, M., and Firouzi, M., 2008. Treatment of chronic thoracic spinal cord injury patients with autologous Schwann cell transplantation: an interim report on safety considerations and possible outcomes. Neurosci. Lett. 443**,** 46-50.

Samadikuchaksaraei, A., 2007. An overview of tissue engineering approaches for management of spinal cord injuries. Journal of NeuroEngineering and Rehabilitation 4**,** 15.

Sambanis, A., 2003. Encapsulated islets in diabetes treatment. Diabetes Technol. Ther. 5**,** 665-668.

Scheff, S., and Roberts, K. N., 2009. Infinite horizon spinal cord contusion model. In: Chen, J., Xu, X.-M., Xu, Z. C., and Zhang, J. H., (Eds.), Animal models of acute neurological injuries. Humana Press, New York.

Scheff, S. W., Rabchevsky, A. G., Fugaccia, I., Main, J. A., and James E. Lumpp, J., 2003. Experimental modeling of spinal cord injury: characterization of a force-defined injury device. J. Neurotrauma 20**,** 179-193.

Segura, T., Anderson, B. C., Chung, P. H., Webber, R. E., Shull, K. R., and Shea, L. D., 2005. Crosslinked hyaluronic acid hydrogels: a strategy to functionalize and pattern. Biomaterials 26**,** 359-371.

Sherman, L. S., Struve, J. N., Rangwala, R., Wallingford, N. M., Tuohy, T. M. F., and Kuntz, C., 2002. Hyaluronate-based extracellular matrix: keeping glia in their place. Glia 38**,** 93-102.

Shi, R., and Borgens, R. B., 1999. Acute repair of crushed guinea pig spinal cord by polyethylene glycol. J. Neurophysiol. 81**,** 2406-2414.

Shi, R., and Borgens, R. B., 2000. Anatomical repair of nerve membranes in crushed mammalian spinal cord with polyethylene glycol. J. Neurocytol. 29**,** 633–643.

Short, D. J., Masry, W. S. E., and Jones, P. W., 2000. High dose methylprednisolone in the management of acute spinal cord injury - a systematic review from a clinical perspective. Spinal Cord 38**,** 273-286.

Silva, G. A., Czeisler, C., Niece, K. L., Beniash, E., Harrington, D. A., Kessler, J. A., and Stupp, S. I., 2004. Selective differentiation of neural progenitor cells by high-epitope density nanofibers. Science 303**,** 1352-1355.

Simpson, N. E., Stabler, C. L., Simpson, C. P., Sambanis, A., and Constantinidis, I., 2004. The role of the CaCl2-guluronic acid interaction on alginate encapsulated [beta]TC3 cells. Biomaterials 25**,** 2603-2610.

Skjåk-Bræk, G., Grasdalen, H., and Smidsrød, O., 1989. Inhomogeneous polysaccharide ionic gels. Carbohydr. Polym. 10**,** 31-54.

Smidsrød, O., and Skjåk-Bræk, G., 1990. Alginate as immobilization matrix for cells. Trends Biotechnol. 8**,** 71-78.

Soon-Shiong, P., 1999. Treatment of type I diabetes using encapsulated islets. Adv. Drug Del. Rev. 35**,** 259-270.

Stabenfeldt, S. E., García, A. J., and LaPlaca, M. C., 2006. Thermoreversible laminin-functionalized hydrogel for neural tissue engineering. J. Biomed. Mater. Res. A 77A**,** 718-725.

Stang, F., Fansa, H., Wolf, G., Reppin, M., and Keilhoff, G., 2005. Structural parameters of collagen nerve grafts influence peripheral nerve regeneration. Biomaterials 26**,** 3083-3091.

Stevens, M. M., Qanadilo, H. F., Langer, R., and Prasad Shastri, V., 2004. A rapid-curing alginate gel system: utility in periosteum-derived cartilage tissue engineering. Biomaterials 25**,** 887-894.

Steward, O., Zheng, B., and Tessier-Lavigne, M., 2003. False resurrections: distinguishing regenerated from spared axons in the injured central nervous system. J. Comp. Neurol. 459**,** 1-8.

Stokes, B. T., and Jakeman, L. B., 2002. Experimental modelling of human spinal cord injury: a model that crosses the species barrier and mimics the spectrum of human cytopathology. Spinal Cord 40**,** 101-109.

Stokols, S., and Tuszynski, M. H., 2004. The fabrication and characterization of linearly oriented nerve guidance scaffolds for spinal cord injury. Biomaterials 25**,** 5839-5846.

Stokols, S., and Tuszynski, M. H., 2006. Freeze-dried agarose scaffolds with uniaxial channels stimulate and guide linear axonal growth following spinal cord injury. Biomaterials 27**,** 443-451.

Stopek, J. B., 2003. Biopolymer-microglia cell compositions for neural tissue repair, (Dissertation), University of Florida, Gainesville, FL.

Stopek, J. B., Streit, W. J., and Goldberg, E. P., 2002. Opportunities for axon repair in the CNS: use of microglia and biopolymer compositions. In: Streit, W. J., (Ed.), Microglia in the regenerating and degenerating central nervous system. Springer, New York, pp. 227-244.

Straatmann, A., and Borchard, W., 2003. Phase separation in calcium alginate gels. Eur. Biophys. J. 32**,** 412-417.

Streit, W. J., 2001. Microglia and macrophages in the developing CNS. Neurotoxicology 22**,** 619-624.

Streit, W. J., 2002. Physiology & pathophysiology of microglial cell function. In: Streit, W. J., (Ed.), Microglia in the regenerating and degenerating central nervous system. Springer, New York, pp. 1-14.

Struve, J., Maher, P. C., Li, Y. Q., Kinney, S., Fehlings, M. G., Kuntz, C., and Sherman, L. S., 2005. Disruption of the hyaluronan-based extracellular matrix in spinal cord promotes astrocyte proliferation. Glia 52**,** 16-24.

Suzuki, K., Suzuki, Y., Ohnishi, K., Endo, K., Tanihara, M., and Nishimura, Y., 1999. Regeneration of transected spinal cord in young adult rats using freeze-dried alginate gel. Neuroreport 10**,** 2891-2894.

Suzuki, Y., Kitaura, M., Wu, S., Kataoka, K., Suzuki, K., Endo, K., Nishimura, Y., and Ide, C., 2002. Electrophysiological and horseradish peroxidase-tracing studies of nerve regeneration through alginate-filled gap in adult rat spinal cord. Neurosci. Lett. 318**,** 121-124.

Talac, R., Friedman, J. A., Moore, M. J., Lu, L., Jabbari, E., Windebank, A. J., Currier, B. L., and Yaszemski, M. J., 2004. Animal models of spinal cord injury for evaluation of tissue engineering treatment strategies. Biomaterials 25**,** 1505-1510.

Teng, Y. D., Lavik, E. B., Qu, X., Park, K. I., Ourednik, J., Zurakowski, D., Langer, R., and Snyder, E. Y., 2002. Functional recovery following traumatic spinal cord injury mediated by a unique polymer scaffold seeded with neural stem cells. Proceedings of the National Academy of Sciences of the United States of America 99**,** 3024-3029.

Tester, N. J., and Howland, D. R., 2008. Chondroitinase ABC improves basic and skilled locomotion in spinal cord injured cats. Exp. Neurol. 209**,** 483-496.

Tewarie, R. S. N., Hurtado, A., Bartels, R. H., Grotenhuis, A., and Oudega, M., 2009. Stem cell–based therapies for spinal cord injury. J. Spinal Cord Med. 32**,** 105-114.

Tian, W. M., Hou, S. P., Ma, J., Zhang, C. L., Xu, Q. Y., Lee, I. S., Li, H. D., Spector, M., and Cui, F. Z., 2005. Hyaluronic acid–poly-D-lysine-based three-dimensional hydrogel for traumatic brain injury. Tissue Eng. 11**,** 513-525.

Tian, W. M., Zhang, C. L., Hou, S. P., Yu, X., Cui, F. Z., Xu, Q. Y., Sheng, S. L., Cui, H., and Li, H. D., 2005. Hyaluronic acid hydrogel as Nogo-66 receptor antibody delivery system for the repairing of injured rat brain: in vitro. J. Controlled Release 102**,** 13-22.

Tomaselli, K. J., Damsky, C. H., and Reichardt, L. E., 1987. Interactions of a neuronal cell line (PC12) with laminin, collagen IV, and fibronectin: identification of integrin-related glycoproteins involved in attachment and process outgrowth. J. Cell Biol. 105**,** 2347-2358.

Tønnesen, H. H., and Karlsen, J., 2002. Alginate in drug delivery systems. Drug Dev. Ind. Pharm. 28**,** 621-630.

Toole, B. P., 2001. Hyaluronan in morphogenesis. Semin. Cell Dev. Biol. 12**,** 79-87.

Trivedi, N., Keegan, M., Steil, G. M., Hollister-Lock, J., Hasenkamp, W. M., Colton, C. K., Bonner-Weir, S., and Weir, G. C., 2001. Islets in alginate macrobeads reverse diabetes despite minimal acute insulin secretory responses. Transplantation 71**,** 203-211.

Tsai, E. C., Dalton, P. D., Shoichet, M. S., and Tator, C. H., 2004. Synthetic hydrogel guidance channels facilitate regeneration of adult rat brainstem motor axons after complete spinal cord transection. J. Neurotrauma 21**,** 789–804.

Tsai, E. C., Dalton, P. D., Shoichet, M. S., and Tator, C. H., 2006. Matrix inclusion within synthetic hydrogel guidance channels improves specific supraspinal and local axonal regeneration after complete spinal cord transection. Biomaterials 27**,** 519-533.

Tung, C.-Y. M., and Dynes, P. J., 1982. Relationship between viscoelastic properties and gelation in thermosetting systems. J. Appl. Polym. Sci. 27**,** 569-574.

Tysseling-Mattiace, V. M., Sahni, V., Niece, K. L., Birch, D., Czeisler, C., Fehlings, M. G., Stupp, S. I., and Kessler, J. A., 2008. Self-assembling nanofibers inhibit glial scar formation and promote axon elongation after spinal cord injury. J. Neurosci. 28**,** 3814-3823.

Wang, C., Liu, H., Gao, Q., Liu, X., and Tong, Z., 2008. Alginate-calcium carbonate porous microparticle hybrid hydrogels with versatile drug loading capabilities and variable mechanical strengths. Carbohydr. Polym. 71**,** 476-480.

Wang, Y.-C., Wu, Y.-T., Huang, H.-Y., Lin, H.-I., Lo, L.-W., Tzeng, S.-F., and Yang, C.-S., 2008. Sustained intraspinal delivery of neurotrophic factor encapsulated in biodegradable nanoparticles following contusive spinal cord injury. Biomaterials 29**,** 4546-4553.

Wei, Y. T., Tian, W. M., yu, X., Cui, F. Z., Hou, S. P., Xu, Q. Y., and Lee, I.-S., 2007. Hyaluronic acid hydrogels with IKVAV peptides for tissue repair and axonal regeneration in an injured rat brain. Biomed. Mater. 2**,** S142-S146.

West, D. C., Hampson, I. N., Arnold, F., and Kumar, S., 1985. Angiogenesis induced by degradation products of hyaluronic acid. Science 228**,** 1324-1326.

Willerth, S. M., and Sakiyama-Elbert, S. E., 2008. Cell therapy for spinal cord regeneration. Adv. Drug Del. Rev. 60**,** 263-276.

Winter, H. H., and Chambon, F., 1986. Analysis of linear viscoelasticity of a crosslinking polymer at the gel point. J. Rheol. 30**,** 367-382.

Woerly, S., Doan, V. D., Evans-Martin, F., Paramore, C. G., and Peduzzi, J. D., 2001. Spinal cord reconstruction using NeuroGel (TM) implants and functional recovery after chronic injury. J. Neurosci. Res. 66**,** 1187-1197.

Woerly, S., Doan, v. D., Sosa, N., de Vellis, J., and Espinosa, A., 2001. Reconstruction of the transected cat spinal cord following NeuroGel(TM) implantation: axonal tracing, immunohistochemical and ultrastructural studies. Int. J. Dev. Neurosci. 19**,** 63-83.

Woerly, S., Doan, V. D., Sosa, N., Vellis, J. d., and Espinosa-Jeffrey, A., 2004. Prevention of gliotic scar formation by NeuroGel (TM) allows partial endogenous repair of transected cat spinal cord. J. Neurosci. Res. 75**,** 262-272.

Woerly, S., Petrov, P., Sykova, E., Roitbak, T., Simonova, Z., and Harvey, A. R., 1999. Neural tissue formation within porous hydrogels implanted in brain and spinal cord lesions: ultrastructural, immunohistochemical, and diffusion studies. Tissue Eng. 5**,** 467-488.

Woerly, S., Pinet, E., de Robertis, L., Bousmina, M., Laroche, G., Roitback, T., Vargová, L., and Syková, E., 1998. Heterogeneous PHPMA hydrogels for tissue repair and axonal regeneration in the injured spinal cord J. Biomater. Sci., Polym. Ed. 9**,** 681-711.

Woerly, S., Pinet, E., de Robertis, L., Van Diep, D., and Bousmina, M., 2001. Spinal cord repair with PHPMA hydrogel containing RGD peptides (NeuroGel(TM)). Biomaterials 22**,** 1095-1111.

Woerly, S., Plant, G. W., and Harvey, A. R., 1996. Cultured rat neuronal and glial cells entrapped within hydrogel polymer matrices: a potential tool for neural tissue replacement. Neurosci. Lett. 205**,** 197-201.

Woerly, S., Plant, G. W., and Harvey, A. R., 1996. Neural tissue engineering: from polymer to biohybrid organs. Biomaterials 17**,** 301-310.

Wong, D. Y., Leveque, J. C., Brumblay, H., Krebsbach, P. H., Hollister, S. J., and Lamarca, F., 2008. Macro-architectures in spinal cord scaffold implants influence regeneration. Journal of neurotrauma 25**,** 1027-1037.

Wu, S., Suzuki, Y., Kitada, M., Kitaura, M., Kataoka, K., Takahashi, J., Ide, C., and Nishimura, Y., 2001. Migration, integration, and differentiation of hippocampus-derived neurosphere cells after transplantation into injured rat spinal cord. Neurosci. Lett. 312**,** 173-176.

Xu, X., Urban, J. P. G., Browning, J. A., Tirlapur, U., Wilkins, R. J., Wu, M. H., Cui, Z., and Cui, Z., 2007. Influences of buffer systems on chondrocyte growth during long-term culture in alginate. Osteoarthritis Cartilage 15**,** 396-402.

Xu, X. M., Chen, A., Guenard, V., Kleitman, N., and Bunge, M. B., 1997. Bridging Schwann cell transplants promote axonal regeneration from both the rostral and caudal stumps of transected adult rat spinal cord J. Neurocytol. 26**,** 1-16.

Yick, L.-W., Cheung, P.-T., So, K.-F., and Wu, W., 2003. Axonal regeneration of Clarke's neurons beyond the spinal cord injury scar after treatment with chondroitinase ABC. Exp. Neurol. 182**,** 160-168.

Yoshii, S., Ito, S., Shima, M., Taniguchi, A., and Akagi, M., 2009. Functional restoration of rabbit spinal cord using collagen-filament scaffold. J.Tissue Eng. Regen. Med. 3**,** 19-25.

Yoshii, S., Oka, M., Shima, M., Akagi, M., and Taniguchi, A., 2003. Bridging a spinal cord defect using collagen filament. Spine 28**,** 2346-2351.

Yoshii, S., Oka, M., Shima, M., Taniguchi, A., Taki, Y., and Akagi, M., 2004. Restoration of function after spinal cord transection using a collagen bridge. J. Biomed. Mater. Res. A 70A**,** 569-575.

Yu, P., Huang, L., Zou, J., Yu, Z., Wang, Y., Wang, X., Xu, L., Liu, X., Xu, X.-M., and Lu, P.-H., 2008. Immunization with recombinant Nogo-66 receptor (NgR) promotes axonal regeneration and recovery of function after spinal cord injury in rats. Neurobiol. Dis. 32**,** 535-542.

Yu, X., Dillon, G. P., and Bellamkonda, R. V., 1999. A laminin and nerve growth factor-laden three-dimensional scaffold for enhanced neurite extension. Tissue Eng. 5**,** 291-304.

Zeng, Q., Yu, Z., You, J., and Zhang, Q., 2007. Efficacy and safety of Seprafilm for preventing postoperative abdominal adhesion: systematic review and meta-analysis. World J. Surg. 31**,** 2125-2131.

Zheng, Z., Liu, C., Zhang, L., Gao, R., Wei, S., Zhang, K., and Zhang, L., 2007. Olfactory ensheathing cell transplantation in 106 patients with old spinal cord injury: differences in ages, sexes, disease courses, injured types and sites. Neural Regen.Res. 2**,** 380-384.

Zhong, Y., and Bellamkonda, R. V., 2008. Biomaterials for the central nervous system. J. R. Soc. Interface 5**,** 957–975.

Zimmer, M. B., Nantwi, K., and Goshgarian, H. G., 2007. Effect of spinal cord injury on the respiratory system: basic research and current clinical treatment options. J. Spinal Cord Med. 30**,** 319-330.

BIOGRAPHICAL SKETCH

Samesha R. Barnes was born in Fort Gordon, Georgia. She was reared in the Richmond County school system in Augusta, Georgia where she attended the award-winning John S. Davidson Fine Arts Magnet High School. Samesha excelled in academics and in the arts and was especially gifted in violin, flute, French and Japanese. Samesha had the opportunity to travel to Takarazuka, Japan as a representative of the Foreign Langauge Department on a school exchange visit for which she was selected on the basis of her academic achievement in Japanese Studies during her senior. In addition to her affection for the arts, Samesha had a love for science, math and engineering which was enhanced by her participation in the Research and Engineering Apprenticeship Program (REAP). She graduated with honors and moved to Atlanta, Georgia to follow her dream of becoming a chemical engineer.

Samesha enrolled in the Atlanta University Center's Dual-Degree Engineering Program where she pursued degrees in chemistry and chemical engineering from Clark Atlanta University (CAU) and the Georgia Institute of Technology. She was a member of the CAU Honors Program and a High Performance Polymers and Ceramics (HiPPAC) fellow which afforded the opportunity to conduct scholarly research throughout her undergraduate matriculation. In addition, Samesha participated in undergraduate research programs in the summer, including the Summer Undergraduate Research Program (SURP) at Virginia Tech.

After graduating in 1996, Samesha began her professional career as a Product Development Engineer in Hewlett-Packard's Inkjet Media Division in San Diego, California where she previously worked as an intern. She served on the recruiting team and also filed an invention disclosure for a product idea. After two years in industry Samesha decided to pursue an advanced degree in materials science and engineering.

Samesha continued her education at the University of Florida and earned a master of science in 2003. During her tenure at the university she received an Alumni Association Fellowship, an NSF Alliance for Graduate Education and the Professoriate (AGEP) Fellowship and was a part of the inaugural class of Bill & Melinda Gates Foundation Millennium Scholars. She completed two internships with Kimberly-Clark in Neenah, WI and Roswell, GA and was also active in leadership roles in organizations on campus and in the Gainesville community. Samesha was competitively selected to serve as a teaching assistant for the College of Engineering's pilot Chem Teach program to promote freshman retention in engineering, which stirred her passion for teaching and mentoring. She earned a PhD in materials science and engineering in 2009 with a concentration in biomaterials and plans to pursue a career in academia.